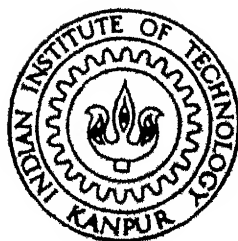


SIMULATION OF BUCK-BOOST CONVERTER WITH FUZZY LOGIC CONTROLLERS

by
RUCHI MALHOTRA



DEPARTMENT OF ELECTRICAL ENGINEERING

INDIAN INSTITUTE OF TECHNOLOGY KANPUR

FEBRUARY 1997

EE
1997
M
MAL
SIM

SIMULATION OF BUCK-BOOST CONVERTER WITH FUZZY LOGIC CONTROLLERS

A Thesis Submitted
in Partial Fulfillment of the Requirements
for the Degree of
Master of Technology

by
RUCHI MALHOTRA

to the
DEPARTMENT OF ELECTRICAL ENGINEERING
INDIAN INSTITUTE OF TECHNOLOGY, KANPUR

February 1997

EE-1997-M-MAL-SIM

Certificate

It is certified that the work contained in the thesis entitled **SIMULATION OF BUCK-BOOST CONVERTER WITH FUZZY LOGIC CONTROLLERS**, by **RUCHI MALHOTRA**, has been carried out under my supervision and that this work has not been submitted elsewhere for a degree

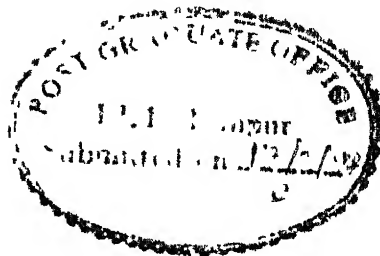
February 1997

x/01/172
Dr A JOSHI

Professor

Department of Electrical Engineering

IIT Kanpur



19 MAR 1937

CENTRAL LIBRARY
111 KANPUR

~~111~~ A 123244

Dedicated To
My Parents

Acknowledgements

I would take this opportunity to express my veneration to the Almighty for having given me this opportunity to come to this prestigious institute

I am ever indebted and express my profound thanks to my honourable thesis supervisor, Dr A Joshi without whose subtle guidance, untiring efforts and patient treatment (when I made blunders) it would not have been possible for me to present this discourse I am grateful to Dr A K Raina, for providing his lab facilities to me.

I am also thankful to my family members and Sanjay who have given me invaluable support during the course I would also like to thank Rajshekar and Shyamla for their invaluable support in Computer Center I am thankful to Rajneesh who has always helped me during the course.

Last but not the least, I would like to thank our group G-7 (Shubha, Bidisha, Pradeep, Jaswant, Groverji, Rajshekar), which has made my stay at I I T K a memorable one

Abstract

A detailed analysis of modelling and behaviour of the Buck-Boost converter is studied. The transfer functions are verified by simulation. The fuzzy logic controller is studied in detail. Equivalence between the Fuzzy Logic Controller and the linear P.I controller is established. Two schemes for self-organisation have been proposed to tune the process output to several desired responses. The response of FLC for a variation in load, line and reference value of voltage has been studied. The response of the system with various auxiliary controllers along with the FLC against the variation in load has been discussed. The Fuzzy Logic Controller is used alone with variable gain factor against load variation.

Contents

1	Introduction	1
1 1	Organisation of the Thesis	2
2	Modelling And Open Loop Behaviour of Buck-Boost Converter	4
2.1	Buck-Boost converter	4
2 1 1	Differential Equation Model	5
2 1 2	Simulation of the Buck-Boost Converter	7
2 1 3	State Space Average Model	9
2.1.4	Equivalent Circuit	11
2 1 5	Small Signal Model	12
2 1 6	$\hat{V}_c(s)$ Vs $\hat{d}(s)$ Transfer Function	14
2 1 7	$\hat{V}_c(s)$ Vs $\hat{u}(s)$ Transfer Function	19
2.2	Open Loop Behaviour Due to Step Change in Load Resistance	23
2 3	Effect of Step Change in Duty Cycle	28
2 4	Conclusions	30
3	Fuzzy Logic Controller	32
3 1	Description of Fuzzy Logic Controller	32
3 1 1	Fuzzifier	33
3 1 2	Fuzzy Control Rules	34
3 1 3	Fuzzy Inference	35
3 1 4	Defuzzification.	35
3 1 5	Calculation Of D_i	36

3 2	Equivalent Gains of the Fuzzy Logic Controller	36
3.2.1	Region 1:	37
3 3	5 Zone Fuzzy Logic Controller	41
3 4	A Simple Integral Controller	44
3 5	A Simple Proportional Controller	46
3 6	Integral Control With Adjustable Weights	48
3 7	A PI Controller	49
3 8	Effect of Fuzzy Output on the Controller Response	50
3 9	Control Surface	53
3.10	Response at 20 kHz	55
3.11	Conclusions	56
4	Self Organising Controller	57
4 1	Performance Measure	58
4 2	Method-1	60
4 3	Method-2	60
4.4	Self Organisation to Obtain a Given Desired Response	61
4 4 1	Method-1	62
4.4 2	Method-2	63
4.4.3	With Zero Initial Constants:	64
4.4 4	With Unity Initial Constants	65
4.5	Response to an Ideal Step	66
4 5 1	With Zero Initial constants	66
4 5 2	With Unity Initial Constants	67
4 6	Response to a Given Exponential	67
4 6 1	With Zero Initial Constants	67
4 6 2	With Unity Initial Constants	68
4.7	Effect of Number of Matching Points	68
4 8	Criterion For Stopping	69
4 9	Dual Table Method	70

4 10	Conclusions	73
5	Fuzzy Regulators	74
5 1	Load Regulation	74
5 2	Line Regulation	75
5 3	Response to Change in V_{ref}	77
5 4	Auxillary Controller	77
5 4 1	Auxillary Controller Using the Small Signal Model	80
5.4.2	Auxillary Controller Using the Simplified Small Signal Model	82
5.4.3	Auxillary Controller Using Low Frequency D.C. Gain	84
5.5	Effect of Variable Gain Factor η_1 on Response to Load Changes	85
5.5.1	Dual Value Gain Factor	86
5 5 2	Variable Gain Factor	87
5 6	Conclusions	89
6	Conclusions	90
6 1	Recommendations for Future Work	91
	References	93
	Appendix A	95

List of Figures

2 1	Buck-Boost Converter	5
2 2	Flow chart for converter simulation	8
2 3	Transient Response of the Buck-Boost Converter	9
2 4	Averaged Equivalent Circuit (Continuous Conduction Mode)	12
2 5	Averaged Equivalent Circuit (Discontinuous Conduction Mode) .	12
2 6	Bode Plot	16
2 7	Simulation Results while Disturbance in Duty Cycle at the Corner Frequency	18
2 8	Bode Plot	21
2 9	Simulation Results While Disturbance in V_{dc} at Corner Frequency	22
2 10	Average Inductor Current For a Change in Load Resistance From 10Ω to 5Ω	23
2 11	Average Output Voltage For a Change in Load Resistance From 10Ω to 5Ω	24
2 12	Average Inductor Current For a Change in Load Resistance From 10Ω to 15Ω	25
2 13	Average Output Voltage For a Change in Load Resistance From 10Ω to 15Ω	25
2 14	Average Inductor Current For a Change in Load Resistance From 10Ω to 20Ω	26
2 15	Average Output Voltage For a Change in Load Resistance From 10Ω to 20Ω	26

2.16	Average Inductor Current For a Change in Load Resistance From 10Ω to 30Ω	27
2.17	Average Output Voltage For a Change in Load Resistance From 10Ω to 30Ω	27
2.18	Average Inductor Current For a Change in Duty Cycle D From 0.2 to 0.4	28
2.19	Average Output Voltage For a Change in Duty Cycle D From 0.2 to 0.4	29
2.20	Average Inductor Current For a Change in Duty Cycle D From 0.2 to 0.25	29
2.21	Average Output Voltage For a Change in Duty Cycle D From 0.2 to 0.25	30
3.1	Block Diagram of Fuzzy Logic Controller	33
3.2	Membership Function for 3 Zone FLC	34
3.3	Division of e-ce Plane Into Zones For Calculation of K_i & K_p	37
3.4	Membership Function For 5 Zone FLC	41
3.5	Fuzzification Routine	42
3.6	Flow Chart For Simulation	43
3.7	Integral Control	45
3.8	Proportional Control	47
3.9	Integral Control With Adjustable Weights	49
3.10	Response With 3 Zone FLC, Linear PI Controller and 5 Zone FLC	50
3.11	Response of 5 zone FLC	52
3.12	Mamdani's Minimum Operation	52
3.13	Membership Function For Output	53
3.14	Response Due to Fuzzy Output and Crisp Output	54
3.15	A 3-D Control Surface For 3 Zone FLC	54
3.16	A 3-D Control Surface For 5 Zone FLC	55
3.17	Response at 20 kHz and 100 kHz	56

4 1	Desired Response and Response of Original 5 Zone FLC	62
4 2	Response to a Given Desired Response Using Method-1 With Initial Constants	63
4 3	For a Given Desired Response Using Method-2 With Initial Constants	64
4 4	For a Given Desired Response Using Method-2 With Zero Initial Constants	66
4 5	Step Response	67
4 6	Exponential Response	68
4 7	Variation in the Value of Constant a_3	69
4 8	Criterion For Stopping	70
4 9	Membership Function For e_p	71
4 10	Dual Table Method	72
5 1	Load Resistance is Changed from $10\ \Omega$ to $30\ \Omega$ & then to $10\ \Omega$	75
5 2	Load Resistance is Changed from $10\ \Omega$ to $5\ \Omega$ & then to $10\ \Omega$	76
5 3	Line Voltage is Changed from 15V to 10V & then back to 15V	76
5 4	Reference Voltage is Changed to 5V	77
5 5	Block Diagram For Auxillary Controller	78
5 6	Nature of Load Variation	78
5 7	Response of Fuzzy Regulator With $D_{max}=0.80$	79
5 8	Response of Fuzzy Regulator With $D_{max}=0.22$	79
5 9	Response of the Auxillary Controller using Small Signal Model ($D_{max}=0.80$)	81
5 10	Response of the Auxillary Controller using Small Signal Model ($D_{max}=0.22$)	82
5 11	Response of the Auxillary Controller using Simplified Small Signal Model ($D_{max}=0.80$)	83
5 12	Response of the Auxillary Controller using Simplified Small Signal Model ($D_{max}=0.22$)	83
5 13	Response of the Auxillary Controller using d c Gain ($D_{max}=0.80$)	84
5 14	Response of the Auxillary Controller using d c Gain ($D_{max}=0.22$)	85
5 15	Response of Dual Gain FLC ($D_{max}=0.80$)	86

5 16	Response of Dual Gain FLC ($D_{max}=0.22$)	87
5 17	Response of Variable Gain FLC ($D_{max}=0.80$) .	88
5 18	Response of Variable Gain FLC ($D_{max}=0.22$) .	88

List of Tables

2 1	Verification of Transfer Function (\hat{V}_c / \hat{d})	17
2 2	Verification of Transfer Function \hat{V}_c / \hat{u}	20
3 1	Rule Table showing C_i For Different Categories of e_i & ce_i	35
3 2	Combinations of e & ce	38
3 3	Equivalent Gains for Fuzzy Controller	39
3 4	Control Action For Boundary Regions	40
3 5	Rule Table For Integral Control	45
3 6	Rule Table For Proportional Control	47
3 7	Rule Table For Integral Control With Adjustable Gains	48
3 8	Rule Table For 5 Zone Fuzzy Controller	51
3 9	Rule Table For Crisp Output	51
3 10	Rule Table For Fuzzy Output	53
4 1	Rule Table For 5 Zone Fuzzy Controller	58
4 2	Performance Measure Table	59
4 3	Constants of Performance Measure Table	62
4 4	Constants of Performance Measure Table	63
4 5	Nature of Deviation With Different Values of $\Delta d's$	65
4 6	Performance Measure Table For C_{pi}	72

Chapter 1

Introduction

For industrial system the problem of controlling a plant involves the determination of the mathematical model and the choice of an appropriate controller. Even if the model of the plant is not known or known inaccurately, the fuzzy logic controller can control the plant. The basis of fuzzy logic controller is the use of linguistic statements [1]. The PID controller is a very common configuration for industrial control. However, the complexity of the plant makes the tuning of the controller difficult and often trial & error is used. The fuzzy logic controller, on the other hand is easy to implement and tune as it is based on the common sense understanding of the nature of the plant to be controlled [2], [3]. Therefore it is worth-while to examine the equivalence between the two types of the controllers [4].

The Buck-Boost converter can be modelled with good accuracy using differential equations [7]. However the design of a linear controller for different converter parameters and operating points requires elaborate calculations. A significant advantage of FLC is the ease with which it can be implemented and tuned for different converters [6]. Also, the fuzzy logic controller is very flexible.

A significant problem in implementation of FLC is the choice of constants in the Rule Table. These constants can be chosen by trial and error using the simulation of the converter. However the self organising scheme is useful in arriving at the values of these constants starting from arbitrary initial values e.g. all zeros [8]. The self organising schemes can also be used to achieve a desired output response obtained

from zero state

Auxillary controllers can be introduced in the system during transients along with the main controller to reduce the overshoot and undershoot in the output after any perturbation. The fuzzy logic allows us to implement such controllers in an easy manner.

1.1 Organisation of the Thesis

The detailed modelling and behaviour analysis of a Buck - Boost converter which is taken as the process to be controlled has been given in Chapter 2. The following models have been derived:

- State space differential equation model (Section 2.1.1)
- Average state space equation and equivalent circuit (Section 2.1.3 & Section 2.1.4)
- Small signal model and transfer function (Section 2.1.5)

The usual assumptions of ideal switch and high switching frequency [7] have been made in deriving above models.

The detailed analysis of several types of fuzzy controllers has been given in chapter 3. The equivalence of Fuzzy Logic Controller (FLC) with the linear P.I controller has been studied in Section 3.2. Response of a 3 zone FLC, 5 zone FLC and with fuzzy output is also studied. The 3-D control surface which gives the characteristics of the controller is given in Section 3.9.

In Chapter 4 the self organising schemes using two different methods are discussed. Rule Table is adjusted to match the different desired responses with different initial conditions given as below.

1. For a given desired response

- With some initial constants (Section 4.4.1 & 4.4.2)

- with zero initial constants (Section 4 4 3)
- With unity initial constants (Section 4 4 4)

2 For a desired step

- with zero initial constants (Section 4 5 1)
- with unity initial constants (Section 4 5 2)

3 For a desired exponential

- with zero initial constants (Section 4 6 1)
- with unity initial constants (Section 4 6 2)

The criterion for stopping this process has been given in Section 4 8

The performance of fuzzy regulators is discussed in Chapter 5 The response to load variation , line variation and reference voltage variation has been studied in Section 5 1, Section 5 2 and Section 5 3 respectively Section 5 4 describes the introduction of the auxillary controller to improve the response of FLC during transients The following three auxillary controllers are discussed in Section 5.

- 1 Auxillary controller based on the small signal model of the converter (Section 5 4 1)
- 2 Auxillary controller based on the simplified small signal model of the converter (Section 5 4 2)
- 3 Auxillary controller based on the d c gain (Section 5 4 3)

The following two auxillary controllers have been dicussed in Section 5 5 and also shown to improve the response of the FLC

- 1 Dual valued gain Auxillary Controller (Section 5 5 1)
- 2 Variable gain Auxillary Controller (Section 5 5 2)

Chapter 2

Modelling And Open Loop Behaviour of Buck-Boost Converter

For applying any control scheme the model of the process to be controlled should be known. This chapter presents the complete modelling of the Buck-Boost converter.

Section 2.1.1 presents the differential equation model of the converter. Section 2.1.2 gives the simulation of the converter and transient behaviour of the converter output voltage. The state space average model has been given in Section 2.1.3. The equivalent circuit of the converter has been derived in Section 2.1.4. Section 2.1.5 gives the small signal model of the converter. The transfer function between small signal capacitor voltage and small signal change in duty cycle D is given in Section 2.1.6. Section 2.1.7 computes the transfer function between small signal capacitor voltage and small signal change in input voltage V_{dc} . The open loop behaviour of the converter for a step change in load resistance and duty cycle has been given in Section 2.1.8 and Section 2.1.9 respectively.

2.1 Buck-Boost converter

The work presented here is based on a Buck-Boost converter shown in Fig 2.1.

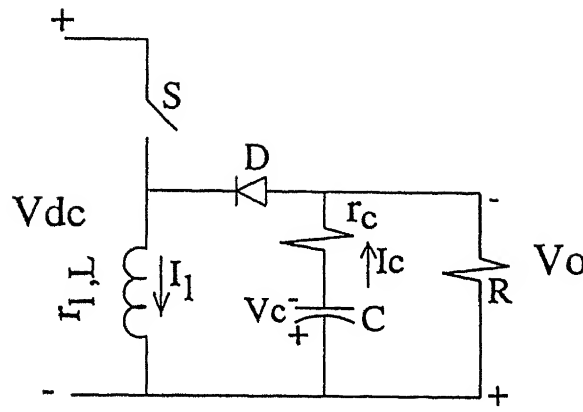


Figure 2 1 Buck-Boost Converter

When the switch S is on and diode D is off, the inductor L stores energy through the supply voltage V_{dc} . The capacitor discharges into the load R . r_l and r_c are the inductor and capacitor series resistances respectively. This is called as Mode 1. When the switch S is off and diode D is on, the inductor L transfers its energy while charging capacitor C and supplying the power to R . This is Mode 2. When the converter goes into discontinuous conduction then it enters into another mode called as Mode 3. In this mode the diode D is off and the inductor current becomes zero before the cycle ends. Capacitor C discharges into the load. The diode prevents inductor current from reversing.

2.1.1 Differential Equation Model

The converter operates in 2 or 3 modes in one cycle during continuous and discontinuous operation of the converter respectively. In Fig 2 1 r_l is the resistance of the inductor winding and r_c is the equivalent series resistance of the capacitor and $R_1 = R + r_c$. The switch S is operated periodically with duty cycle D . Thus S is on for duration DT and off for duration $(1-D)T$. If I_l is continuous, the following equations and their solutions are obtained.

Mode 1:

In this mode S is on and $0 \leq t \leq DT$

$$V_c = \frac{-V_c}{R_1 C}$$

$$I_l = V_{dc} - \frac{r_l I_l}{L}$$

The above state equations give the following solution

$$V_c = V_{c0} e^{\frac{-t}{R_1 C}} \quad (2.1)$$

$$I_l = \frac{V_{dc}}{r_l} + (I_{l0} - \frac{V_{dc}}{r_l}) e^{\frac{-r_l t}{L}} \quad (2.2)$$

where V_{c0} & I_{l0} are the initial capacitor voltage and the inductor current respectively

Mode 2:

In this mode S is off and diode D conducts and $DT \leq t \leq T$ It is assumed that the LC circuit is underdamped

$$V_c = \frac{-V_c}{R_1 C} + \frac{R I_l}{R_1 C}$$

$$I_l = \frac{-V_c(1 - \frac{r_c}{R_1})}{L} - \frac{r_l I_l}{L} - \frac{R r_c I_l}{R_1 L}$$

The above state equations give the following solution.

$$V_c = e^{\sigma t} (c_1 \cos \omega t' + c_2 \sin \omega t') \quad (2.3)$$

$$I_l = e^{\sigma t} (c_3 \cos \omega t' + c_4 \sin \omega t') \quad (2.4)$$

$$c_1 = V_{c0}$$

$$c_2 = \frac{1}{\omega} \left[\frac{R I_{l0}}{R_1 C} - V_{c0} \left(\sigma + \frac{1}{R_1 C} \right) \right]$$

$$c_3 = I_{l0}$$

$$c_4 = -\frac{1}{\omega} \left(\frac{V_{c0}(1 - \frac{r_c}{R_1})}{L} + I_{l0} \left(\sigma + \frac{r_l}{L} + \frac{R r_c}{R_1 L} \right) \right)$$

$$\sigma = -\frac{\frac{1}{R_1 C} + \frac{r_l}{L} + \frac{R r_c}{R_1 L}}{2}$$

$$\omega = \frac{\sqrt{\frac{4(R_1 I_{L1})}{R_1 L C} - \left(\frac{1}{R_1 C} + \frac{1}{L} + \frac{R_1}{R_1 L}\right)^2}}{2}$$

where V_{c1} & I_{L1} are the initial capacitor voltage and the inductor current respectively for mode 2. Time t' is given by $t' = (t - DT)$ and therefore $0 \leq t' \leq (1 - D)T$.

Mode 3.

For discontinuous conduction there is an additional mode apart from mode 1 & mode 2. The time for mode 2, given above becomes $DT \leq t \leq T_1$ where T_1 is the time when the inductor current becomes zero. Therefore capacitor C discharges into the load and the diode D is off. The state equations are as follows

$$V_c = \frac{-V_c}{R_1 C}$$

$$I_L = 0$$

The above state equations give the following solution

$$V_c = V_{c1} e^{\frac{-t''}{R_1 C}} \quad (2.5)$$

$$I_L = 0 \quad (2.6)$$

where V_{c1} is the initial capacitor voltage for mode 3 and t'' is given as $t'' = t - T_1$ and therefore $0 \leq t'' \leq (T - T_1)$. For simulation purpose the analytical solution for converter given in equations (2.1) to (2.6) is used.

2.1.2 Simulation of the Buck-Boost Converter

The buck-boost converter is simulated by its analytical solution given in Section 2.1.1. The flow chart for converter simulation is given in Fig 2.2. The parameters of the converter are given in Appendix A. It is to be noted that the output voltage V_o of the converter is the averaged voltage over one time period T . The transient variation of the output voltage V_o of the converter starting from zero initial conditions with $D=0.2$ is shown in Fig 2.3. The output voltage reaches a steady state value of 3.69V.

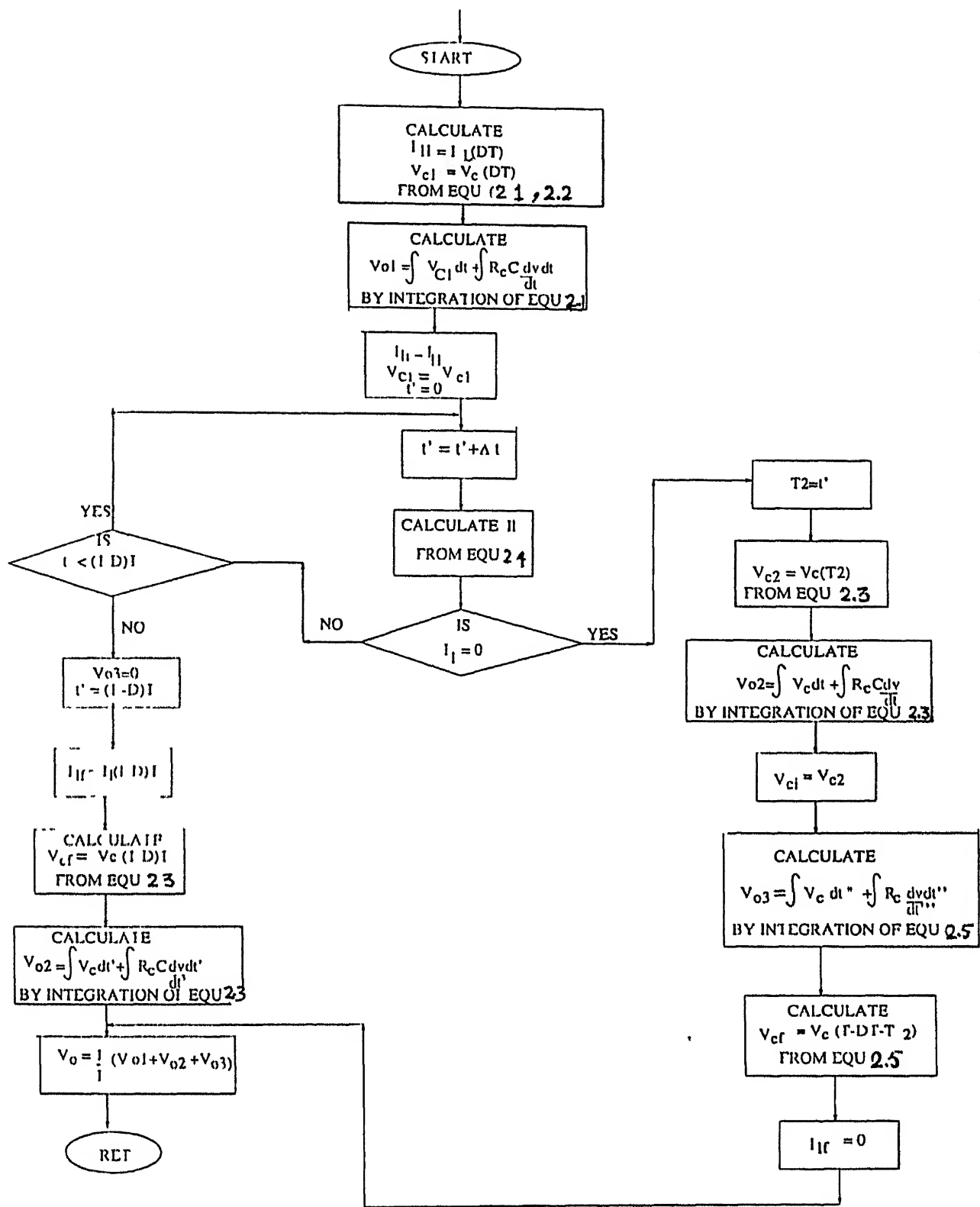


Figure 2.2. Flow chart for converter simulation

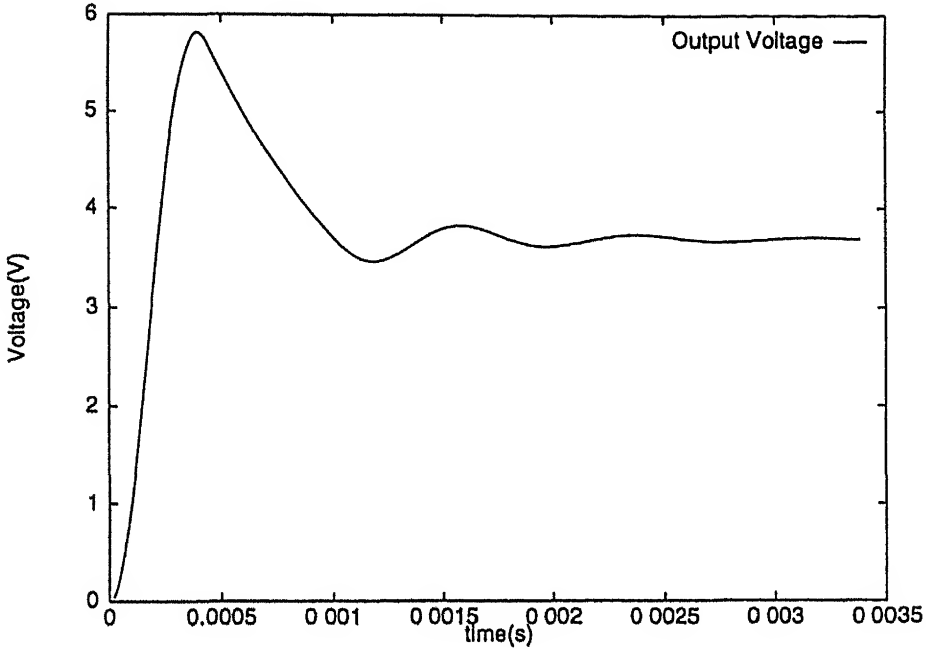


Figure 2.3 Transient Response of the Buck-Boost Converter

2.1.3 State Space Average Model

To study the small signal behaviour of the converter, state space averaging and linearization are the analytical approximation techniques that, allow switching regulators to be represented as linear systems. State space averaging allows the switched system to be approximated as a continuous but nonlinear system and linearization allows the resulting nonlinear system to be approximated as a linear system around an operating point. The state space equation is of the form

$$\dot{X} = AX + BU$$

where X is the state variable. From the state equations given in Section 2.1.1 and V_c and I_L as the state variables the system matrices are given as following

Mode 1:

$$A_1 = \begin{bmatrix} \frac{-1}{R_1 C} & 0 \\ 0 & \frac{1}{L} \end{bmatrix} \quad B_1 = \begin{bmatrix} 0 \\ \frac{1}{L} \end{bmatrix}$$

Mode 2:

$$A_2 = \begin{bmatrix} \frac{-1}{R_1 C} & \frac{R}{R_1 C} \\ \frac{1 - \frac{r_c}{R_1}}{L} & -(\frac{1}{L} + \frac{R_1 r_c}{R_1 L}) \end{bmatrix} \quad B_2 = \begin{bmatrix} 0 \\ 0 \end{bmatrix}$$

The continuous-time state space averaged representation is

$$\dot{X} = AX + BU$$

where

$$A = A_1 D + A_2 (1 - D)$$

$$B = B_1 D + B_2 (1 - D)$$

which results in the following

$$A = \begin{bmatrix} \frac{-1}{R_1 C} & \frac{(1-D)R}{R_1 C} \\ \frac{(1-D)(1 - \frac{r_c}{R_1})}{L} & \frac{-1}{L} - \frac{(1-D)Rr_c}{R_1 L} \end{bmatrix} \quad B = \begin{bmatrix} 0 \\ \frac{D}{L} \end{bmatrix}$$

Mode 3:

For discontinuous conduction from the state space equations for mode 3, A_3 and B_3 are given as

$$A_3 = \begin{bmatrix} \frac{-1}{R_1 C} & 0 \\ 0 & 0 \end{bmatrix} \quad B_3 = \begin{bmatrix} 0 \\ 0 \end{bmatrix}$$

$$A = A_1 D + A_2 D_1 + A_3 (1 - D - D_1)$$

$$B = B_1 D + B_2 D_1 + B_3 (1 - D - D_1)$$

where $D_1 = \frac{T_1 - DT}{T}$

which results in the following

$$A = \begin{bmatrix} -\frac{1}{R_1 C} & \frac{D_1 R}{R_1 C} \\ -\frac{D_1 (1 - \frac{r_c}{R_1})}{L} & -\frac{r_l (D + D_1)}{L} - \frac{D_1 R r_c}{R_1 L} \end{bmatrix} \quad B = \begin{bmatrix} 0 \\ \frac{D}{L} \end{bmatrix}$$

2.1.4 Equivalent Circuit

An averaged equivalent circuit can be drawn on the basis of continuous-time averaged equations. The averaged state equations given in Section 2.1.2 are rewritten in the following form

$$V_c = \frac{-V_c}{R_1 C} + \frac{(1 - D) R I_l}{R_1 C} \quad (2.7)$$

$$I_l = \frac{-(1 - D)(1 - \frac{r_c}{R_1}) V_c}{L} - \frac{r_l I_l}{L} - \frac{(1 - D) R r_c I_l}{R_1 L} + \frac{D V_{dc}}{L} \quad (2.8)$$

From equation (2.8)

$$\frac{D V_{dc}}{1 - D} = \frac{L}{(1 - D)} \frac{dI_l}{dt} + (1 - \frac{r_c}{R_1}) V_c + \frac{r_l I_l}{(1 - D)} + \frac{R r_c I_l}{R_1} \quad (2.9)$$

From equation (2.7)

$$I_l = \frac{R_1 C}{R(1 - D)} \frac{dV_c}{dt} + \frac{V_c}{R(1 - D)} \quad (2.10)$$

Equations (2.9) & (2.10) can be described by an equivalent circuit given in Fig 2.4

For discontinuous conduction the averaged system's equations are given as

$$\frac{dV_c}{dt} = \frac{-V_c}{R_1 C} + \frac{D_1 R I_l}{R_1 C} \quad (2.11)$$

$$\frac{dI_l}{dt} = \frac{-D_1 (1 - \frac{r_c}{R_1}) V_c}{L} - \frac{r_l (D + D_1) I_l}{L} - \frac{D_1 R r_c I_l}{R_1 L} \quad (2.12)$$

From equation (2.11)

$$I_l = \frac{R_1 C}{D_1 R} \frac{dV_c}{dt} + \frac{V_c}{D_1 R}$$

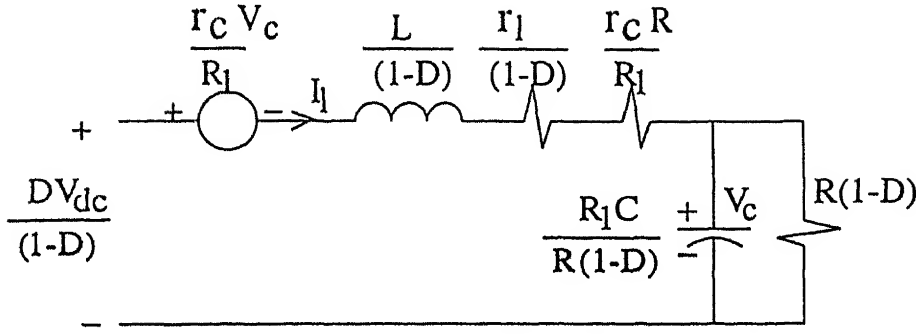


Figure 2.4 Averaged Equivalent Circuit (Continuous Conduction Mode)

$$\frac{DV_{dc}}{D_1} = \frac{L}{D_1} \frac{dI_l}{dt} + V_c - \frac{r_c V_c}{R_l} + r_l \left(1 + \frac{D}{D_1}\right) I_l$$

Equation (2.11) & (2.12) can be described by an equivalent circuit given in Fig 2.5

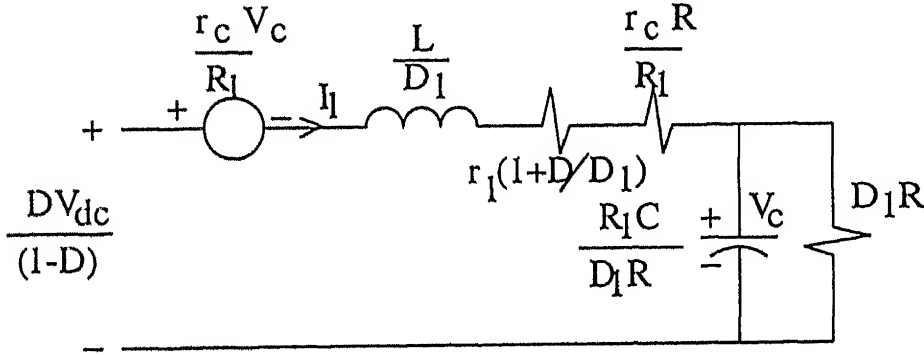


Figure 2.5. Averaged Equivalent Circuit (Discontinuous Conduction Mode)

2.1.5 Small Signal Model

This continuous nonlinear system can be approximated as a linear system with in a small enough neighbourhood, around its dc operating point, which results in a linear system as

$$\hat{X} = A_o \hat{X} + B_o \hat{u} + E \hat{d}$$

where \hat{X} is a small deviation in state variable X

\hat{u} is a small deviation in input U

\hat{d} is a small deviation in duty cycle D .

A_o and B_o are the matrices at a particular operating point Matrix E is given as

$$E = (A_1 - A_2)X_o + (B_1 - B_2)U_o$$

For continuous conduction

$$E = \begin{bmatrix} 0 & \frac{-R}{R_1 C} \\ \frac{(1-\frac{r_c}{R_1})}{L} & \frac{R r_c}{R_1 L} \end{bmatrix} \begin{bmatrix} V_{co} \\ I_{lo} \end{bmatrix} + \begin{bmatrix} 0 \\ \frac{1}{L} \end{bmatrix} V_{dc}$$

$$E = \begin{bmatrix} \frac{-I_{lo} R}{R_1 C} \\ \frac{(1-\frac{r_c}{R_1})V_{co}}{L} + \frac{R r_c I_{lo}}{R_1 L} + \frac{V_{dc}}{L} \end{bmatrix}$$

For discontinuous conduction

$$E = (A_1 - A_2 - A_3)X_o + (B_1 - B_2 - B_3)U_o$$

$$E = \begin{bmatrix} -\frac{1}{R_1 C} & -\frac{R}{R_1 C} \\ \frac{(1-\frac{r_c}{R_1})}{L} & \frac{R r_c}{R_1 L} \end{bmatrix} \begin{bmatrix} V_{co} \\ I_{lo} \end{bmatrix} + \begin{bmatrix} 0 \\ \frac{1}{L} \end{bmatrix} V_{dc}$$

$$E = \begin{bmatrix} \frac{V_{co}}{R_1 C} - \frac{I_{lo} R}{R_1 C} \\ \frac{V_{co}(1-\frac{r_c}{R_1})}{L} + \frac{I_{lo} R r_c}{R_1 L} + \frac{V_{dc}}{L} \end{bmatrix}$$

The small signal average model is given as

$$\hat{X} = A_o \hat{X} + B_o \hat{u} + E \hat{d}$$

taking its Laplace transformation results in

$$s\hat{X}(s) = A_o \hat{X}(s) + B_o \hat{u}(s) + E \hat{d}(s)$$

$$\hat{X}(sI - A_o) = B_o \hat{u}(s) + E \hat{d}(s)$$

$$\hat{X}(s) = (sI - A_o)^{-1} B_o \hat{u}(s) + (sI - A_o)^{-1} E \hat{d}(s)$$

2.1.6 $\hat{V}_c(s)$ Vs $\hat{d}(s)$ Transfer Function

When the input dc voltage is fixed $\hat{u}(s)=0$

$$\hat{X}(s) = (sI - A_o)^{-1} E \hat{d}(s)$$

$$\begin{bmatrix} \hat{V}_c(s) \\ \hat{I}_l(s) \end{bmatrix} = \begin{bmatrix} (s + \frac{1}{R_1 C}) & -\frac{(1-D)R}{R_1 C} \\ \frac{(1-D)(1-\frac{r_c}{R_1})}{L} & (s + \frac{r_l}{L} + \frac{(1-D)Rr_c}{R_1 L}) \end{bmatrix} \begin{bmatrix} \frac{-I_{lo}R}{R_1 C} \\ \frac{(1-\frac{r_c}{R_1})V_{co}}{L} + \frac{Rr_c I_{lo}}{R_1 L} + \frac{V_{dc}}{L} \end{bmatrix} \hat{d}(s)$$

$$(sI - A_o)^{-1} = \frac{1}{\Delta} \begin{bmatrix} (s + \frac{r_l}{L} + \frac{(1-D)Rr_c}{R_1 L}) & \frac{(1-D)R}{R_1 C} \\ -\frac{(1-D)(1-\frac{r_c}{R_1})}{L} & (s + \frac{1}{R_1 C}) \end{bmatrix}$$

where

$$\Delta = (s + \frac{r_l}{L} + \frac{(1-D)Rr_c}{R_1 L})(s + \frac{1}{R_1 C}) + \frac{(1-D)^2 R(1 - \frac{r_c}{R_1})}{R_1 LC}$$

Considering only the first row

$$\begin{aligned} \hat{V}_c(s) &= \frac{1}{\Delta} [(s + \frac{r_l}{L} + \frac{(1-D)Rr_c}{R_1 L}) (\frac{-RI_{lo}}{R_1 C}) \\ &\quad + \frac{(1-D)R}{R_1 C} (\frac{V_{dc}}{L} + \frac{Rr_c I_{lo}}{R_1 L} + (1 - \frac{r_c}{R_1}) \frac{V_{co}}{L})] \hat{d}(s) \end{aligned}$$

The transfer function is given as follows

$$\begin{aligned} \frac{\hat{V}_c(s)}{\hat{d}(s)} &= \frac{1}{\Delta} [(s + \frac{r_l}{L} + \frac{(1-D)Rr_c}{R_1 L}) (\frac{-RI_{lo}}{R_1 C}) \\ &\quad + \frac{(1-D)R}{R_1 C} (\frac{V_{dc}}{L} + \frac{Rr_c I_{lo}}{R_1 L} + (1 - \frac{r_c}{R_1}) \frac{V_{co}}{L})] \end{aligned}$$

substituting the values in above from the Appendix A and $I_{lo}=0.4614$, $V_{co}=3.69$

$$\begin{aligned} \Delta &= s^2 + 2.781 \times 10^3 s + 64.46 \times 10^6 \\ &= \frac{(1475 \times 10^8 - 4.56 \times 10^3) \hat{d}(s)}{\Delta} \end{aligned}$$

$$\frac{\hat{V}_c(s)}{\hat{d}(s)} = \frac{14.75 \times 10^8 - 4.56 \times 10^3 s}{s^2 + 2.781 \times 10^3 s + 64.46 \times 10^6}$$

substituting $s=j\omega$

$$\begin{aligned} \frac{\hat{V}_c(j\omega)}{\hat{d}(j\omega)} &= \frac{14.75 \times 10^8 - 4.56 \times 10^3 j\omega}{-\omega^2 + 2.78 \times 10^3 j\omega + 64.46 \times 10^6} \\ &= \frac{22.88(1 - 0.309 \times 10^{-5} j\omega)}{1 + 0.04 \times 10^{-3} j\omega - \frac{\omega^2}{64.46 \times 10^6}} \end{aligned} \quad (2.13)$$

The transfer function has a zero at 3.23×10^5 rad/sec and a pole at 8.02×10^3 rad/sec. The Bode plot for this transfer function is shown in Fig 2.6

The Bode plot is verified by giving a small disturbance in the duty cycle in the simulation of the converter. It is verified for frequencies 500 Hz, 1 kHz, 5 kHz, 10 kHz and the corner frequency of 8.02×10^3 rad/sec (1276.42 Hz). Fig 2.7 shows the response of the converter for a disturbance in duty cycle D given as $\hat{d} = 0.005 \sin(\omega t)$ having frequency equal to the corner frequency i.e. 8.02×10^3 rad/sec. The values of the gain and phase computed from the above transfer function and obtained from the results of simulation are given in Table 2.1.

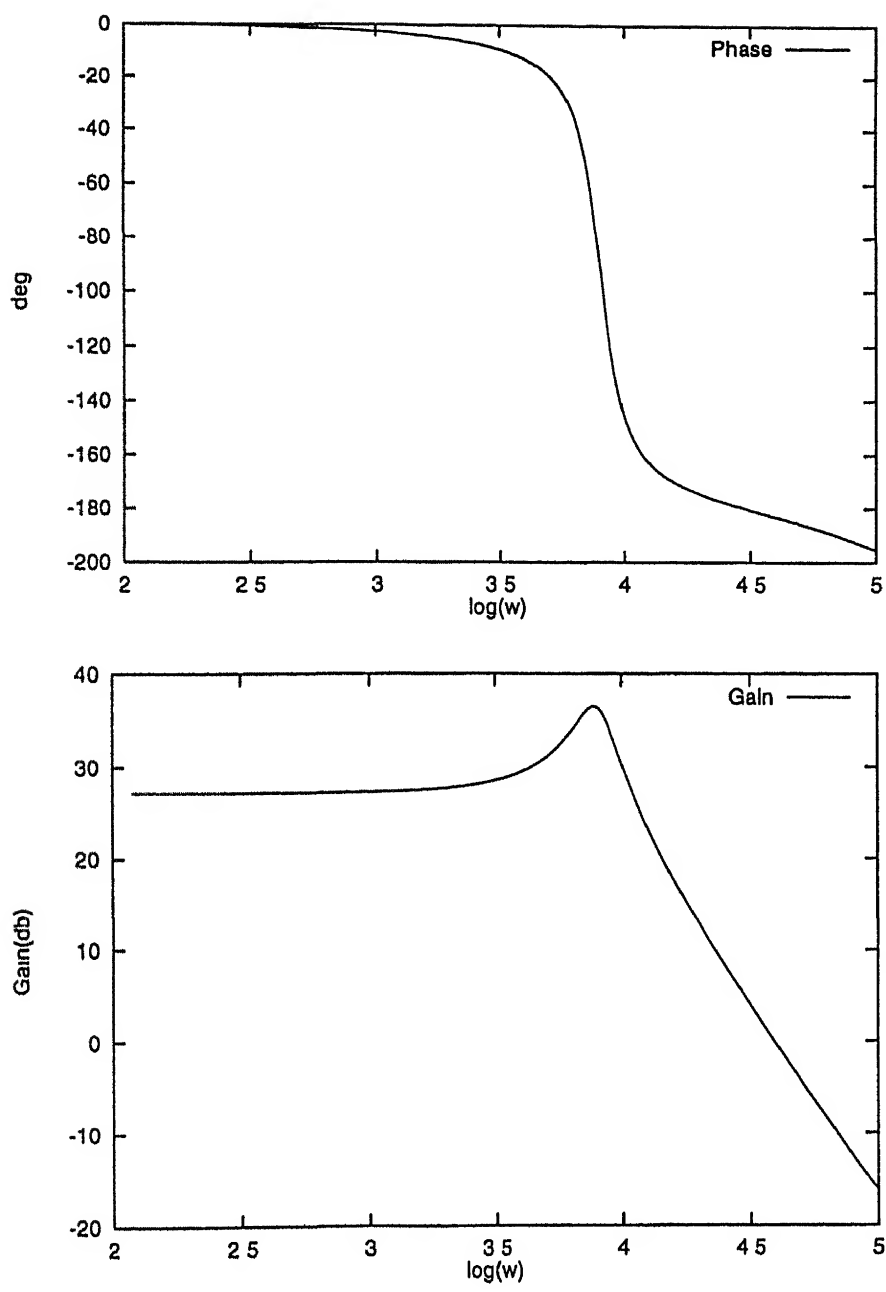


Figure 2 6 Bode Plot

Table 2.1 Verification of Transfer Function (\hat{V}_c / \hat{d})

Frequency (Hz)	Gain (db)		Phase (deg)	
	Simulation	Transfer Function	Simulation	Transfer Function
500	28.57	28.58	-9.22	-12.8
1000	33.73	34.03	-34.37	-38.57
1276.42	36.43	36.12	-90.14	-90
5000	4.08	4.76	-180.57	-180
10000	-8.27	-7.6	-188.64	162

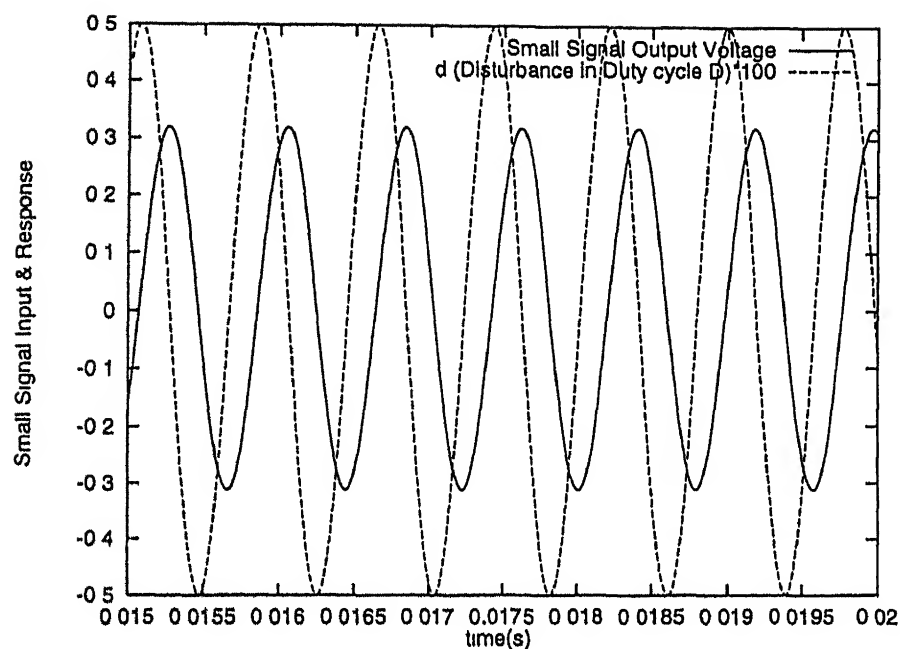


Figure 2.7. Simulation Results while Disturbance in Duty Cycle at the Corner Frequency

2.1.7 $\hat{V}_c(s)$ Vs $\hat{u}(s)$ Transfer Function

When there is a disturbance in supply voltage \hat{u} at a fixed value of duty cycle D , the transfer function between $\hat{V}_c(s)$ & $\hat{u}(s)$ is given as below

$$\hat{X}(s) = (sI - A_o)^{-1}B_o\hat{u}(s) + (sI - A_o)^{-1}E\hat{d}(s)$$

substituting $\hat{d}(s)=0$

$$\begin{aligned} \hat{X}(s) &= (sI - A_o)^{-1}B_o\hat{u}(s) \\ \begin{bmatrix} \hat{V}_c(s) \\ \hat{I}_l(s) \end{bmatrix} &= \frac{1}{\Delta} \begin{bmatrix} (s + \frac{r_l}{L} + \frac{(1-D)Rr_c}{R_1L}) & \frac{(1-D)R}{R_1C} \\ -\frac{(1-D)(1-\frac{r_c}{R_1})}{L} & (s + \frac{1}{R_1C}) \end{bmatrix} \begin{bmatrix} 0 \\ \frac{D}{L} \end{bmatrix} \hat{u}(s) \\ \hat{V}_c(s) &= \frac{(1-D)RD\hat{u}(s)}{\Delta R_1LC} \end{aligned}$$

The transfer function is given as following

$$\frac{\hat{V}_c(s)}{\hat{u}(s)} = \frac{(1-D)RD}{\Delta R_1LC}$$

substituting the values in above

$$\frac{\hat{V}_c(s)}{\hat{u}(s)} = \frac{1.58 \times 10^7}{s^2 + 2.78 \times 10^3 s + 64.46 \times 10^6} \quad (2.14)$$

The transfer function has a pole at 8.02×10^3 rad/sec. The Bode plot for this transfer function is shown in Fig 2.8.

The Bode plot is now verified by giving a small disturbance in the dc supply voltage in the simulation of the converter. It is verified for frequencies 500 Hz, 1 kHz, 5 kHz, 10 kHz and the corner frequency of 8.02×10^3 rad/sec (1276.42 Hz). Fig 2.9 shows the response of the converter for a disturbance in the supply voltage given as, $\hat{V}_{dc} = 1 \sin(\omega t)$ having frequency equal to the corner frequency i.e. 8.02×10^3 rad/sec.

The values of the gain computed from the above transfer function and obtained from the results of simulation are given in Table 2.2. Same equations, as the model for constant V_{dc} have been used for modelling the perturbation. The ac component of the input voltage has been sampled in each cycle and this value is assumed constant. As sampling is at 100 kHz, this approximation is valid.

Table 2.2 Verification of Transfer Function \hat{V}_c / \hat{u}

Frequency (Hz)	Gain (db)		Phase (deg)	
	Simulation	Transfer Function	Simulation	Transfer Function
500	-10.8	-10.5	-9.31	-8.56
1000	-5.66	-6.16	-35.26	-22.5
1276.42	-3.08	-7.7	-88.81	-80
5000	-35.35	-34.88	-174.60	-162
10000	-47.83	-47.13	-177.42	-170

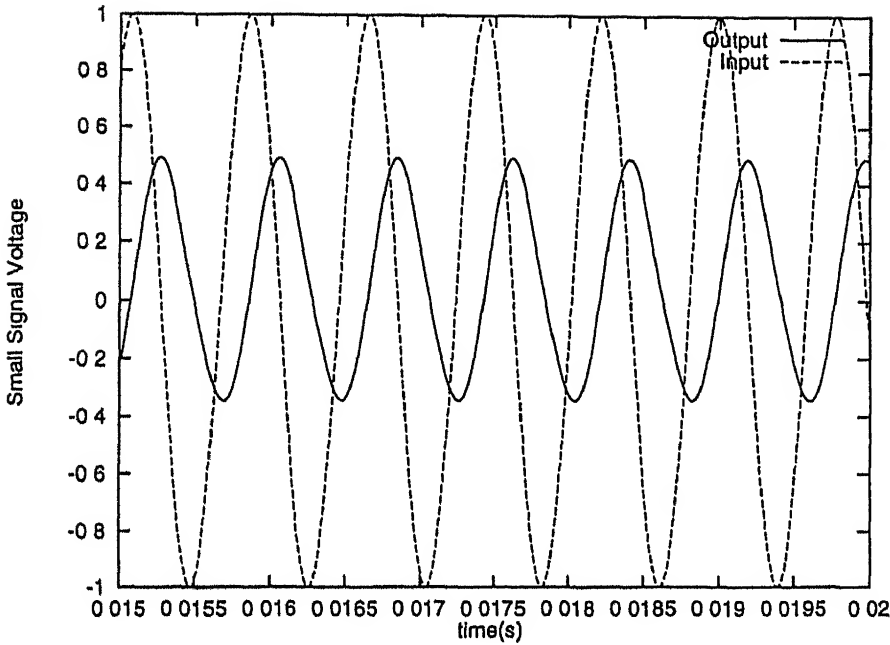


Figure 2 9 Simulation Results While Disturbance in V_{dc} at Corner Frequency

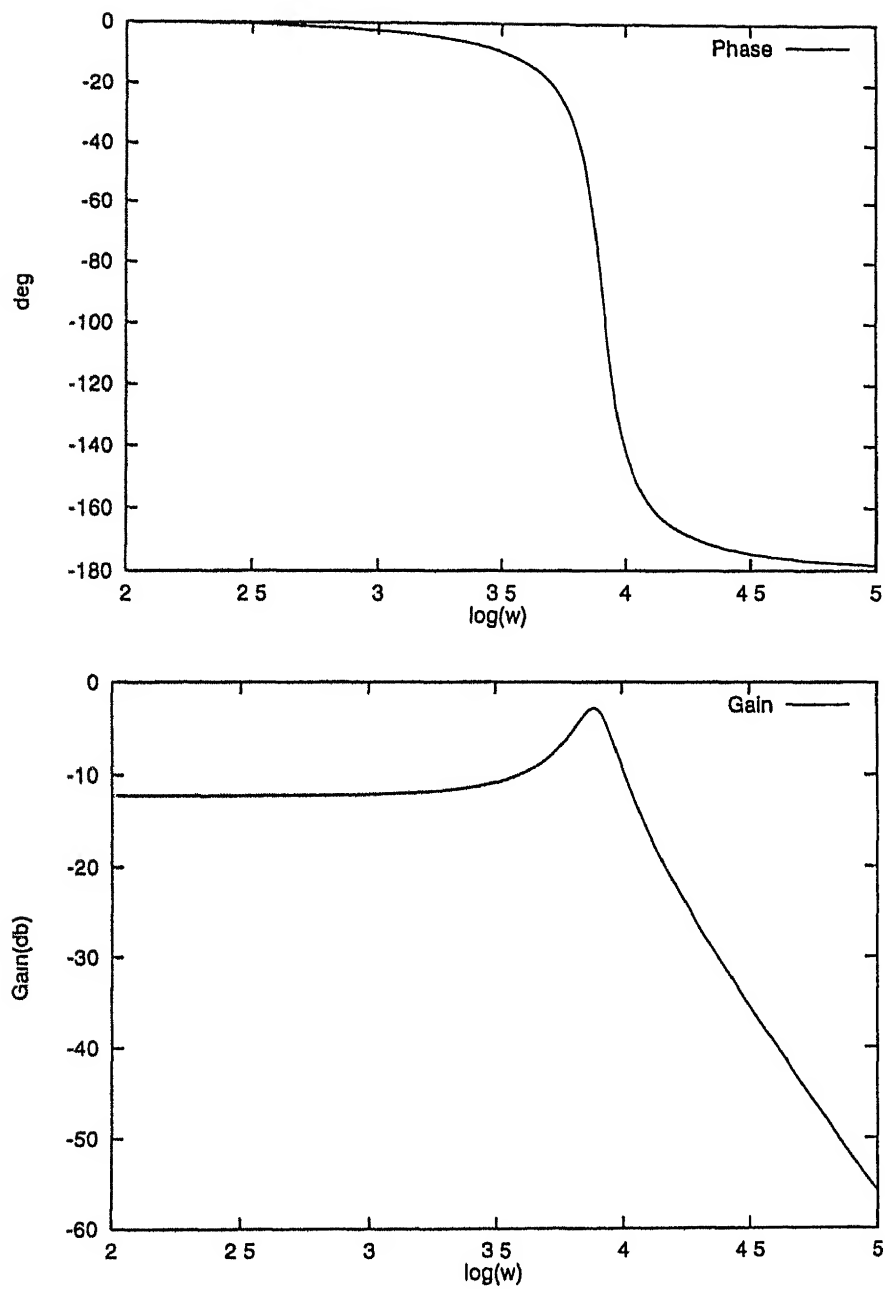


Figure 2 8 Bode Plot

2.2 Open Loop Behaviour Due to Step Change in Load Resistance

The converter behaviour for a step change in the load resistance from a stable operating point i.e. $D=0.200$ & $V_o=3.69$ is shown through the average inductor current and average output voltage. Fig 2.10 and Fig 2.11 shows the response for load injection i.e. the load resistance is decreased from 10 ohms to 5 ohms with the differential equation model and the averaged equivalent model of the converter.

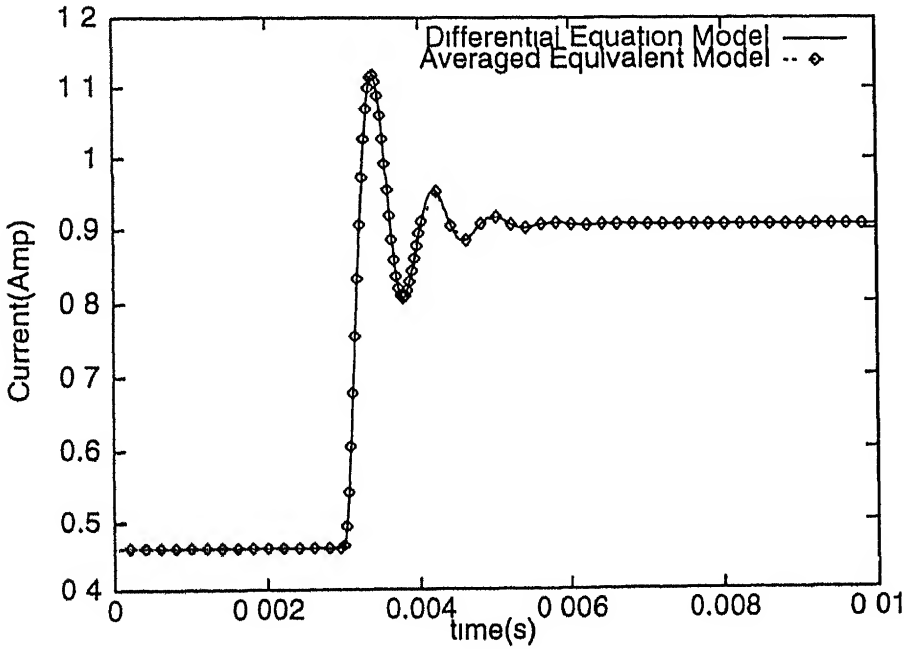


Figure 2.10. Average Inductor Current For a Change in Load Resistance From 10Ω to 5Ω

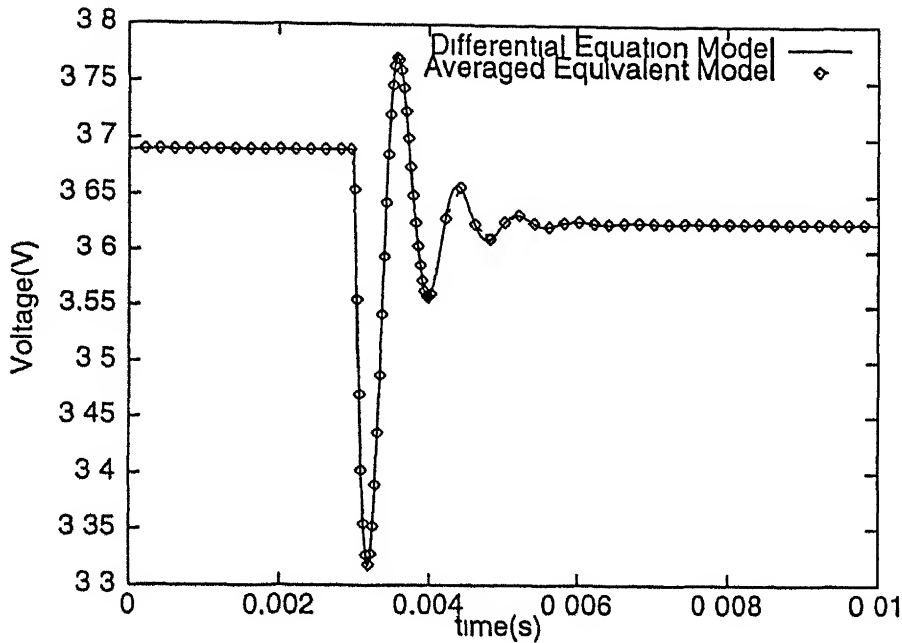


Figure 2.11 Average Output Voltage For a Change in Load Resistance From 10Ω to 5Ω

The inductor current overshoots transiently to feed the load and settles to a value greater than the previous value. There is a dip in the output voltage. In the absence of any controller, the output voltage settles to a value less than the previous value of voltage i.e. 3.69V . Fig 2.12 and Fig 2.13 shows the response of the converter in terms of output voltage and inductor current respectively, for the load rejection i.e. load resistance is increased from 10 ohms to 15 ohms with the differential equation model and the averaged equivalent model of the converter. The inductor current undershoots and settles to a value less than the previous one. The output voltage has an overshoot and its steady state value is greater than that of at $R=10$ ohms. Fig 2.14 and Fig 2.15 shows the response of both the models to a load rejection of 10 ohms to 20 ohms. The constant part of the inductor current corresponds to the discontinuous conduction of the converter. As the load is rejected more, the converter remains in discontinuous conduction for more number of cycles. This can be seen by a load rejection of 10 ohms to 30 ohms in Fig 2.16 and Fig 2.17.

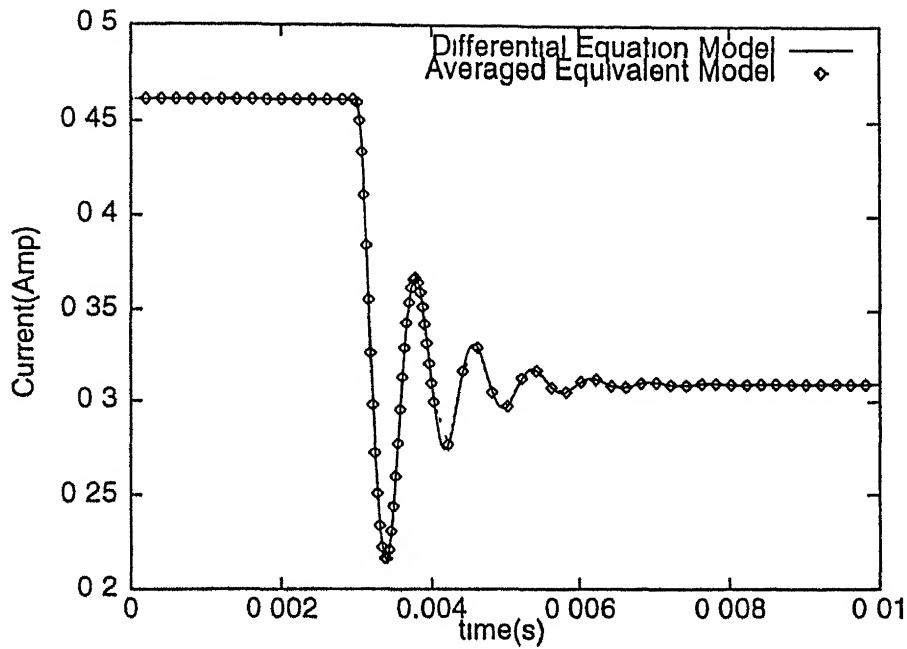


Figure 2.12 Average Inductor Current For a Change in Load Resistance From 10Ω to 15Ω

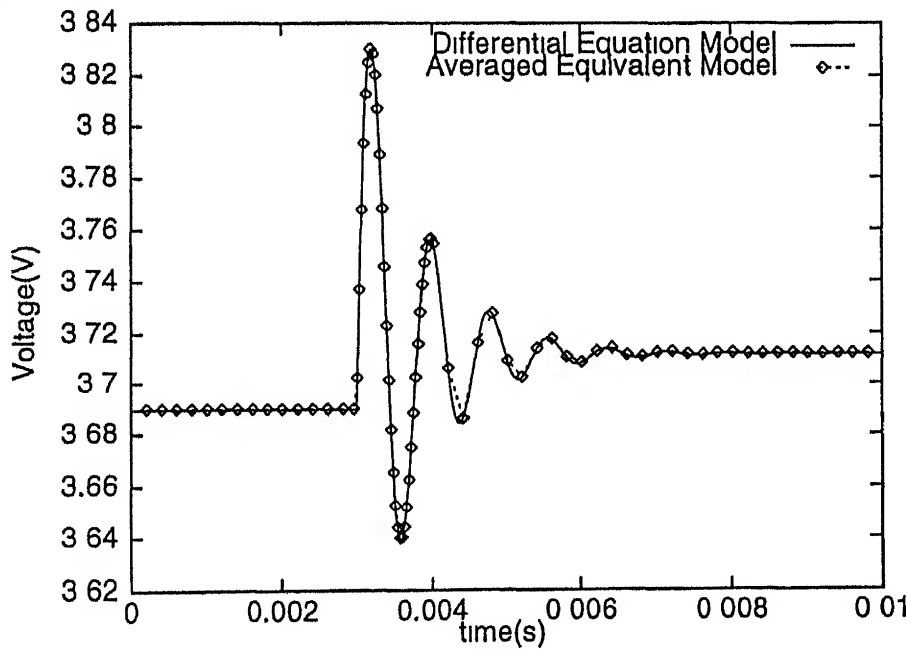


Figure 2.13 Average Output Voltage For a Change in Load Resistance From 10Ω to 15Ω

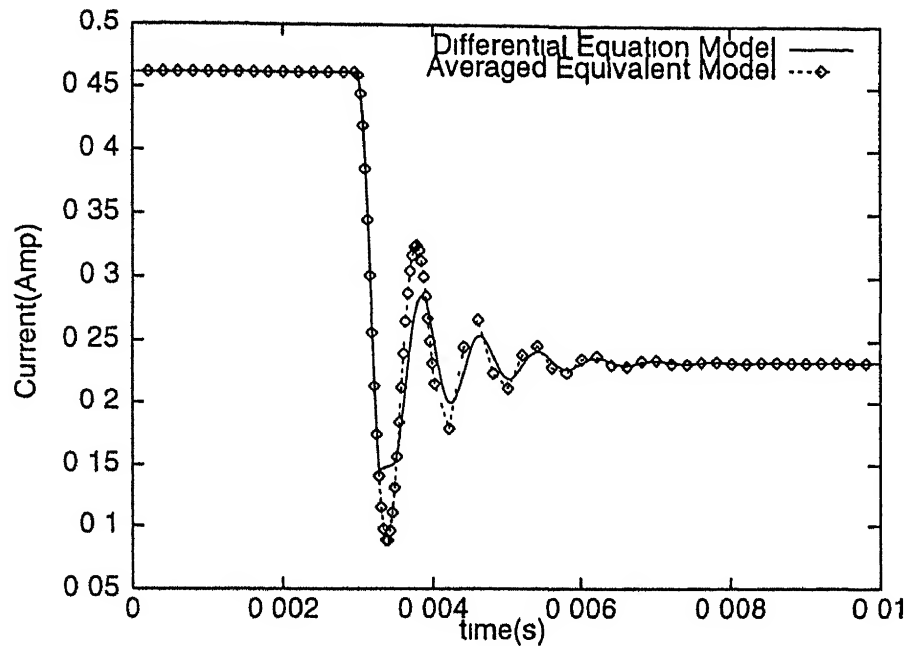


Figure 2 14. Average Inductor Current For a Change in Load Resistance From 10Ω to 20Ω

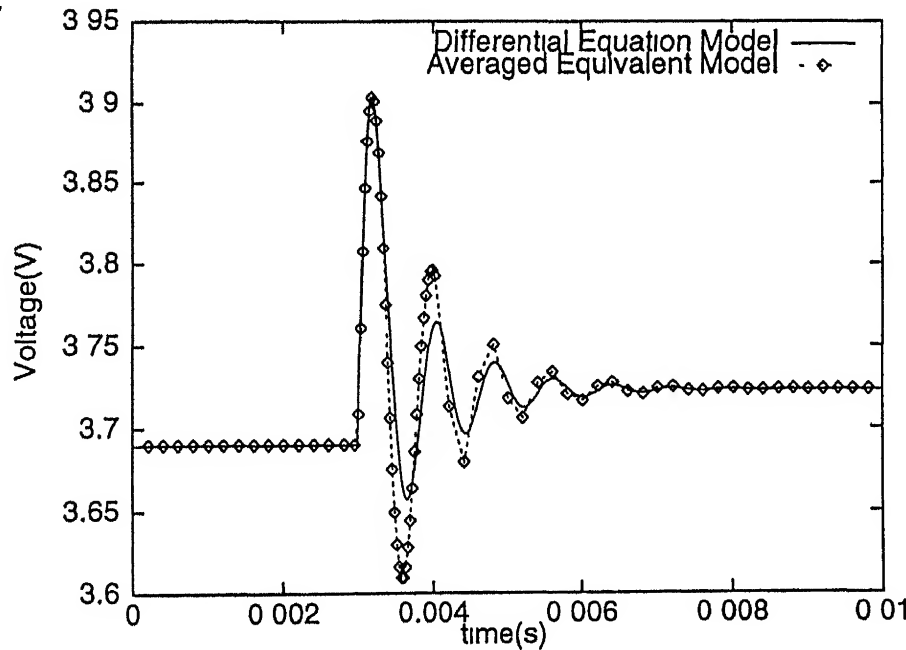


Figure 2 15 Average Output Voltage For a Change in Load Resistance From 10Ω to 20Ω

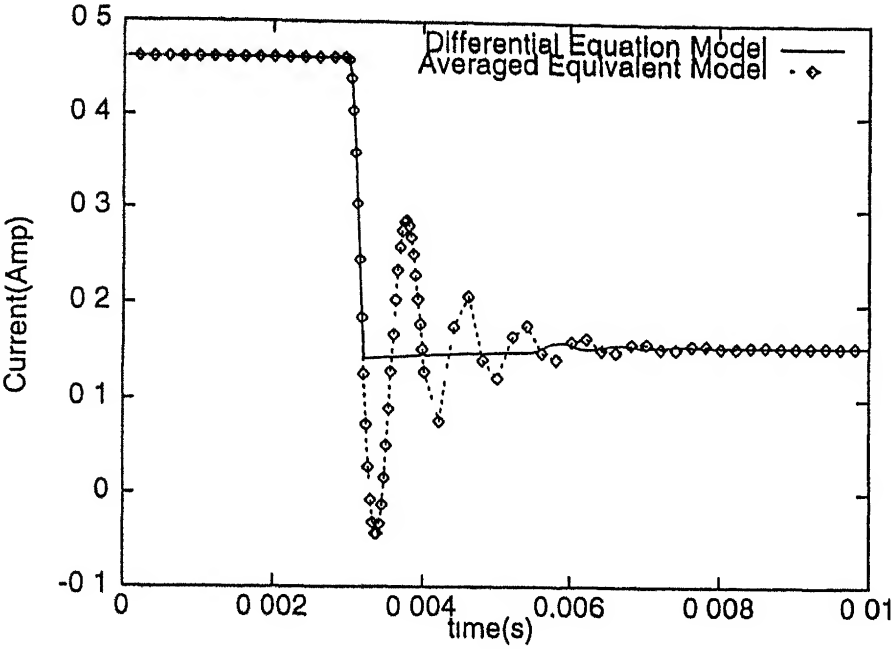


Figure 2.16 Average Inductor Current For a Change in Load Resistance From 10Ω to 30Ω

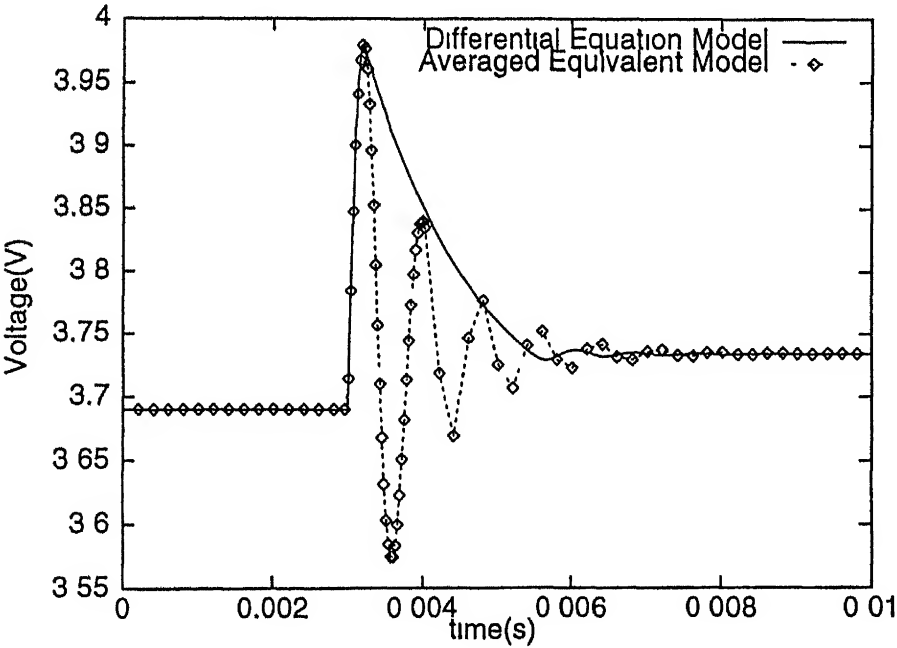


Figure 2.17. Average Output Voltage For a Change in Load Resistance From 10Ω to 30Ω

2.3 Effect of Step Change in Duty Cycle

In the absence of any controller the converter output voltage is decided by the duty factor D . The approximate value of the output voltage is given by,

$$V_o = \frac{DV_{dc}}{(1-D)}$$

Fig 2.18 and Fig 2.19 shows the response of the differential equation model and averaged equivalent circuit model to a change in D from 0.2 to 0.4. The response

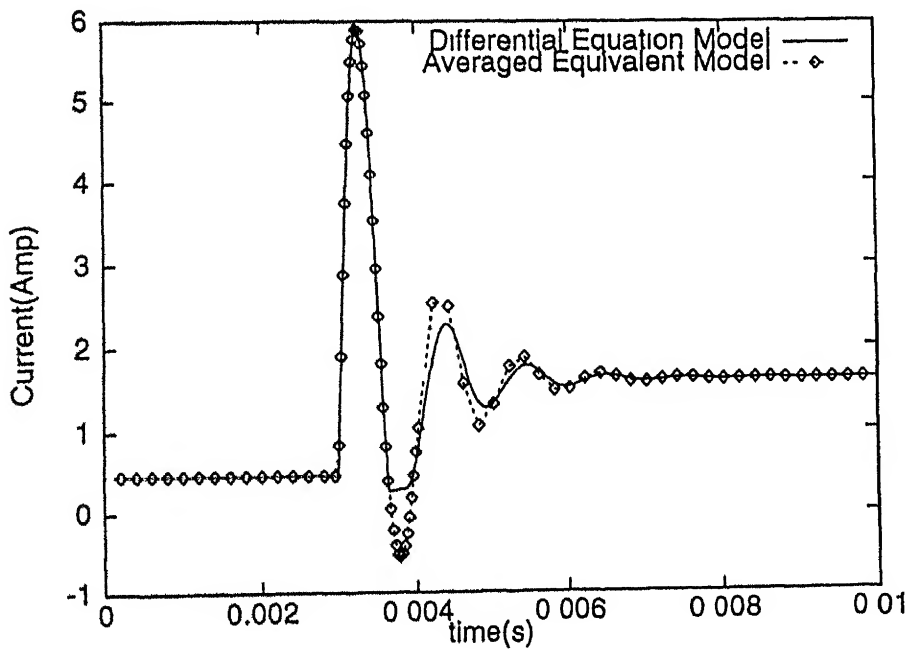


Figure 2.18 Average Inductor Current For a Change in Duty Cycle D From 0.2 to 0.4

due to change in duty cycle D from 0.2 to 0.25 is shown in Fig 2.20 and Fig 2.21.

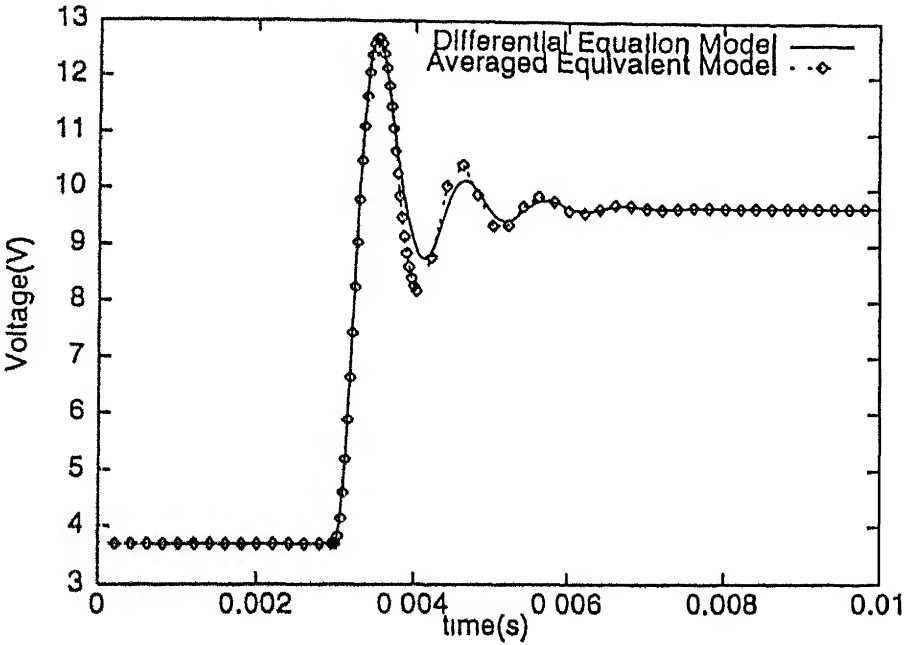


Figure 2.19. Average Output Voltage For a Change in Duty Cycle D From 0.2 to 0.4

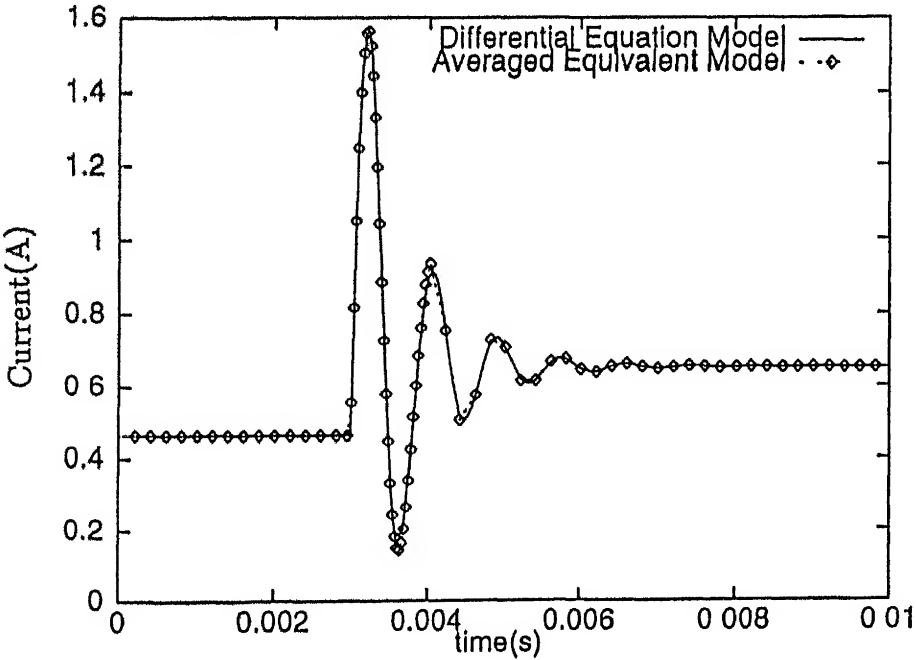


Figure 2.20. Average Inductor Current For a Change in Duty Cycle D From 0.2 to 0.4

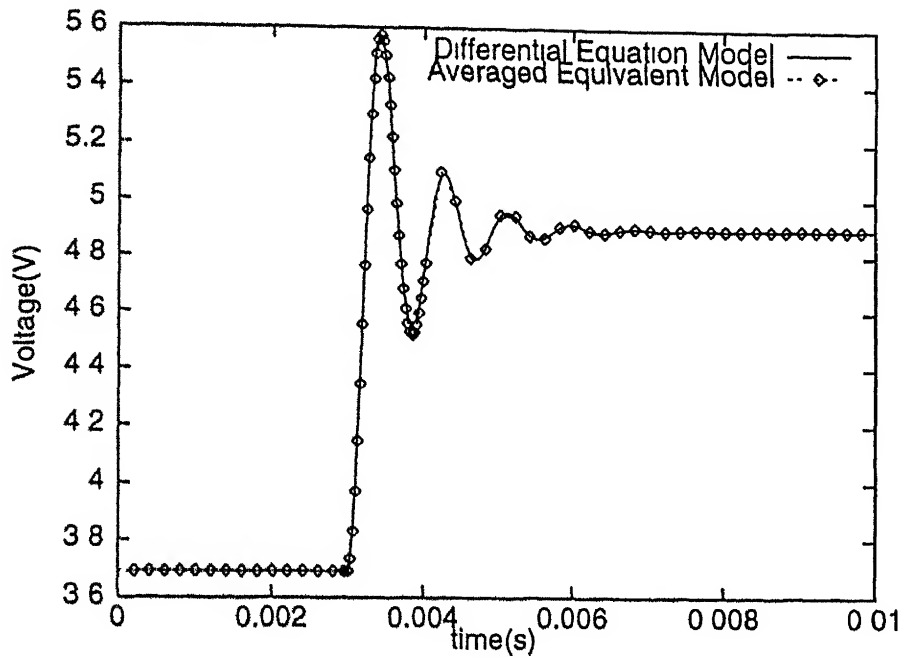


Figure 2.21. Average Output Voltage For a Change in Duty Cycle D From 0.2 to 0.25

The voltage oscillates with its natural frequency and then settles down to a steady state value. The converter enters into discontinuous conduction mode for $D=0.4$. For $D=0.25$, the converter remains in discontinuous conduction mode for less time. The averaged equivalent model does not show the discontinuous behaviour of the converter

2.4 Conclusions

In this chapter the converter models based on following are given

- State space differential equations
- Averaged state space equations and equivalent circuits based on them
- Small signal model and transfer functions based on state space averaging

The results of averaging have been compared with the differential equation model. The average equivalent model is a good approximation of the differential equation model at a frequency as high as 100 kHz. For continuous conduction mode the response from the two models is exactly the same. But the average equivalent model cannot predict the discontinuous conduction of the converter. In the differential equation model the average inductor current becomes almost constant in discontinuous conduction mode but in the average equivalent model the variation is smooth, damped sinusoid. From Fig 2.16 it can be concluded that if the inductor current is negative or zero then the converter must be in discontinuous conduction mode but the converse is not always true.

Using the differential equation model, a sinusoidal perturbation in D & u has been added to their respective d.c. values one at a time. The results of deviations in the output voltage has been determined. This is compared with the values obtained from the transfer function given by equation 2.13 & 2.14 and equation and the corresponding Bode plots shown in Fig 2.6 and Fig 2.8. The results of comparison have been given in Table 2.1 and Table 2.2. There is a close agreement between these values. In the 5 kHz to 10 kHz range of signal frequencies, there is deviation in the values of phase shift in case of \hat{V}_c/\hat{d} . In the case of \hat{V}_c/\hat{u} there is deviation in the value of gain at corner frequency. These errors are due to stepped approximation of the ac input perturbation in the differential model and due to linearisation in the small signal model.

Chapter 3

Fuzzy Logic Controller

In this chapter the fuzzy logic controller (FLC), its equivalence with linear PI controller and some simple fuzzy logic controllers have been discussed. The building blocks of the Fuzzy Logic Controller are explained in Section 3.1. Section 3.2 establishes the equivalence between a linear PI controller and a 3 zone Fuzzy Logic Controller. Section 3.3 and onwards, a 5 zone membership function has been used for fuzzification. A simple integral controller with 5 zone membership function for error (e) is discussed in Section 3.4. In Section 3.5 a simple proportional controller with 5 zone membership function for change of error (ce) is discussed. Integral control with adjustable weights is discussed in Section 3.6. Response of a linear PI controller, a 3 zone FLC, a 5 zone FLC are given in Section 3.7. Section 3.8 compares the responses at switching frequency of 20 kHz and 100 kHz.

3.1 Description of Fuzzy Logic Controller

The block diagram of fuzzy logic controller is shown in Fig 3.1. Different blocks of controller are described below.

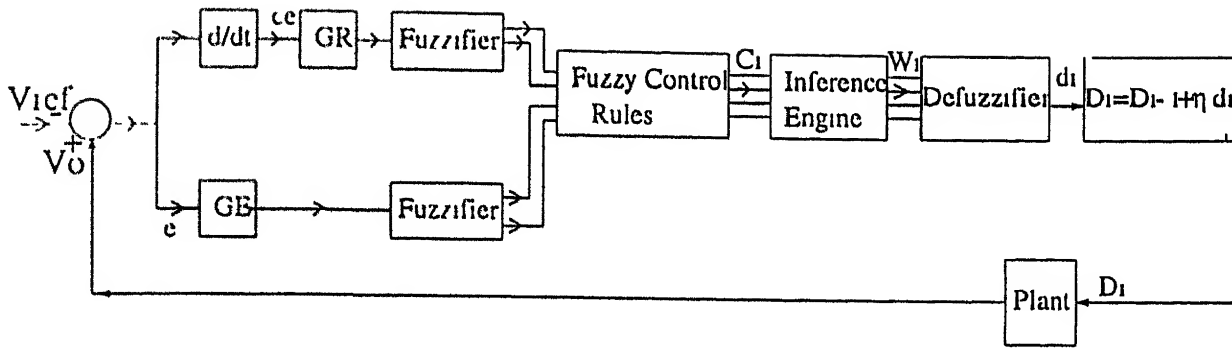


Figure 3.1 Block Diagram of Fuzzy Logic Controller

3.1.1 Fuzzifier

The inputs to the fuzzy logic controller are the error e and rate of change of error ce . These are defined as

$$e = V_o - V_{ref} \quad (3.1)$$

$$ce = e_i - e_{i-1} \quad (3.2)$$

where V_o = output voltage of the converter

V_{ref} = reference voltage of the converter

The symbol i is the suffix denoting the present sampling instant

The values of e and ce are scaled by gains GE & GR respectively to match the range of inputs used by the fuzzifier. Both fuzzifiers are described by the input-output characteristics given in Fig 3.2. The input-output characteristics of the fuzzifier consists of three piecewise linear curves called "Membership Functions". These are shown as N, Z & P in Fig 3.2. These correspond to the classification of input as Negative, Zero and Positive respectively. The fuzzifier assigns two values of the output $\mu_A(x)$ and $\mu_B(x)$ i.e. membership functions to each value of the input x . If input is greater than or equal to L or, less than or equal to $-L$ or, zero these values go to 0 & 1. If the input is between $-L$ & L , the membership functions have values between 0 & 1. Due to linear nature of curves the sum of the two values of membership functions is always unity i.e. $\mu_A(x) + \mu_B(x) = 1$, for all x .

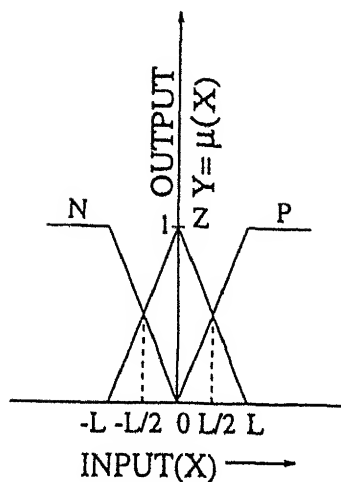


Figure 3.2: Membership Function for 3 Zone FLC

The notion of fuzzification implies that each input may belong to more than one category with a specific value of the membership function. In the fuzzifier shown in Fig 3.1 an input value is classified as Negative, Zero or Positive with membership function values equal to those given by the respective N & Z or P & Z curves. For large values i.e. magnitude greater than L, the membership function for Zero, curve Z is zero.

3.1.2 Fuzzy Control Rules:

A control rule relates the category of inputs to the output C_i . It is of the form: If e_i is A_i and ce_i is B_i , then output is C_i . In above A_i and B_i may each be P, Z or N. Since there are 3 categories of e and 3 categories of ce , therefore total of $3 \times 3 = 9$ rules must be enumerated. These are usually expressed in the form of a control rule table as shown below in Table 3.1. The table given below gives the values of C_i for each of the nine possible combinations of e_i and ce_i . The zero entries in the table indicate that the converter output voltage is approaching the set point and therefore no control action is required. The positive entries indicate that the converter output voltage is below the set point. So a positive control action is required in order to increase the output. The entries are negative in the table when the output is above

Table 3.1 Rule Table showing C_i For Different Categories of e_i & ce_i

		ce		
		P	Z	N
e	P	-Lo	-Lo	0
	Z	-Lo	0	Lo
	N	0	Lo	Lo

the set point, so a negative control action is required. For any given value of e and ce there are two categories to which it belongs with two values of μ ie. $\mu_A(e_i)$ & $\mu_B(e_i)$. Similarly for ce . Therefore there are 4 control rules operative for any combination of e_i and ce_i out of possible 9 shown in Table 3.1 above.

3.1.3 Fuzzy Inference:

The fuzzy inference method used is the 'Mamdani's Minimum Fuzzy Implication' which selects a weight factor for C_i and gives a weighted output W_i given by

$$W_{ik} = \min(\mu_A(e_i), \mu_B(ce_i))C_{ik} = \mu_{ik}C_{ik} \quad (3.3)$$

In above equation k varies from 1 to 4 to cover the 4 combinations of $\mu(e)$ and $\mu(ce)$ which have two values each.

3.1.4 Defuzzification:

A nonlinear defuzzification algorithm called 'centre of gravity' method is used. The defuzzifier produces a single crisp value of the output from the multiple weighted values produced by the inference engine. The control action d_i is inferred by

$$d_i = \frac{\sum_{k=1}^4 \mu_{ik}C_{ik}}{\sum_{k=1}^4 \mu_{ik}} \quad (3.4)$$

3.1.5 Calculation Of D_i :

The duty cycle of converter is defined as $D_i = D_{i-1} + \eta d_i$

where η is the gain factor of the fuzzy controller

3.2 Equivalent Gains of the Fuzzy Logic Controller

The membership function for the curves P, Z & N in X-Y plane are given as

$$\text{Curve P} \cdot \mu_P(x) = \frac{|X|}{L} \quad (3.5)$$

$$\text{Curve Z} \cdot \mu_Z(x) = 1 - \frac{|X|}{L} \quad (3.6)$$

$$\text{Curve N} \cdot \mu_N(x) = \frac{|X|}{L} \quad (3.7)$$

in the range $-L \leq X \leq L$. The curves P & N saturate at 1 and curve Z falls to zero outside the above range. For every inference corresponding to a pair of e_i & ce_i , the weighting factors μ_i ($i=1-4$) are chosen on the basis of relative values of $\mu_A(e_i)$ & $\mu_B(ce_i)$. But these depend upon the relative values of scaled error and scaled change of error. Therefore e-ce plane is divided into zones as shown in Fig 3.3. In the first quadrant each variable can be divided into two ranges $0 - L/2$ and $L/2 - L$. This gives 4 large regions. These are subdivided further into 2 zones each by straight lines of slope -1 & +1 passing through the point $(L/2, L/2)$. Each quadrant of e-ce plane can be similarly divided into 8 zones. These are shown in Fig 3.3. The division allows us to predict μ_i the minimum between $\mu_A(e_i)$ & $\mu_B(ce_i)$ stated in equation (3.3) for W_i . Therefore analytical expressions for μ_i are calculated. These are used to calculate d_i . An example for Region 1 is given below

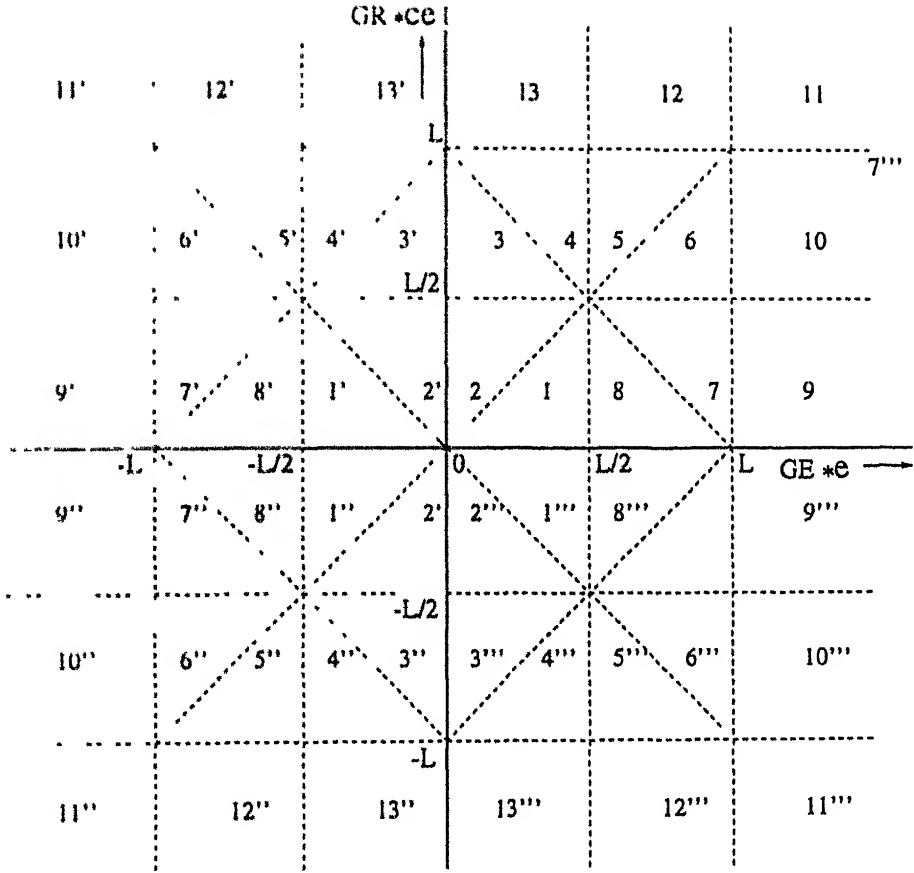


Figure 3.3: Division of e-ce Plane Into Zones For Calculation of K_i & K_p

3.2.1 Region 1:

In this region $e > ce$ and both the inputs are in the category P & Z (equation (3.5) & (3.6)). The possible combinations of e & ce are given in Table 3.2

Therefore according to equation (3.4) d_i is given by

$$d_i = \frac{(-GE|e| - 2GR|ce|)Lo}{(2GR|ce|) + L}$$

Table 3.2 Combinations of e & ce

e	ce	μ_{ik}	output(C_{ik})
Z	Z	$\mu_Z(e)$	0
P	P	$\mu_P(ce)$	-Lo
Z	P	$\mu_P(ce)$	-Lo
P	Z	$\mu_P(e)$	-Lo

In this region $e > 0$, $ce > 0$, therefore $|e| = e$, $|ce| = ce$. Comparing this equation with conventional PI controller

$$d_i = -(K_i e + K_p ce)$$

$$K_i = \frac{LoGE}{(2|ce|GR) + L}$$

$$K_p = \frac{2LoGR}{(2|ce|GR) + L}$$

The equivalent constants for other regions are given in Table 3.3. For ranges greater than or equal to L and less than or equal to -L the membership function becomes 0 & 1 and effectively the number of control rules are two. The control action d_i for this range is given in Table 3.4

Table 3.3 Equivalent Gains for Fuzzy Controller

REGION	K_i	K_p
1,1'',8,8''	$\frac{LoGE}{(2GR ce)+L}$	$\frac{2LoGR}{(2GR ce)+L}$
2,2'',3,3''	$\frac{2LoGE}{(2GE e)+L}$	$\frac{LoGR}{(2GE e)+L}$
4,4'',5,5''	0	$\frac{Lo(GR-\frac{2L}{ce})}{(2GR ce)-3L}$
6,6'',7,7''	$\frac{Lo(GE-\frac{2L}{e})}{(2GE e)-3L}$	0
1',1''',8',8'''	$\frac{LoGE}{(2GR ce)+L}$	$\frac{2LoGR}{(2GR ce)+L}$
2',2''',3',3'''	$\frac{2LoGE}{(2GE e)+L}$	$\frac{LoGR}{(2GE e)+L}$
4',4''',5',5'''	$\frac{LoGE}{3L-(2GR ce)}$	$\frac{LoGR}{3L-(2GR ce)}$
6',6''',7',7'''	$\frac{LoGE}{3L-(2GE e)}$	$\frac{LoGR}{3L-(2GE e)}$

Table 3.4. Control Action For Boundary Regions

REGION	CONTROL ACTION(d_i)
9,10,11,12,13	$-L_o$
9'	d_{i1}
10'	d_{i1}
11'	0
12'	$-d_{i2}$
13'	$-d_{i2}$
9'',10'',11'',12'',13''	L_o
9'''	$-d_{i1}$
10'''	$-d_{i1}$
11'''	0
12'''	$-d_{i2}$
13'''	$-d_{i2}$

where

$$d_{i1} = \frac{Lo(L - GR|ce|)}{L}$$

$$d_{i2} = \frac{Lo(L - GE|e|)}{L}$$

The above given gains are equal for quadrant 1 & 3 and quadrant 2 & 4, if e and ce both lie in the range $0 < |e|(|ce|) < L$. There are 4 gains for each quadrants of 8 regions. We have taken 2 ranges of e and ce and the number of gains are 8. For n ranges the number of gains will be $2n^2$. Moreover, the number of gains are independent of the levels of output. The change in output level only affects the value of gains. As seen from the Table 3.3 & 3.4, the gains are functions of e & ce . Therefore the fuzzy logic controller is a nonlinear controller.

3.3 5 Zone Fuzzy Logic Controller

A more complex controller can be achieved by the classification of e and ce in 5 zones. Positive Big, Positive Small, Zero, Negative Small, Negative Big called as PB, PS, Z, NS, NB respectively with 50% overlap. The membership function for 5 zones is shown in Fig 3.4. As the number of membership function increases the

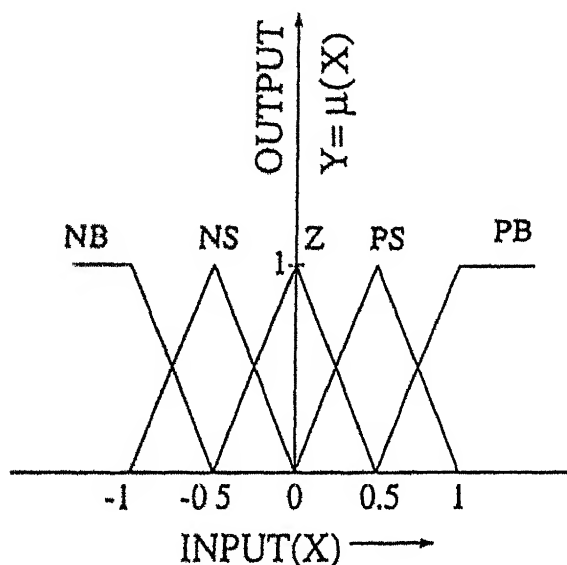


Figure 3.4: Membership Function For 5 Zone FLC

response becomes better and smooth. In the following sections 5 zone membership function has been used for different controllers. The flow chart for fuzzification is given Fig 3.5. Fig 3.6 shows the flow chart for simulation of the Buck-Boost converter using the fuzzy logic controller for the output voltage regulation.

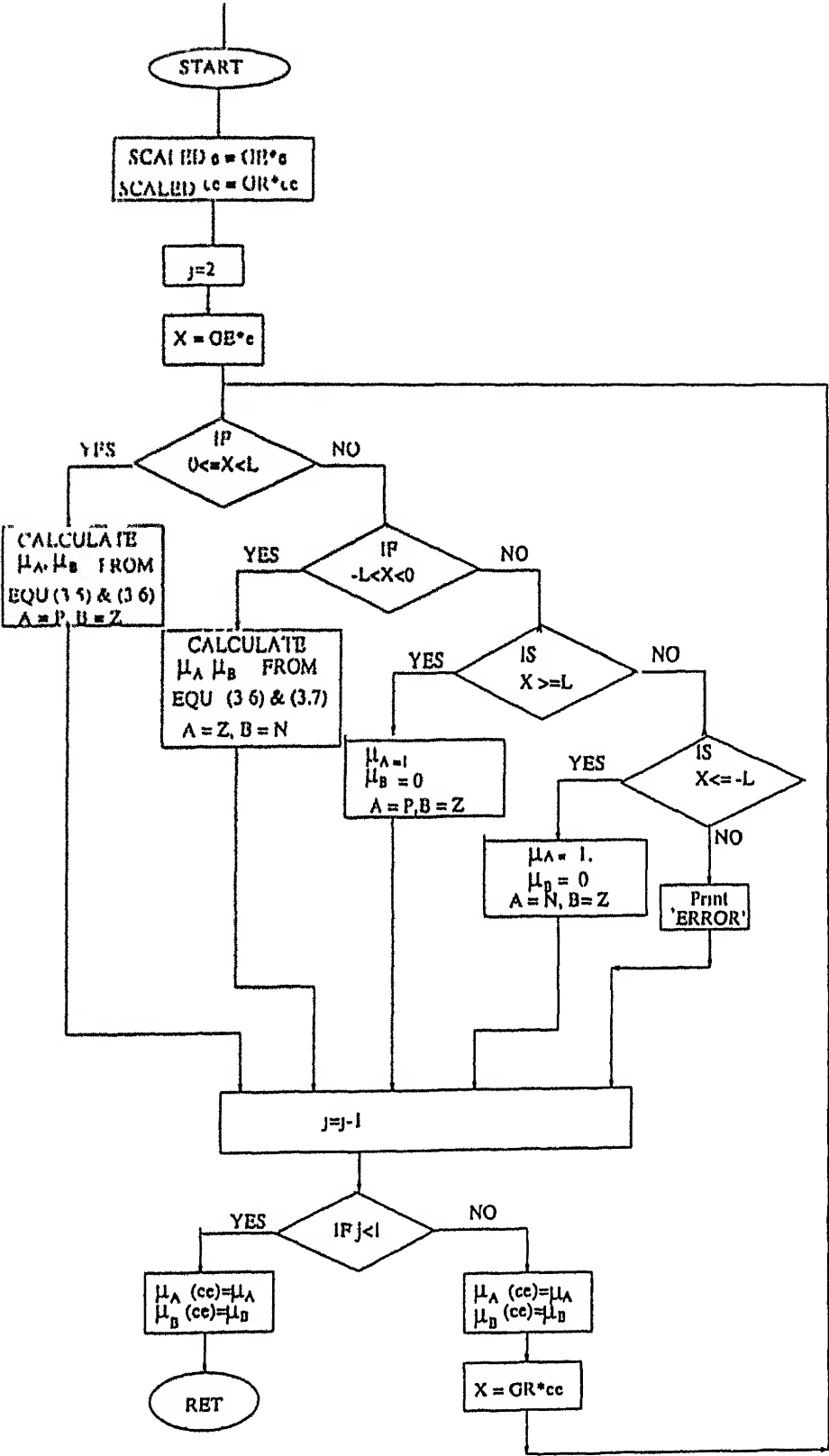


Figure 3.5: Fuzzification Routine for 3 zone FLC

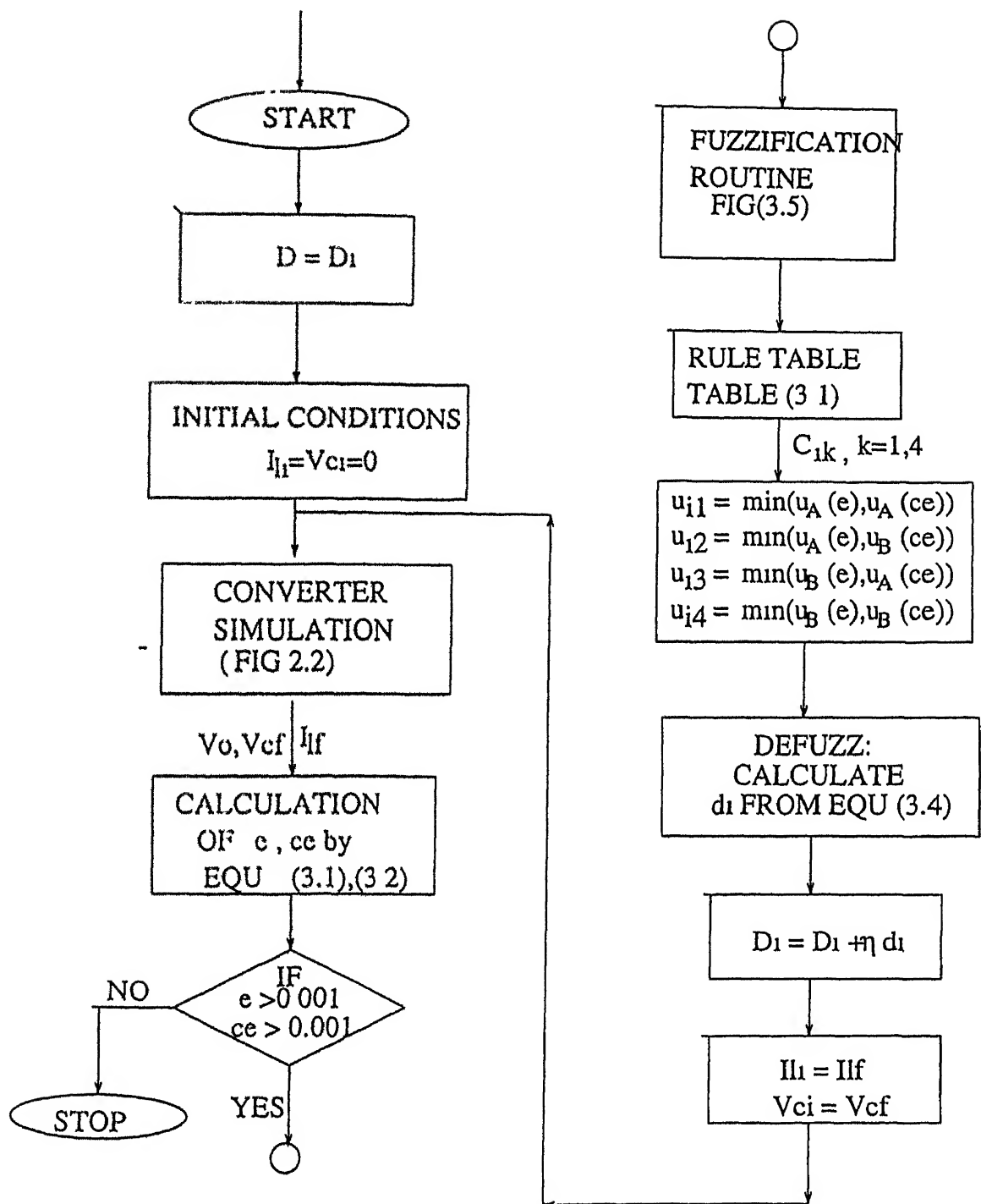


Figure 3.6 Flow Chart For Simulation

3.4 A Simple Integral Controller

Integral control action using fuzzy logic can be obtained by taking into consideration only error at every sampling instant. The value of controller output D_i is the cumulative addition of controller outputs d_i after every sampling instant which is proportional to the error. This results into integral action.

$$D_i = D_{i-1} + d_i$$

$$d_i = K_i c_i$$

where D_i =controller output

c_i =error at i^{th} sampling instant

K_i =gain constant

$$D_i = \sum_i K_i e_i$$

In the steady state e_i is driven to the value zero and d_i is zero.

Five zone membership functions for error is chosen according to the Fig 3.4. The control rules are given below.

- R1 : if c_i is PB then C_i is NB.
- R2 : if c_i is PS then C_i is NS
- R3 : if c_i is ZE then C_i is Z.
- R4 : if c_i is NS then C_i is PS
- R5 : if c_i is NB then C_i is PB

where C_i is the singleton output given by $a_2, a_1, a_0, -a_1, -a_2$ for NB, NS, Z, PS and PB respectively. The fuzzy rule table is given in Table 3.5

Integral control action using fuzzy logic control is performed on a Buck-Boost converter for different values of gain constants. The simulation results for different values of control action is shown in Fig 3.7.

Table 3.5 Rule Table For Integral Control

e_i	C_i
NB	a_2
NS	a_1
Z	a_0
PS	$-a_1$
PB	$-a_2$

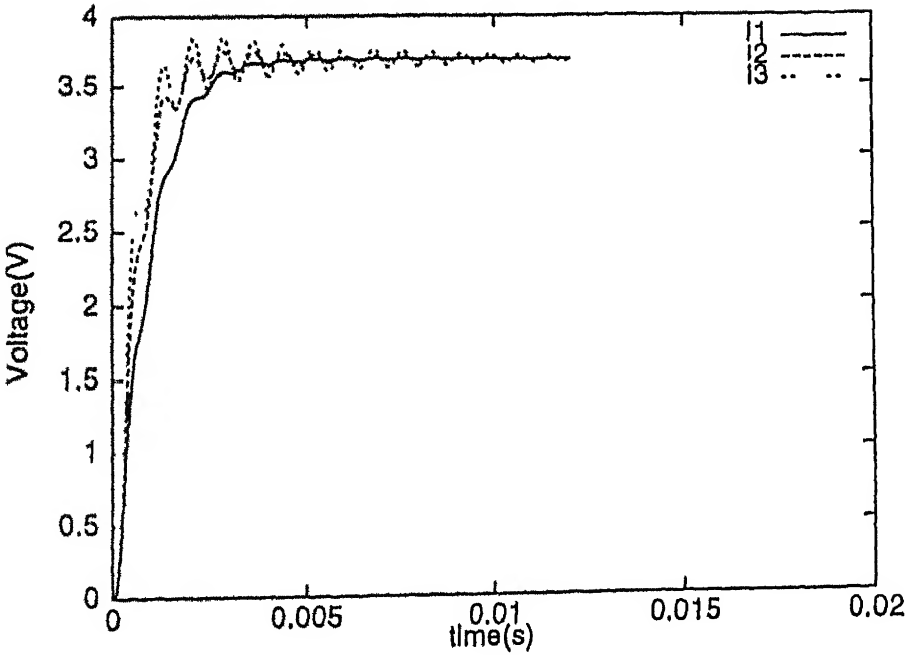


Figure 3.7: Integral Control

- For controller I1 $a_0=0$, $a_1=0.15$, $a_2=0.25$.
- For controller I2 $a_0=0$, $a_1=0.22$, $a_2=0.30$
- For controller I3 $a_0=0$, $a_1=0.25$, $a_2=0.40$.

It is observed that there are oscillations at high gain, where as the system stabilizes at lower values of gain.

3.5 A Simple Proportional Controller

Fuzzy logic control taking into consideration only change of error (ce) results into a "P" type controller. If N is the number of samples then

$$e_i = e_1 + (e_2 - e_1) + (e_3 - e_2) + \dots - (e_i - e_{i-1}) + \dots$$

The fuzzy control action will be given by

$$D_i = D_{i-1} + d_i, \quad d_i = K_p(ce_i)$$

The magnitude of controller output is proportional to magnitude of ce and sign of controller output is opposite to the sign of e_i . The membership function for ce is shown in Fig 3.4. The fuzzy control rules are given below.

- R1 if $|ce_i|$ is PB then $|C_i|$ is B.
- R2 if $|ce_i|$ is PS then $|C_i|$ is S
- R3 if $|ce_i|$ is ZE then $|C_i|$ is Z

where $|C_i|$ is the singleton output given by a_2 , a_1 , a_0 for B, S and Z respectively. The fuzzy rule table is given in Table 3.6. Proportional control action using fuzzy logic control is performed on a Buck-Boost converter for a value of gain constants. Simulation results for this controller for different values of gain is shown in Fig 3.8.

- For controller P1 $a_0=0$, $a_1=0.4$, $a_2=1$
- For controller P2 $a_0=0$, $a_1=0.45$, $a_2=1$

Table 3 6 Rule Table For Proportional Control

ce_i	C_i
PB	a_2
PS	a_1
Z	a_0

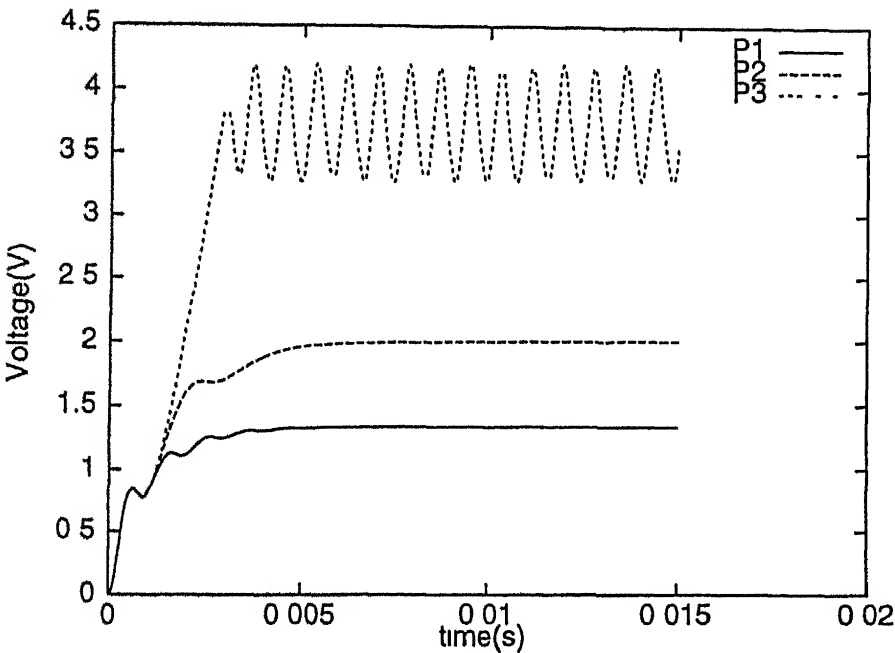


Figure 3 8 Proportional Control

- For controller P3 $a_0=0$, $a_1=0.5$, $a_2=1$

It has been seen from the simulation results that there is a steady state error for lower values of gain. As the values of gain is increased the steady state error decreases. A limit is reached when increasing the gain makes the system unstable.

3.6 Integral Control With Adjustable Weights

This control action is modified form of the integral control action given above. The change of error i.e. ce is divided into 3 zones according to the magnitude. So instead of one column of output C_i , there are 3 columns. Therefore only two rules are selected for control action at every sampling instant. The ranges of ce are as given below.

Z: $0 < |ce| < 0.25$

S: $0.25 < |ce| < 0.75$

B: $|ce| > 0.75$

The membership function for e is same as shown in Fig 3.4. The fuzzy rule table is given in Table 3.7.

Table 3.7 Rule Table For Integral Control With Adjustable Gains

		ce		
		Z	S	B
e	PB	$-a_1$	$-a_2$	$-a_3$
	PS	$-a_4$	$-a_5$	$-a_6$
	Z	a_0	a_0	a_0
	NS	a_4	a_5	a_6
	NB	a_1	a_2	a_3

The simulation result on a Buck-Boost converter is shown in Fig 3.9.

- For controller PI1 $a_0=0, a_1=0.10, a_2=0.15, a_3=0.30, a_4=0.05, a_5=0.08, a_6=0.15$
- For controller PI2 $a_0=0, a_1=0.10, a_2=0.20, a_3=0.35, a_4=0.06, a_5=0.10, a_6=0.18$
- For controller PI3 $a_0=0, a_1=0.1, a_2=0.25, a_3=0.45, a_4=0.08, a_5=0.15, a_6=0.25$

It has been seen from the simulation results that as the gain is increased, the response time reduces but there is a limit for increasing the gain after which the system

becomes unstable

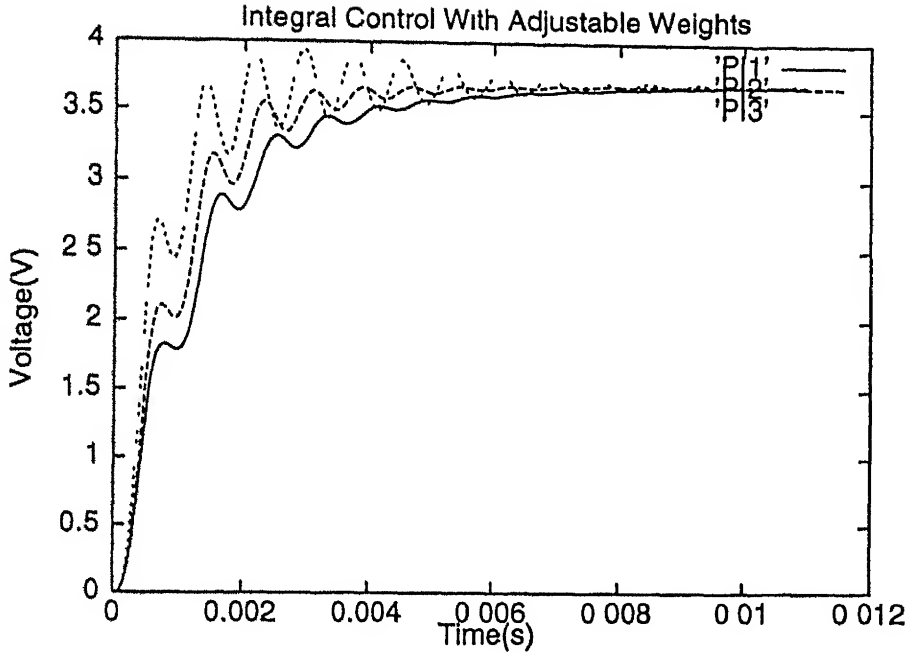


Figure 3.9 Integral Control With Adjustable Weights

3.7 A PI Controller

Fuzzy logic control taking into consideration both e and ce results in a nonlinear PI controller. Fig 3.10 shows the response of 3 zone FLC for $L_o = 0.6$, response of a linear PI controller for $K_i = 0.0003$ and $K_p = 0.012$ and of a 5 zone FLC corresponding to the constants of controller PI1 in Fig 2.11. The control rule Table for 5 zones is shown in Table 3.8. As the number of zones increases the response becomes better and smooth. The transient behaviour of the the output voltage starting from zero initial conditions with 5 zone FLC is shown in Fig 3.11

- For Controller PI1 . $a_0=0$, $a_1=0.1$, $a_2=0.2$, $a_3=0.3$, $a_4=0.35$, $a_5=0.45$, $a_6=0.5$, $a_7=0.65$, $a_8=1$
- For Controller PI2 $a_0=0$, $a_1=0.3$, $a_2=0.4$, $a_3=0.6$, $a_4=1.05$, $a_5=1.35$, $a_6=1.5$, $a_7=1.95$, $a_8=3$

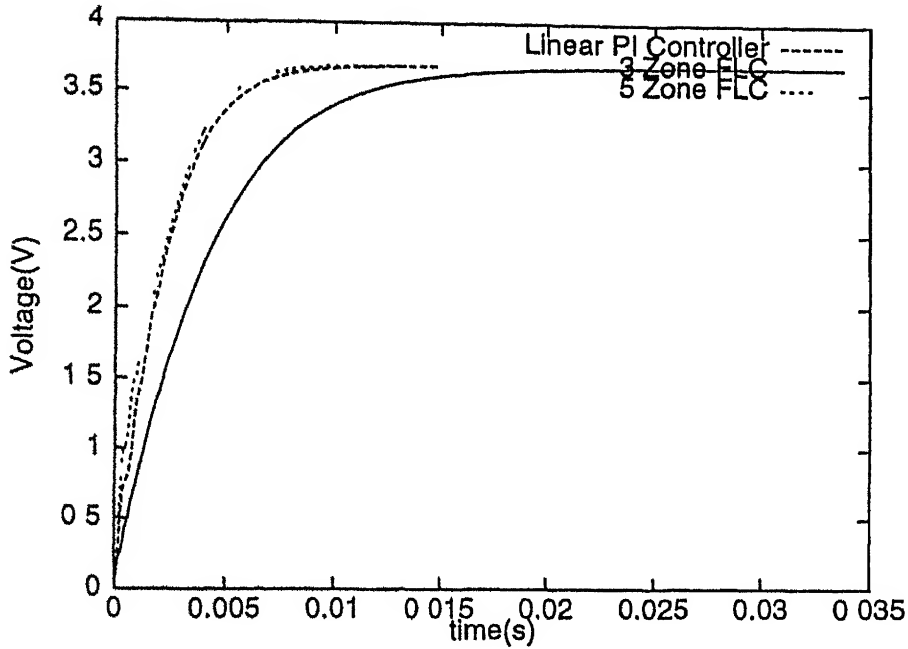


Figure 3.10 Response With 3 Zone FLC, Linear PI Controller and 5 Zone FLC

- For Controller PI3 : $a_0=0$, $a_1=0.5$, $a_2=1.0$, $a_3=1.5$, $a_4=1.75$, $a_5=2.25$, $a_6=2.5$, $a_7=3.25$, $a_8=5$.

The result shows that the system becomes unstable at high gains

3.8 Effect of Fuzzy Output on the Controller Response

The fuzzy control rule is of the form

If e_i is A_i & ce_i is B_i then output is C_i

Instead of a singleton value, C_i is also a fuzzy variable like e_i & ce_i , as shown in Fig 3.13. The corresponding crisp outputs used for comparison of controller responses equal the central values of each zone. More computations are required in the inference engine. Mamdani's minimum fuzzy implication is used to find the minimum of $\mu_A(e_i)$ and $\mu_B(ce_i)$ called μ_i as in equation (3.3). This minimum is used along with the membership function for C_i . A modified membership function for the output C_i is

Table 3.8. Rule Table For 5 Zone Fuzzy Controller

		ce				
		NB	NS	Z	PS	PB
e	PB	$-a_3$	$-a_4$	$-a_5$	$-a_7$	$-a_8$
	PS	a_0	$-a_1$	$-a_2$	$-a_4$	$-a_6$
	Z	a_2	a_1	a_0	$-a_1$	$-a_2$
	NS	a_6	a_4	a_2	a_1	a_0
	NB	a_8	a_7	a_5	a_4	a_3

calculated which saturates at μ_1 . This process is shown in Fig 3.12 [2]. There would be four such minimum operations for a value of e , and ce . μ_c is found by taking the maximum of the shaded areas of μ_{c1} , μ_{c2} , μ_{c3} & μ_{c4} . For defuzzification center of gravity of the maximum area is calculated. The Rule Tables for fuzzy output and the corresponding crisp output are given in Table 3.9 and Table 3.10. Fig 3.14 shows the response of the controller with fuzzy output and singleton output for $L_{o1} = 0.24$ and $L_o = 0.12$. The nature of the response is similar to that of with the crisp output. However the response due to fuzzy output is slightly slower than that with the crisp output.

Table 3.9. Rule Table For Crisp Output

		ce		
		P	Z	N
e	P	$-L_{o1}$	$-L_{o2}$	0
	Z	$-L_{o2}$	0	L_{o2}
	N	0	L_{o2}	L_{o1}

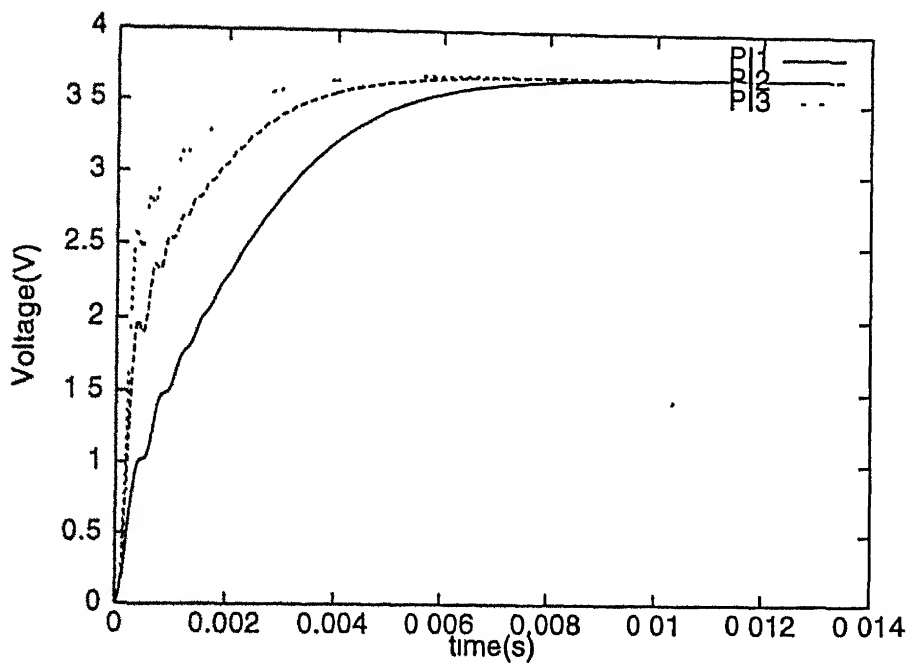


Figure 3.11 Response of 5 zone FLC

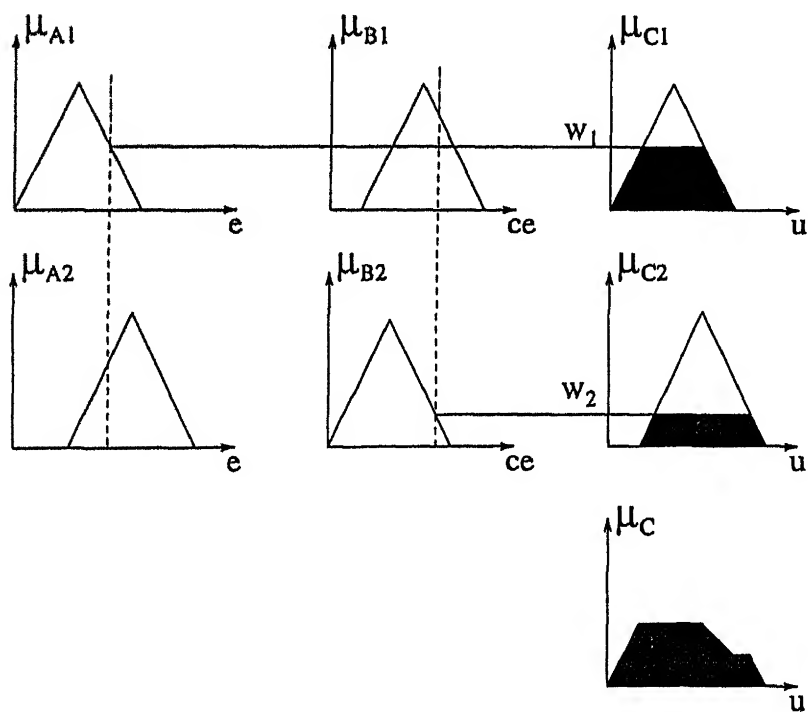


Figure 3.12: Mamdani's Minimum Operation

Table 3.10: Rule Table For Fuzzy Output
ce

e		P	Z	N
	P	NB	NS	0
	Z	NS	0	PS
	N	0	PS	PB

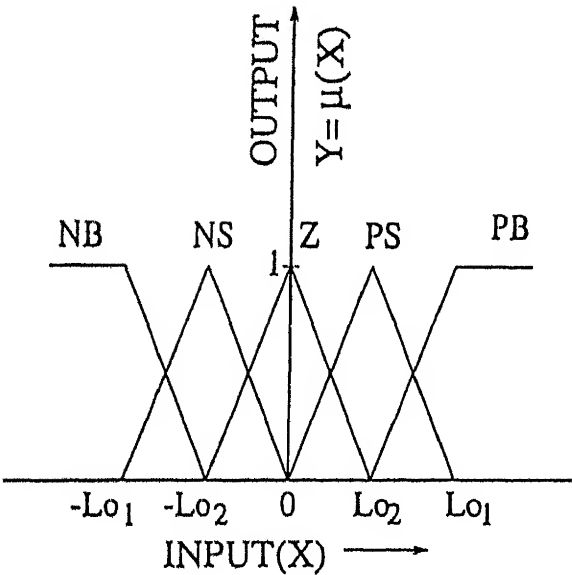


Figure 3.13: Membership Function For Output

3.9 Control Surface

The control surface of the controller describes the characteristics of the controller. This characteristics is independent of the process to be controlled. The characteristics have been drawn relating the fuzzifier inputs to the crisp control output d_c . The fuzzifier inputs are scaled error e and scaled change of error ce (which includes the factors GE & GR), ranging from -2.0 to $+2.0$. A 3-D control surface for 3 zone FLC and 5 zone FLC is shown in Fig 3.15 and Fig 3.16

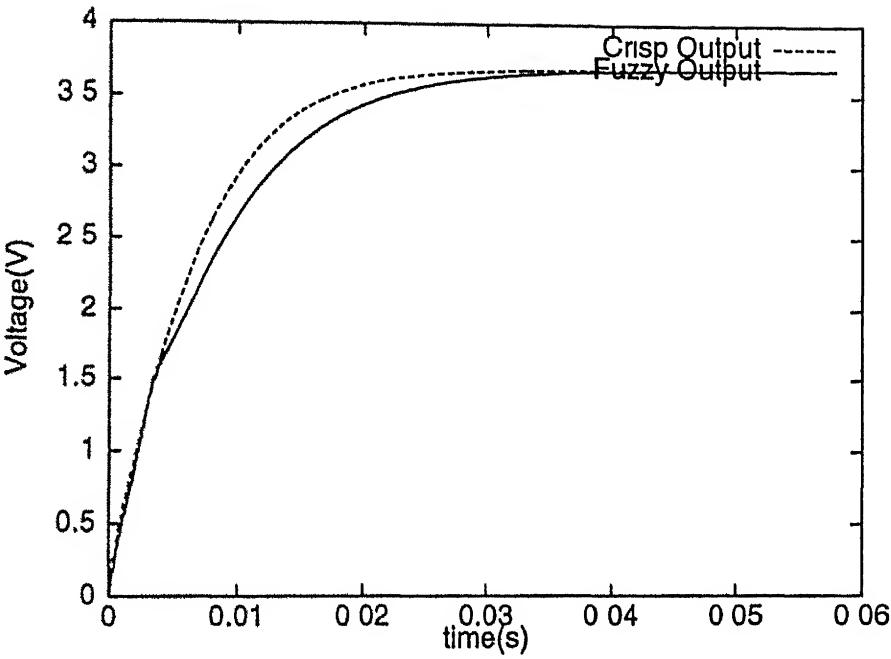


Figure 3 14: Response Due to Fuzzy Output and Crisp Output

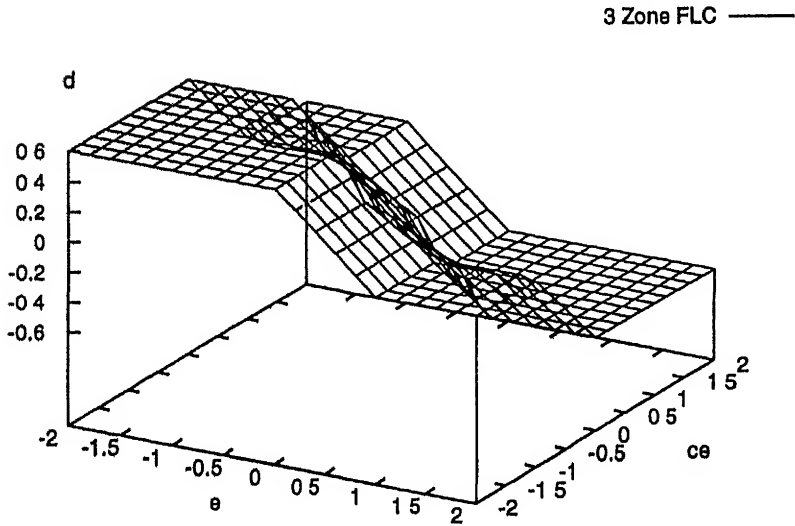


Figure 3 15 A 3-D Control Surface For 3 Zone FLC

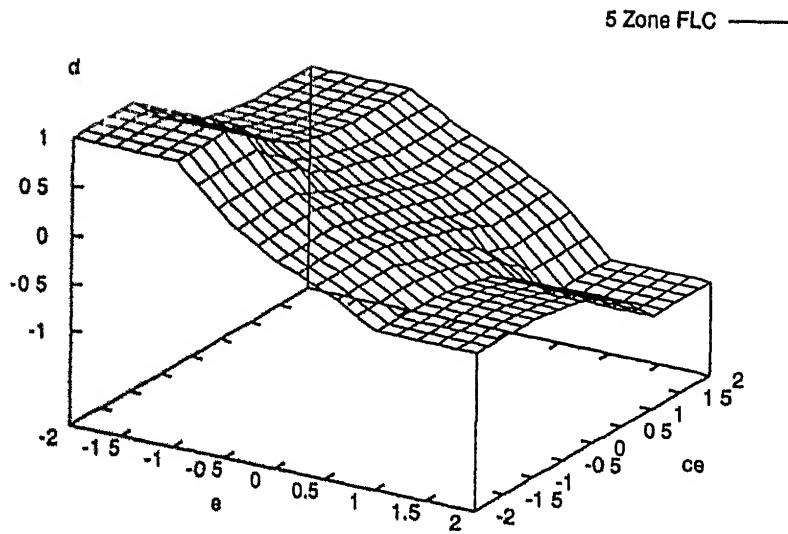


Figure 3.16: A 3-D Control Surface For 5 Zone FLC

3.10 Response at 20 kHz

The response of the controller on a converter which is operating at 20 kHz i.e. at a frequency lower than 100 kHz is shown in Fig 3.17. As the frequency is decreased the value of inductor and capacitor has to be increased. Therefore these values are set at $500\ \mu\text{H}$ and $500\ \mu\text{F}$ respectively. The response shows that the system is stable but the response time increases. As the value of the inductor and capacitor is increased the response time increases but a limit is reached when the response becomes unstable.

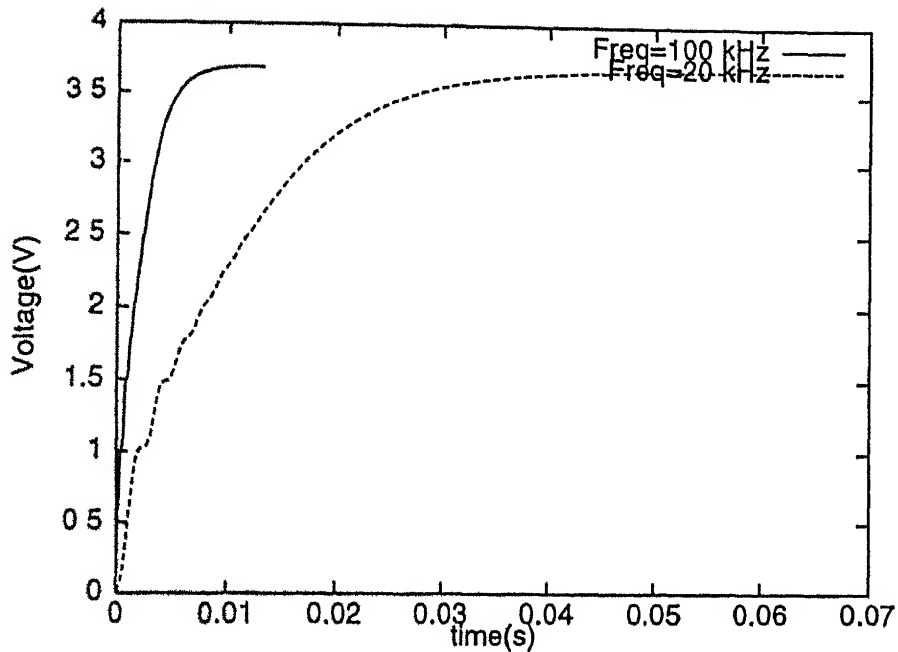


Figure 3.17: Response at 20 kHz and 100 kHz

3.11 Conclusions

In this chapter different types of controller based on fuzzy logic control are discussed. It has been seen that as the gain is increased the system becomes unstable. There is a large steady state error in case of Proportional Control. The fuzzy controller has been seen to be equivalent to a nonlinear PI controller. The expressions for these equivalent gains have been given in table 3 & 4. Simulation results show that the transient response of a linear PI controller is similar to that of a fuzzy controller. However the line and load regulation will be better with 3 zone and 5 zone fuzzy controller as this is a nonlinear controller. The transient response of a 5 zone fuzzy controller is better than that of a 3 zone fuzzy controller but more computation is required. As the value of inductor and capacitor is increased the response time increases.

Table 4 1: Rule Table For 5 Zone Fuzzy Controller

	NB	NS	Z	PS	PB
PB	$-a_3$	$-a_4$	$-a_5$	$-a_7$	$-a_8$
PS	a_0	$-a_1$	$-a_2$	$-a_4$	$-a_6$
Z	a_2	a_1	a_0	$-a_1$	$-a_2$
NS	a_6	a_4	a_2	a_1	a_0
NB	a_8	a_7	a_5	a_4	a_3

4.7. Section 4 8 gives the criterion for stopping. Dual Table Method is discussed in Section 4.9.

4.1 Performance Measure

The performance measure, measures the deviation from the path of the desired trajectory and issues appropriate changes that are required at the output of the controller.

If V_o =output voltage of the converter at any sampling instant.

V_{od} =desired output voltage at the same sampling instant.

Then the difference between the actual output and the desired output is a measure of deviation. The performance index is given by an Integral Square Error criterion

$$P.I. = \int_0^{NT} (V_o - V_{od})^2 dt$$

where NT is the total time over which error is measured and T is the converter cycle time. It is desirable to take samples of error at intervals synchronized with the converter cycle time T. Then the integral given above is modified to

$$P.I. = \sum_{i=1}^{N/k} (V_o - V_{od})^2 \cdot kT$$

where k is the number of converter cycles after which the error is measured. The term T above is the constant 100 μs cycle time of the converter and may be dropped

Therefore

$$P I = \sum_{i=1}^{N/k} (V_o - V_{od})^2 k \quad (4.1)$$

A performance measure table is shown in Table 4.2 where $\text{dev} = V_o - V_{od}$. For the

Table 4.2. Performance Measure Table

Dev	Δd
PVL	$-\Delta d_1$
PL	$-\Delta d_2$
PM	$-\Delta d_3$
PS	$-\Delta d_4$
Z	0
NS	Δd_4
NM	Δd_3
NL	Δd_2
NVL	Δd_1

results shown in this chapter, the P.I. at 18th run has been calculated for all the cases. The value of P.I. varies between 1 & 4. The effect of changing the numbers of matching points on the P.I. has been studied and results are given in Section 4.7. The deviation has been divided into 9 categories - Positive Very Large (PVL), Positive Large (PL), Positive Medium (PM), Positive Small (PS), Zero (Z), Negative Very Large (NVL), Negative Large (NL), Negative Medium (NM), Negative Small (NS). Some matchings points are chosen at which the modification to the constants of the rule table (Table 4.1) is applied. The modification in the entries of the rule table is proportional to Δd in Table 4.2. The modification in the entries of the rule table i.e. in the values of a_0 to a_8 can be done by two methods. The control action d as defined in the equation (3.4) is given by

$$d = \frac{\sum \mu_i a_i}{\sum \mu_i}$$

or

$$d = \frac{\mu_1 a'_1 + \mu_2 a'_2 + \mu_3 a'_3 + \mu_4 a'_4}{\mu_1 + \mu_2 + \mu_3 + \mu_4}$$

where a'_1 , a'_2 , a'_3 and a'_4 are any four constants of the rule table.

4.2 Method-1

This method proposes an equal contribution to the change in control output d but unequal modification in the individual constants. For a given value of deviation from the (Table 4.2) a value of Δd is chosen and the modification in the value of constant is Δa_i . The part of control action contributed by any individual constant say a_1 is given by:

$$u_1 = \frac{\mu_1 a_1}{\sum \mu_i}$$

With modified constants the control action due to a_1 i.e. u_1 is given by

$$u_1 = \frac{\mu_1 (a_1 + \Delta a_1)}{\sum \mu}$$

The change in the control action given by $\frac{\mu_1 \Delta a_1}{\sum \mu}$ produces an equal change in control output i.e

$$\frac{\mu_1 \Delta a_1}{\sum \mu} = \frac{\Delta d}{4}$$

Therefore

$$\Delta a_1 = \frac{\Delta d \sum \mu}{4 \mu_1}$$

Therefore every a_i will produce $\frac{\Delta d}{4}$.

4.3 Method-2

This method proposes an equal change in all the relevant four constants. The modified control action is given by

$$\frac{\mu_1 (a_1 + \Delta a) + \mu_2 (a_2 + \Delta a) + \mu_3 (a_3 + \Delta a) + \mu_4 (a_4 + \Delta a)}{\sum \mu_i} = d + \Delta d \quad (4.2)$$

where d is the unmodified control action given by

$$d = \frac{\mu_1 a_1 + \mu_2 a_2 + \mu_3 a_3 + \mu_4 a_4}{\sum \mu_i} \quad (4.3)$$

comparing equation (4.2) and equation (4.3) we get

$$\frac{\mu_1 \Delta a + \mu_2 \Delta a + \mu_3 \Delta a + \mu_4 \Delta a}{\sum \mu_i} = \Delta d$$

$$\frac{\Delta a \sum \mu_i}{\sum \mu_i} = \Delta d$$

Therefore

$$\Delta a = \Delta d$$

This amounts to correction proportional to $\frac{\mu_i}{\sum \mu_i}$. At the end of one run the various modified values of a particular constant is averaged and this averaged value is used in the next run. In order to make the response faster the slope of desired response and the present response is also taken into consideration. The absolute value of error in slope is also discretised as Small, Medium and Big. The scaling factor for error in slope is taken as 10.

$$ce_1 = \text{error in slope} * 10$$

According to these slopes there are three tables like Table 4.2 with increasing value of Δd .

4.4 Self Organisation to Obtain a Given Desired Response

The unmodified converter response of a five zone FLC with constants a_0 to a_8 equal to that used in controller PI1 in Section 3.7 shown in Fig 4.1. The desired response whose rise time and settling time both are less than that of the present response is also shown in Fig 4.1. The self-organising algorithm changes the constants of Table 4.2 to achieve the desired response. Method-1 & Method-2 given in Section 4.3 are used for this purpose.

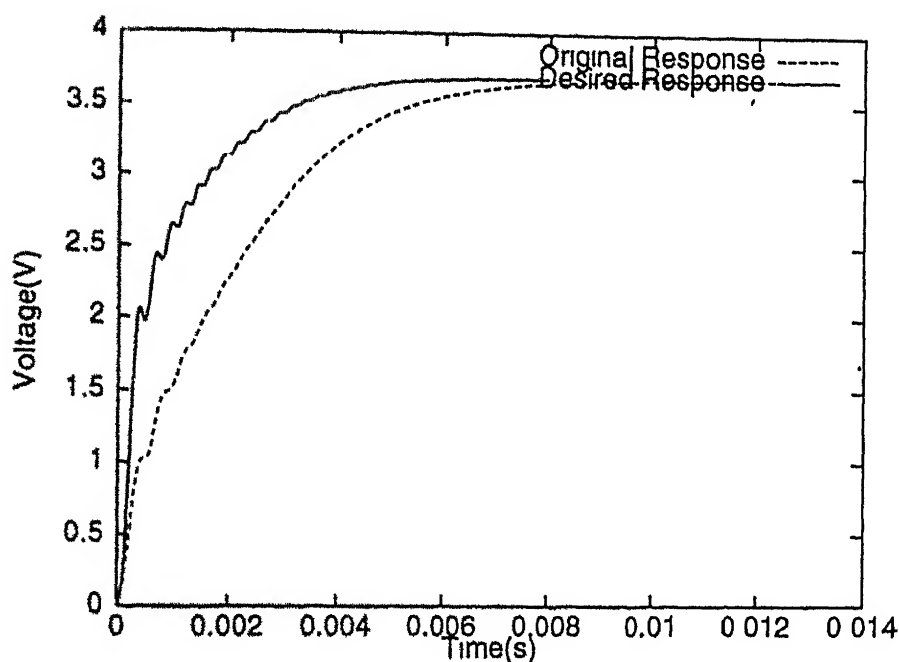


Figure 4.1 Desired Response and Response of Original 5 Zone FLC

4.4.1 Method-1

The values of Δd 's for the performance measure table are given in Table 4.3.

The constants a_0 - a_8 have their initial values according to the original response shown in Fig 4.1 for five zone FLC. Fig 4.2 shows the response with a performance table given above, the desired response and the original response of the converter. The

Table 4.3 Constants of Performance Measure Table

	$0 \leq ce_1 < 0.25$	$0.25 \leq ce_1 < 0.75$	$ce_1 \geq 0.75$
Δd_1	0.03	0.035	0.040
Δd_2	0.025	0.028	0.035
Δd_3	0.0165	0.0185	0.0195
Δd_4	0.0088	0.0128	0.0148

P.I. is 2.56 at 18th run. The average output voltage at every fifth converter cycle is taken as the matching point for measuring P.I. i.e. $k=5$ in equation (4.1). It can be

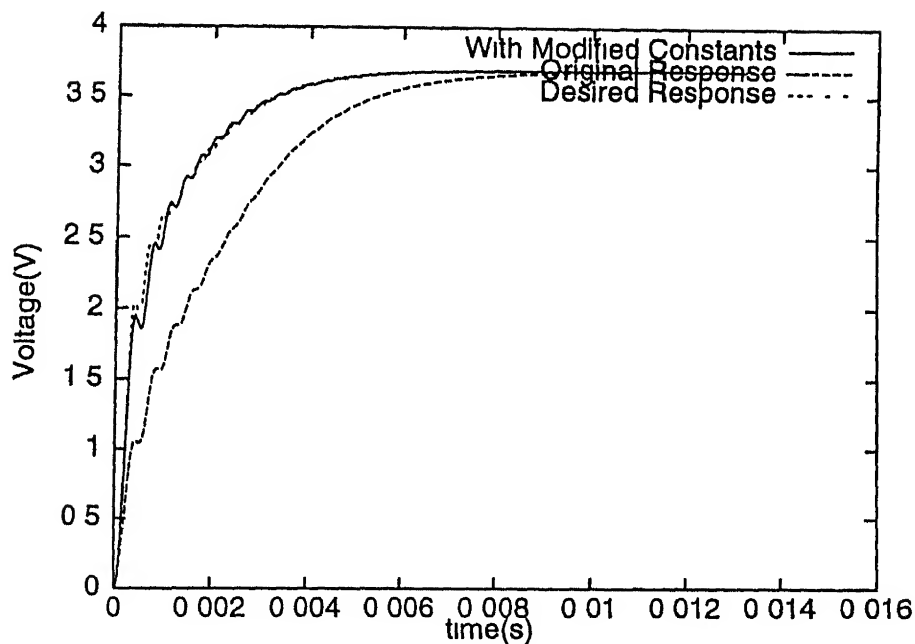


Figure 4.2 Response to a Given Desired Response Using Method-1 With Initial Constants

seen that the response of the converter is very close to the desired response

4.4.2 Method-2

The values of Δd 's for the performance measure table are given in Table 4.4

Fig. 4.3 shows the response with a performance measure table given above, the

Table 4.4 Constants of Performance Measure Table

	$0 \leq ce_1 < 0.25$	$0.25 \leq ce_1 < 0.75$	$ce_1 \geq 0.75$
Δd_1	0.3	0.35	0.40
Δd_2	0.25	0.28	0.35
Δd_3	0.165	0.185	0.195
Δd_4	0.088	0.128	0.148

desired response and the present response. The constants $a_0 - a_8$ have their initial

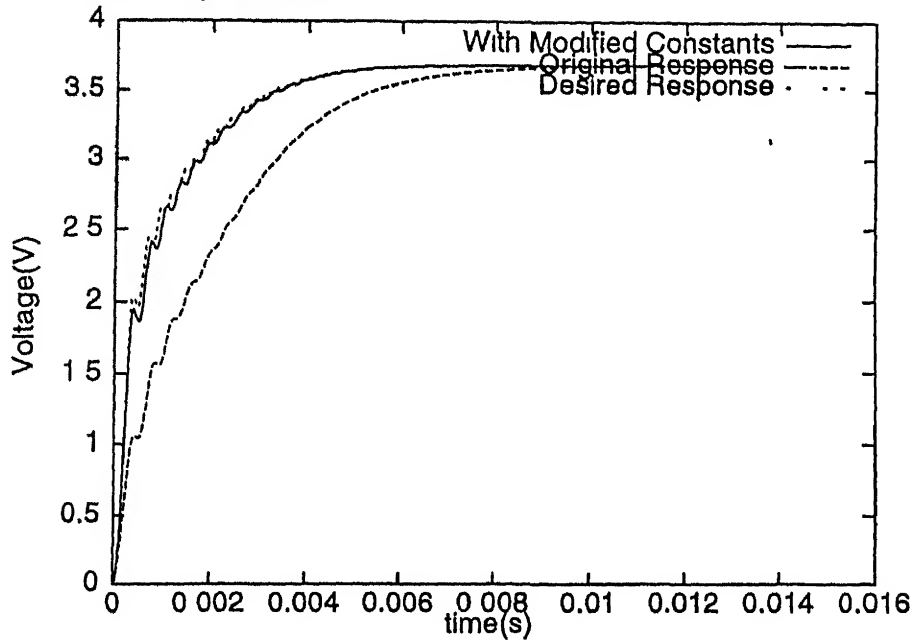


Figure 4.3 For a Given Desired Response Using Method-2 With Initial Constants

values according to the response shown in Fig 4.1 for five zone FLC. The P I is 2.58 in 18th run. Every fifth sampling instant is taken as the matching point for measuring P I. It is seen that the response is very close to the desired response.

It is observed that as the value of Δd increases the number of runs taken to achieve a particular P I decrease. But if the value of Δd is increased much then the correction will be too large and the response becomes unstable.

4.4.3 With Zero Initial Constants:

Method-1 :

Method-1 does not give good results in this case. Since the correction in a particular constant say a_i is proportional to $\frac{\sum \mu_i}{\mu_i}$, the correction to the values of constants is too large in this case. With all zero as initial constants the error (e) is very large so $\sum \mu_i$ is very large and also μ_i is always less than one. So the correction becomes large and system becomes unstable. If the value of Δd is decreased then the system becomes stable but then the number of runs required to achieve a particular value of P I increases.

Table 4.5 shows the nature of P I. with different values of $\Delta d's$ in 50th run where M.F. is the multiplying factor for the values of $\Delta d's$ in Table 4.3

Table 4.5. Nature of Deviation With Different Values of $\Delta d's$

M.F	P.I.
0.0001	11867.78
0.001	844.34
0.01	3.59
0.1	9243332

Method-2 .

This method gives good results. The values of $\Delta d's$ chosen for this method are given in Table 4.4. The result is shown in Fig 4.4 with the desired response. The response is very close to the desired response. The P I is 1.46 in 18th run.

4.4.4 With Unity Initial Constants

All the constants i.e. from a_0 to a_8 are assumed to be one.

Method-1:

This method does not give good result in this case also. The correction to the constants is too large. Moreover it takes more number of runs to achieve a particular minimum value of deviation.

Method-2

All the constants from a_0 to a_8 are initially taken as one. The performance table used is same as Table 4.4. Fig 4.4 shows the response for this case and the desired output voltage. The performance index is 4.08 in 18th run. The response is very close to the desired response.

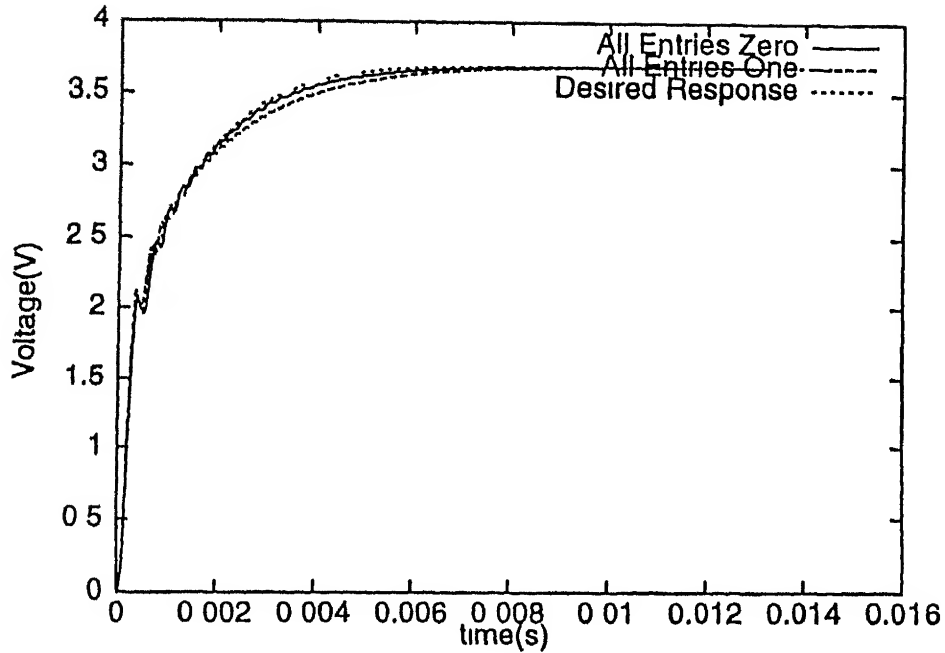


Figure 4.4 For a Given Desired Response Using Method-2

4.5 Response to an Ideal Step

Response to an ideal step using Method-2 for all the constants having values zero and one is studied. The desired output voltage $V_{od}=3.69V$.

4.5.1 With Zero Initial constants

The performance measure table used is same as Table 4.2. Fig 4.5 shows the response to an ideal step. The PI is 18.79 in 18th run.

It is observed that the rise time is considerably less. The output voltage rises very sharply and then oscillates. In the steady state the system is not stable. The output voltage oscillates around the desired steady state, although the deviation is small.

4.5.2 With Unity Initial Constants

The performance measure table is same as Table 4.2. The response to this step with all one as initial constants is shown in Fig 4.5. The P I is 18.45 in 18th run.

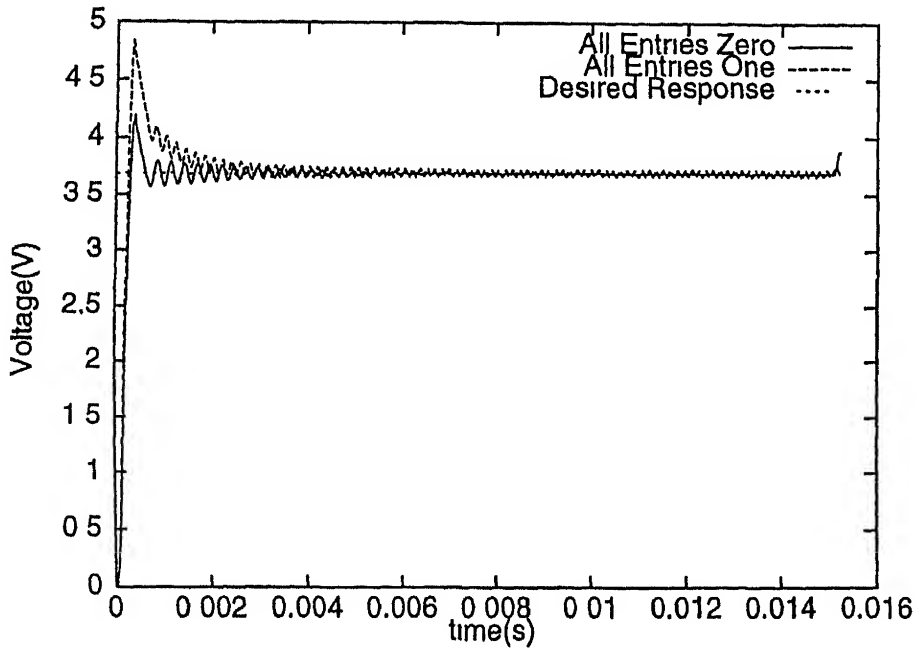


Figure 4.5. Step Response

4.6 Response to a Given Exponential

It is clear from the results of simulation that the rise time is considerably less. The output voltage rises very sharply and the output voltage oscillates around the desired steady state. Response to a given exponential using Method-2 for all the constants having values zero and one is studied. The desired output voltage is taken as $V_{od} = (1 - e^{-t/\tau})$ where $\tau = 200T$ and T is the time period of one cycle.

4.6.1 With Zero Initial Constants

The performance measure table used is same as Table 4.2. Fig 4.6 shows the response to a given exponential and the desired response. The P I is 1.96 in 18th run. The

response is very close to the desired exponential.

4.6.2 With Unity Initial Constants

The performance table used for this case is also same as Table 4.2. The response to a given exponential for this case is shown in Fig 4.6. The P.I. is 9.7 in 18th run. The response is very close to the desired exponential.

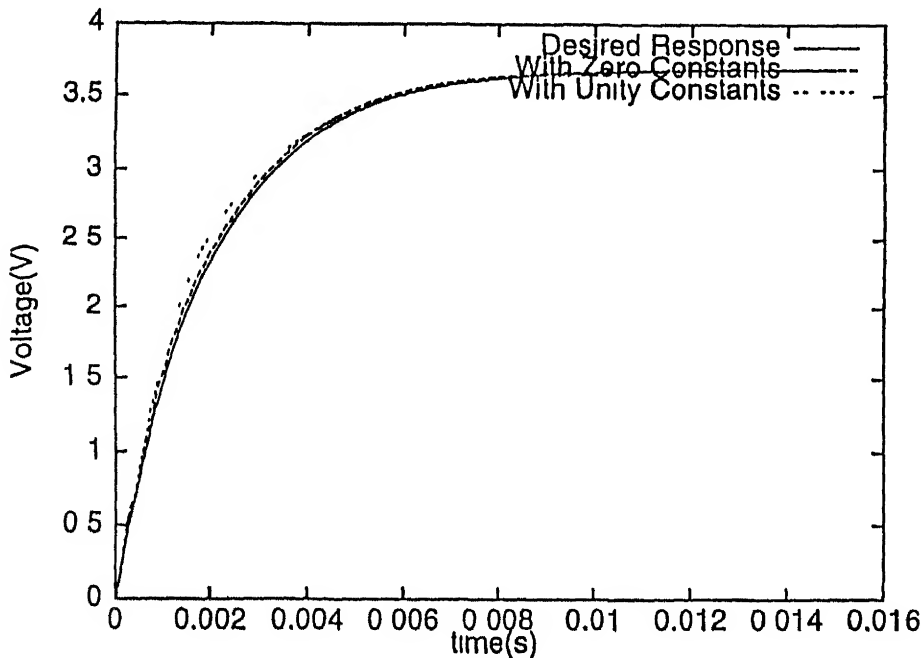


Figure 4.6. Exponential Response

The choice of constants for the performance measure table is dependent on the time constant of the exponential. The same table, if used for slower exponentials causes over correction and the system becomes unstable. Therefore the constants should be decreased as τ increases.

4.7 Effect of Number of Matching Points

The sampling points where the P.I. is calculated are called matching points. The responses shown so far in this chapter are for matching points as every 5th sampling

instants. Fig 4.7 shows the relationship between the values of a particular constant (a_3) and number of matching points at a particular run. It can be concluded from the figure that after a certain point the value of the constant saturates, so increasing the number of matching points further does not affect the value of the constants. Choosing more number of matching points reduces the number of runs required for a particular value of P.I.

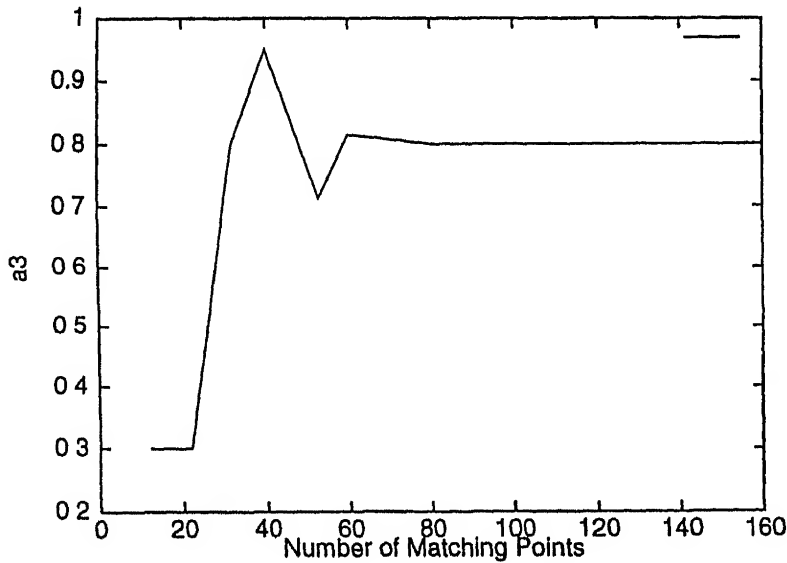


Figure 4.7 Variation in the Value of Constant a_3

4.8 Criterion For Stopping

For matching a response and stopping the process, it is needed to know how many runs are required to achieve the best possible response, which is close to the desired one. Either one can fix the desired value of minimum P I or one can choose the minimum P I as the stopping criterion. Fig 4.8 shows the relationship between the number of runs and P I for a particular case.

It is observed from the figure that after some runs the P I. remains almost constant. Fixing the value of P I for stopping criterion may give the problem, if the controller is not at all able to achieve that desired P I. Then another higher value

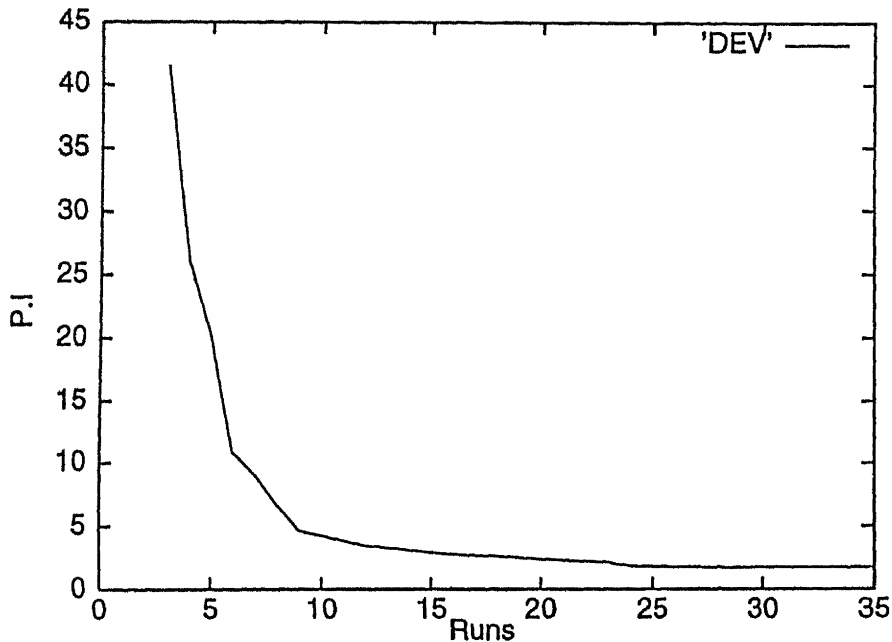


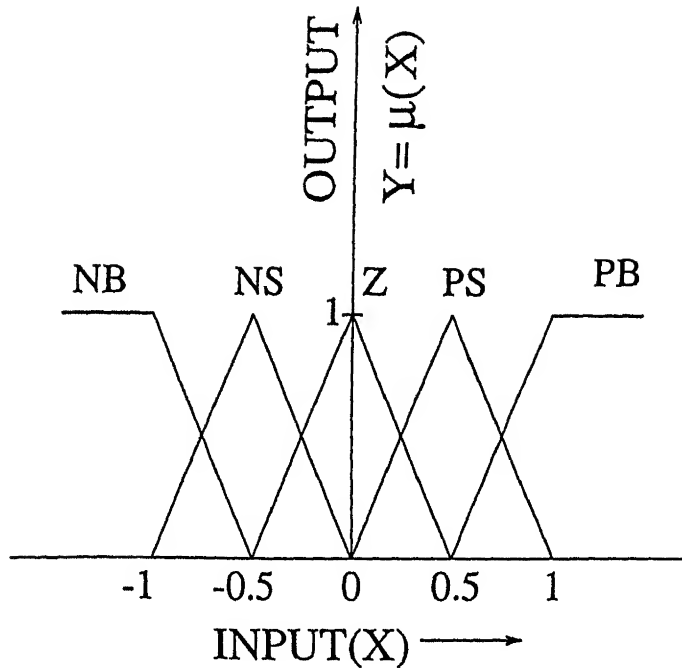
Figure 4.8 Criterion For Stopping

of P.I. is to be chosen, whereas choosing the minimum value of P.I. as stopping criterion gives the best possible response that the controller can produce

4.9 Dual Table Method

In this case the original fuzzy rule table is not changed. There is another table called as performance measure table which is responsible in achieving the desired response. Instead of modifying the constants in fuzzy rule table it directly modifies the controller output. The error in the actual output and desired output is scaled by a factor and the scaled error is called as e_p . This quantity is fuzzified according to the membership function as shown in Fig 4.9. There is a performance measure table given in Table 4.6 which selects the output C_p , according to the scaled error e_p .

For a particular value of error there are two categories of e_p and two values of C_p . Center of gravity method is used for defuzzification to obtain d_2 . The duty

Figure 4.9 Membership Function For e_p

cycle without the performance measure table is given by

$$D_i = D_{i-1} + \eta_1 d_1$$

where d_1 is the fuzzy controller output

η_1 is the gain factor

i is the sampling instant

The duty cycle with the performance measure is given by

$$D_i = D_{i-1} + \eta_1 d_1 + \eta_2 d_2$$

where d_2 is the output of the performance measure table

η_2 is the gain factor for d_2

Fig 4.10 shows the response for this method with $\eta_2=0.1$. The scaling factor for e_p is 0.1. It is observed that the method of modifying the constants is not reciprocal i.e. if the desired response corresponds to a particular fuzzy rule table then the final table obtained from this method is not same as the table of desired response.

Table 4 6: Performance Measure Table For C_{pi}

e_{pi}	C_{pi}
NB	0.80
NS	0.25
Z	0.00
PS	-0.25
PB	-0.80

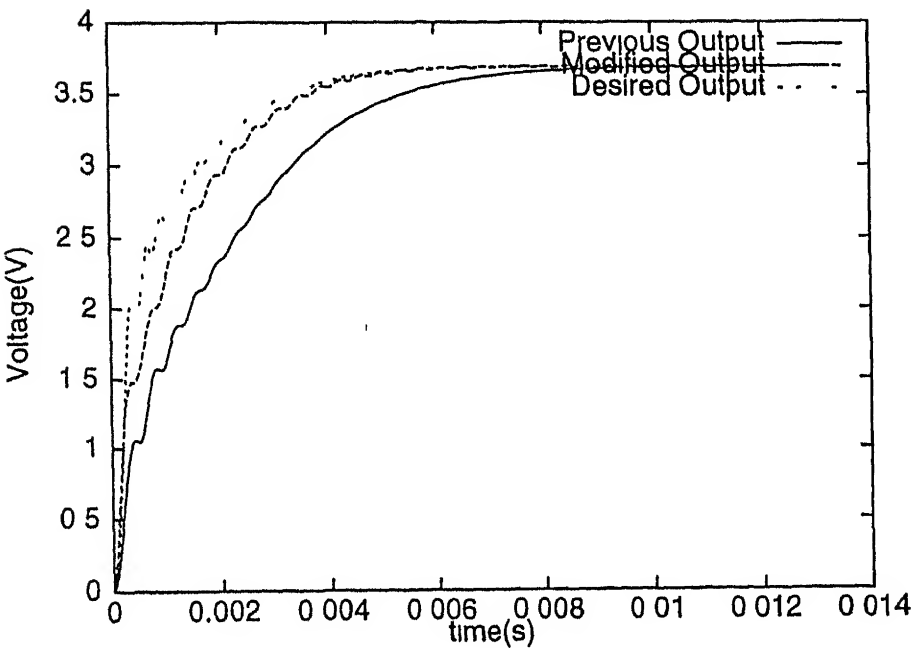


Figure 4 10 Dual Table Method

4.10 Conclusions

In this chapter two methods for self-organisation are discussed. Method 2 is better than Method 1. The response is very close to the desired response in every case. Operation of the self organising algorithm shows that the final values for constants $a_0 - a_8$ are a function of the initial values chosen in the table. Therefore many choices of $a_0 - a_8$ produce nearly same response. If the desired response corresponds to some known values of $a_0 - a_8$, the self organisation does not result in the same values of constants for zero initial values and unity initial values. Some sample values other than the known constants also resulted in a different table. The reason is that the self organisation may not cover all cases of e & ce . The new table with zero & unity initial values resulted in larger values of constants which affects the response due to load and line variation adversely.

If the number of matching points in the algorithm is increased the constants saturate after a particular number of matching points (Fig 4.7). In the dual table method the original constants of fuzzy rule table are not changed.

Chapter 5

Fuzzy Regulators

The quality of any controller is decided on the basis of its ability to damp out the oscillations i.e. to reduce the overshoot & undershoot and time to reach the set value after the perturbation. In this chapter different types of fuzzy regulators are studied. Section 5.1 gives the voltage regulation for load injection and rejection. Line regulation for variation in the supply voltage is given in Section 5.2. The response of the controller to a step change in the reference value of voltage is given in Section 5.3. Section 5.4 describes different auxiliary controllers for reducing the voltage overshoot and undershoot due to load disturbances. The auxiliary controller described in Section 5.4.1 is based on the small signal model for the Buck-Boost converter in the state space. A simplified small signal model is used in Section 5.4.2. Section 5.4.3 describes an auxiliary controller using the small signal model in the frequency domain. The response of the system with variable gain factor η_1 is described in Section 5.5.

5.1 Load Regulation

The fuzzy logic controller is tested against load variation. Fig 5.1 and Fig 5.2 shows the response of FLC to load variation. In Fig 5.1 load resistance is changed from 10 ohms to 30 ohms and then back to 10 ohms. The FLC is able to achieve the steady state voltage i.e. 3.69V in approximately 600 cycles. Fig 5.2 shows the FLC response

to a load change of 10 ohms to 5 ohms and then back to 10 ohms. The FLC is able to achieve the steady state voltage i.e. 3.69V in approximately 600 cycles. It is clear from the simulation results that the fuzzy regulator is able to regulate the output voltage against the variation in load.

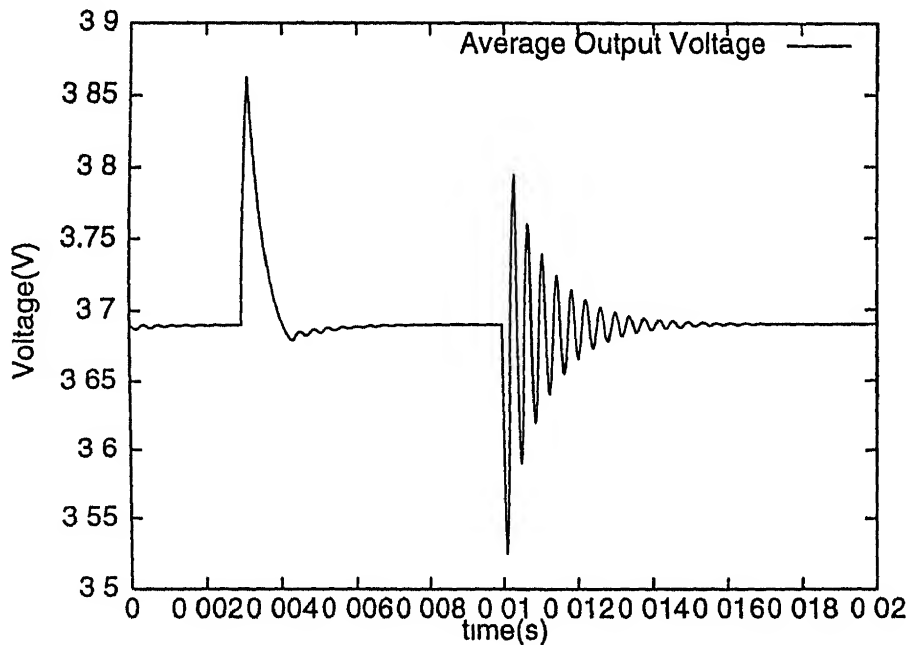


Figure 5.1 Load Resistance is Changed from 10 Ω to 30 Ω & then to 10 Ω

5.2 Line Regulation

The supply voltage is not always constant. So the FLC is tested against a variation in the supply voltage. Fig 5.3 shows the response of the FLC to a variation in line voltage from 15V to 10V and then back to 15V. It can be seen from the figure that the converter voltage reaches the reference voltage within 200 cycles.

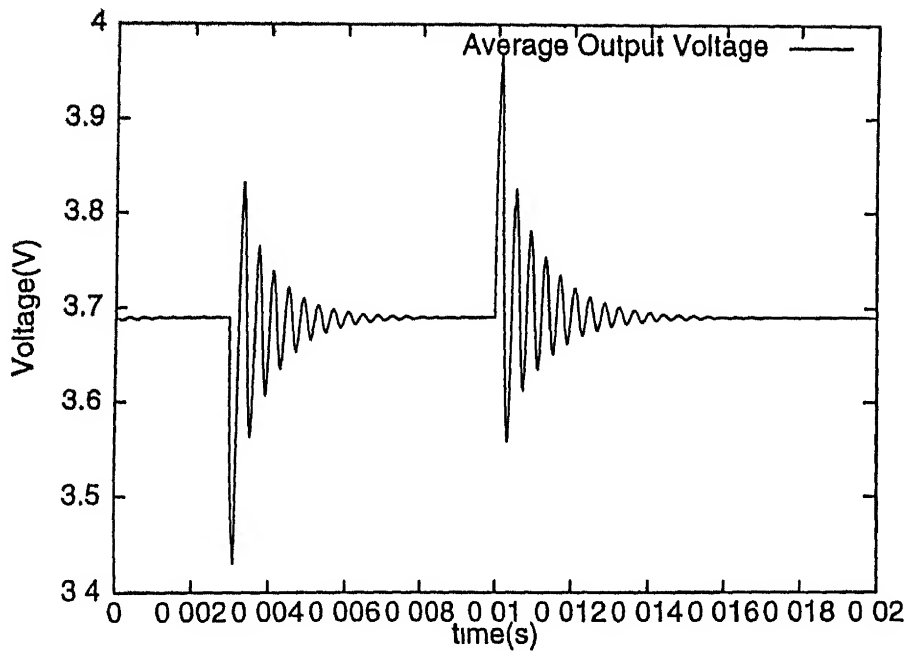


Figure 5 2 Load Resistance is Changed from 10 Ω to 5 Ω & then to 10 Ω

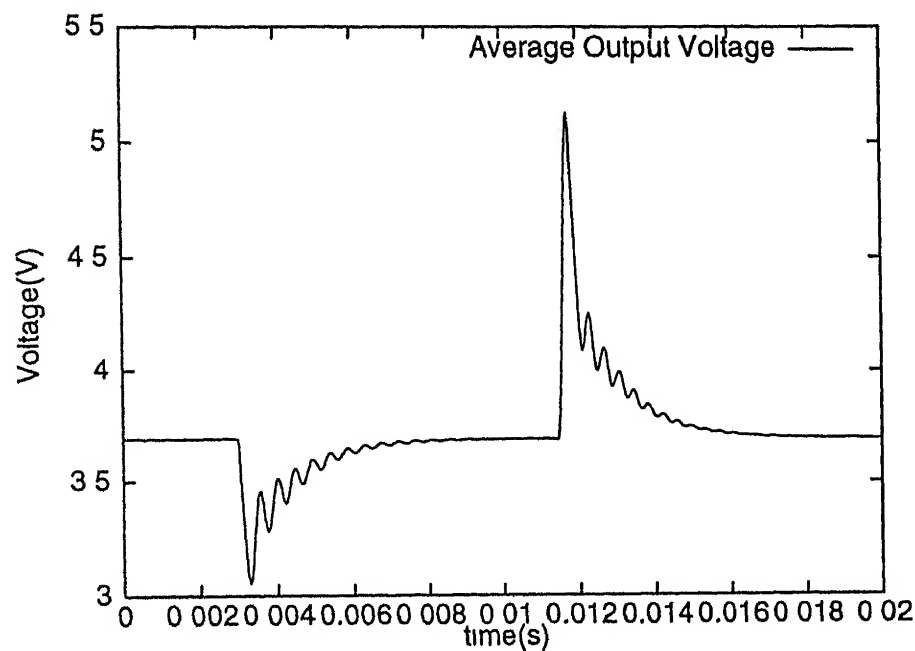


Figure 5 3 Line Voltage is Changed from 15V to 10V & then back to 15V

5.3 Response to Change in Vref

To change the output voltage of the converter, the reference voltage to the controller is changed. Fig 5.4 shows the response of FLC to a change in the reference voltage. The reference voltage is changed from 3.69V to 5V.

It can be seen that the voltage follows the reference voltage.

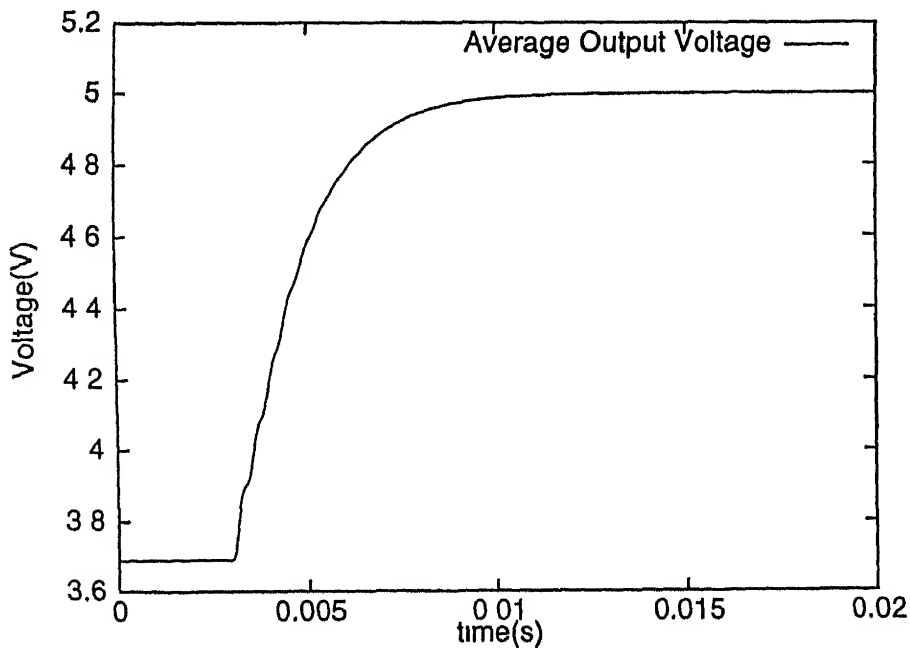


Figure 5.4 Reference Voltage is Changed to 5V

5.4 Auxillary Controller

Fig 5.5 shows the block diagram of a system using FLC and an auxillary controller. When there is a change in the load, the converter output voltage overshoots or undershoots according to the variation in the load. If an auxillary controller is introduced into the system only for some cycles, during these oscillations, then the undershoot and overshoot in the output voltage can be reduced. After that the fuzzy controller alone regulates the voltage and the auxillary controller is disconnected. The three auxillary controllers discussed in this section use the following

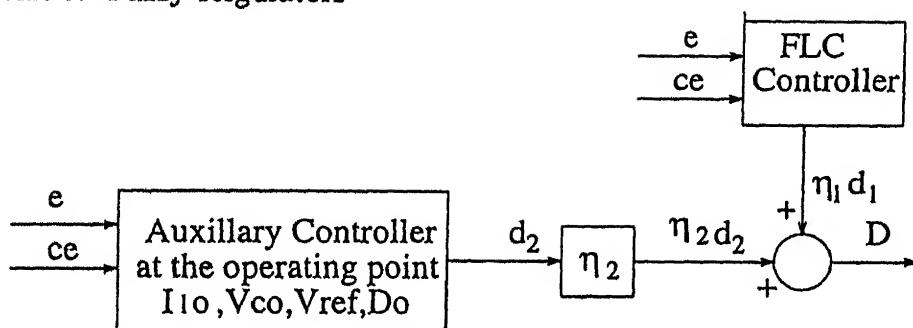


Figure 5.5: Block Diagram For Auxillary Controller

strategies

- Computation of \hat{d} using small signal model
- Computation of \hat{d} using simplified small signal model
- computation of \hat{d} using low frequency d c gain

In the following sections a load change of the type as shown in Fig 5.6 is used.

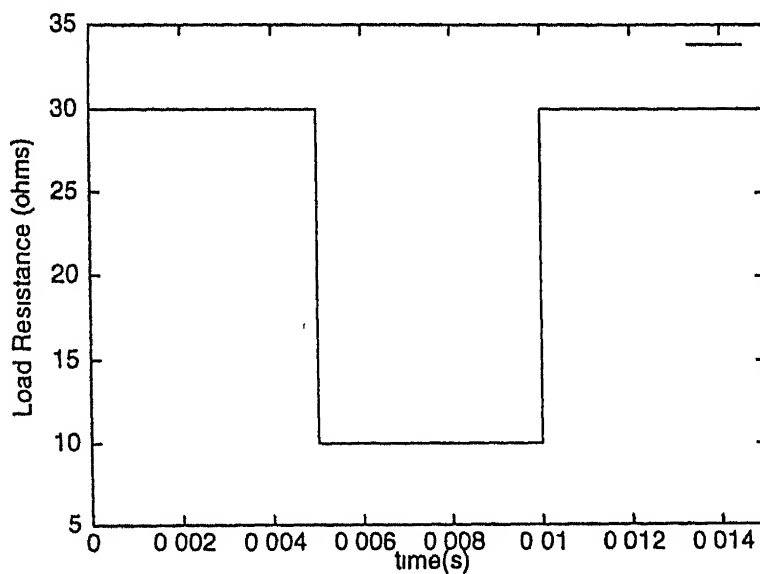
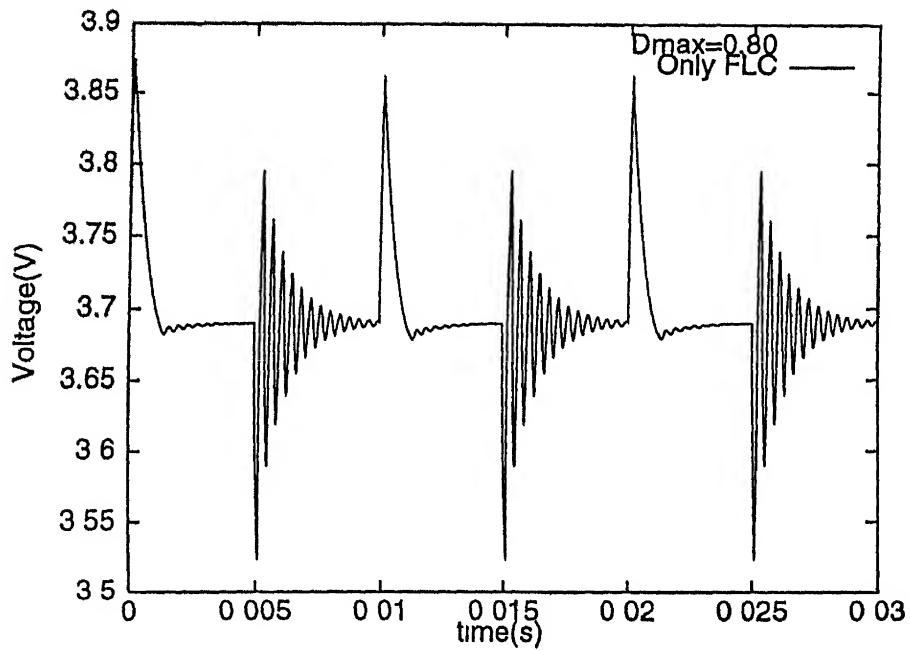
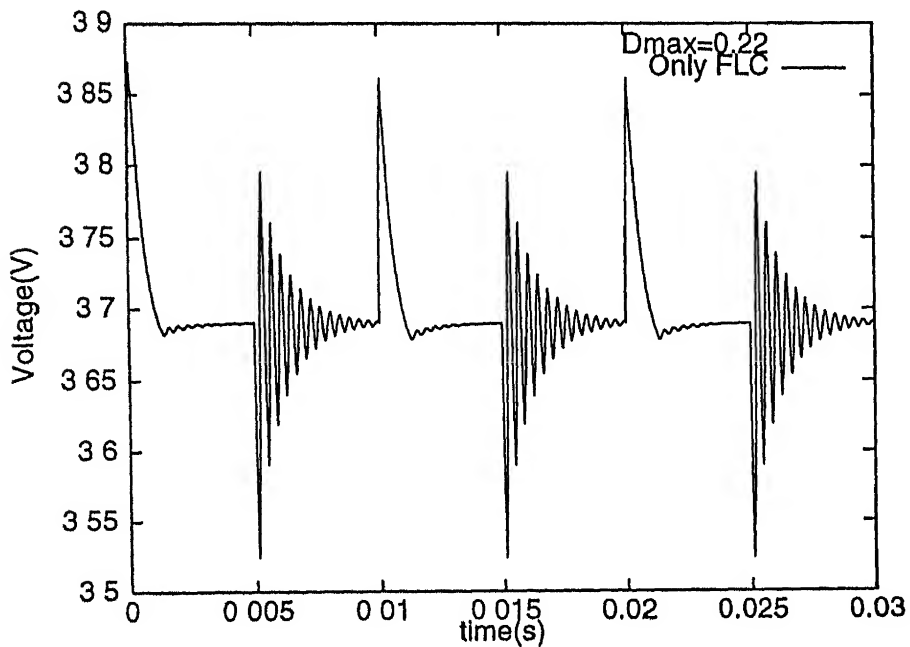


Figure 5 6 Nature of Load Variation

Figure 5.7: Response of Fuzzy Regulator With $D_{max}=0.80$ Figure 5.8 Response of Fuzzy Regulator With $D_{max}=0.22$

The response of the FLC alone, without the auxillary controller, with D_{max} (max limit to duty to duty cycle) =0.80 and with D_{max} =0.22 is shown in Fig 5.7 and Fig 5.8 respectively. The Y-axis represents the average output voltage in the figures showing the response with and without auxillary controller.

5.4.1 Auxillary Controller Using the Small Signal Model

The small signal model of the converter, discussed in Section 2.1.5 gives the following equation:

$$\hat{X} = A_o \hat{X} + B_o \hat{u} + E \hat{d} \quad (5.1)$$

The dc voltage is constant, therefore $\hat{u}=0$

$$\begin{aligned} \hat{\dot{X}} &= A_o \hat{X} + E \hat{d} \\ \frac{(\hat{X}_k - \hat{X}_{k-1})}{\Delta t} &= A_o \hat{X}_k + E \hat{d} \end{aligned}$$

Where k is the current sampling instant and Δt is the sampling time.

$$\frac{(\hat{X}_k - \hat{X}_{k-1})}{\Delta t} - A_o \hat{X}_k = E \hat{d}$$

substituting the state variables as V_c , I_l and the value of A_o & E from Section 2.1.3 and Section 2.1.5 respectively:

$$\frac{1}{\Delta t} \begin{bmatrix} \hat{V}_{ck} - \hat{V}_{ck-1} \\ \hat{I}_{lk} - \hat{I}_{lk-1} \end{bmatrix} - \begin{bmatrix} -\frac{1}{R_1 C} & \frac{(1-D)R}{R_1 C} \\ -\frac{(1-D)(1-\frac{r_c}{R_1})}{L} & -\frac{r_l}{L} - \frac{(1-D)Rr_c}{R_1 L} \end{bmatrix} \begin{bmatrix} \hat{V}_{ck} \\ \hat{I}_{lk} \end{bmatrix} = \begin{bmatrix} -\frac{I_{lo}R}{R_1 LC} \\ \frac{V_{dc}}{L} + \frac{V_{co}(1-\frac{r_c}{R_1})}{L} + \frac{Rr_c I_{lo}}{R_1 L} \end{bmatrix}$$

Considering only first row

$$\frac{(\hat{V}_{ck} - \hat{V}_{ck-1})}{\Delta t} + \frac{\hat{V}_{ck}}{R_1 C} - \frac{(1-D_o)I_{lk}}{C} = -\frac{I_{lo}\hat{d}}{C} \quad (5.2)$$

Since $r_c \ll R$, it is assumed that $R_1 \approx R$

substituting the values of converter parameters from Appendix A Therefore

$$10^5(\hat{V}_{ck} - \hat{V}_{ck-1}) + 10^3 \hat{V}_{ck} - 0.7997 \times 10^4 \hat{I}_{lk} = -4614 \hat{d}$$

$$\hat{d} = \frac{7997 \hat{I}_{lk} - 10^5(\hat{V}_{ck} - \hat{V}_{ck-1}) - 10^3 \hat{V}_{ck}}{4614}$$

Therefore an auxillary controller can calculate \hat{d} from measured values of the state variables \hat{V}_c and \hat{I}_l . The \hat{d} calculated above is the output of the auxillary controller called d_2 in Fig 5.5. The duty cycle is given by

$$D = D_{i-1} + \eta_1 d_1 + \eta_2 d_2 \quad (5.4)$$

where d_1 is the output of the FLC

d_2 is the output of the auxillary controller i.e. \hat{d}

η_2 is chosen as 0.03. The maximum limit to duty cycle (D) is chosen as $D_{max}=0.80$.

The auxillary controller remains in the system until the output reaches the first zero crossing. After that only the FLC regulates the voltage and d_2 is assumed to be zero. Fig 5.9 shows the response with an auxillary controller where $D_{max}=0.80$. Fig 5.7 shows the response with only FLC to the same load variation with $D_{max}=0.80$. Comparison of two results shows that in both load rejection and injection the overshoot and undershoot reduces respectively.

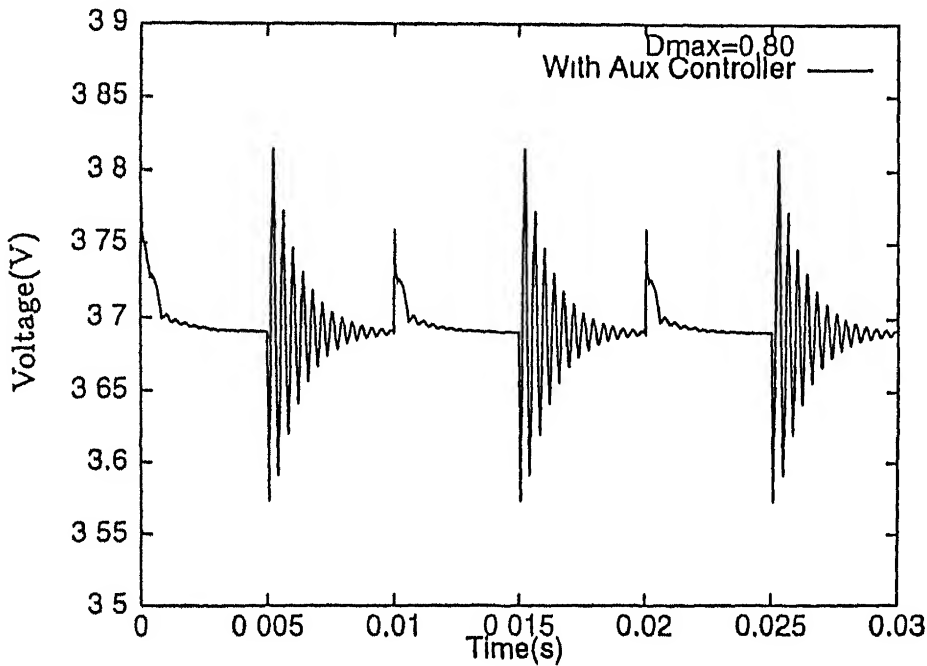


Figure 5.9: Response of the Auxillary Controller using Small Signal Model ($D_{max}=0.80$)

Fig 5 10 shows the response with an auxillary controller where $D_{max}=0.22$. The response improves considerably during load rejection and injection both.

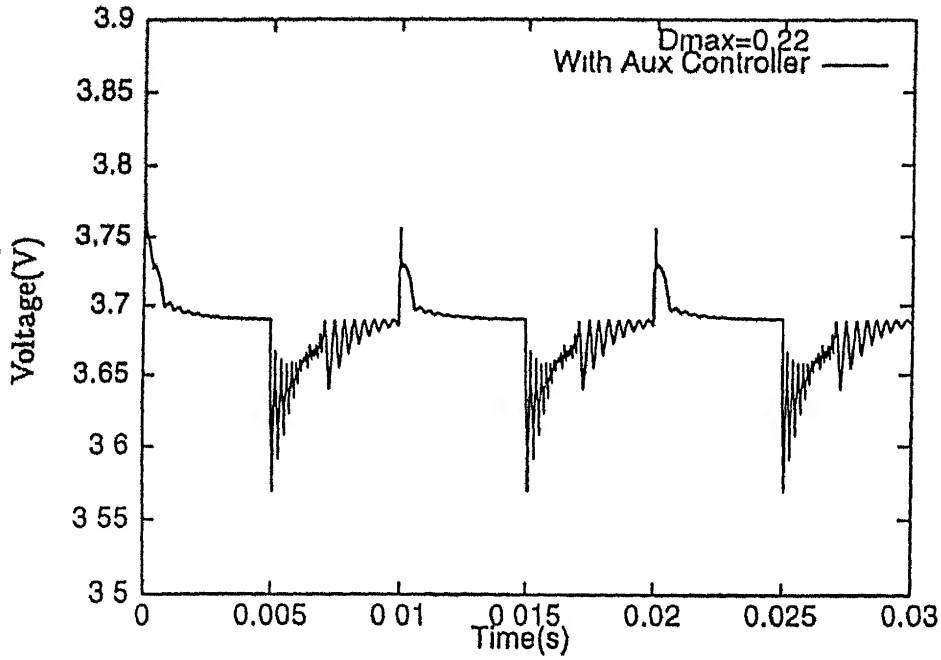


Figure 5 10. Response of the Auxillary Controller using Small Signal Model ($D_{max}=0.22$)

5.4.2 Auxillary Controller Using the Simplified Small Signal Model

In order to judge the relative importance of feedback of \hat{I}_l & \hat{V}_c , a simplified equation for \hat{d} can be obtained by assuming \hat{V}_c to be zero for all k . This results into following equation:

$$\hat{d} = \frac{7997\hat{I}_{lk}}{4614}$$

The value of η_2 in equation (5.4) is reduced to 0.003 from 0.03 to compensate for the effect of above assumption.

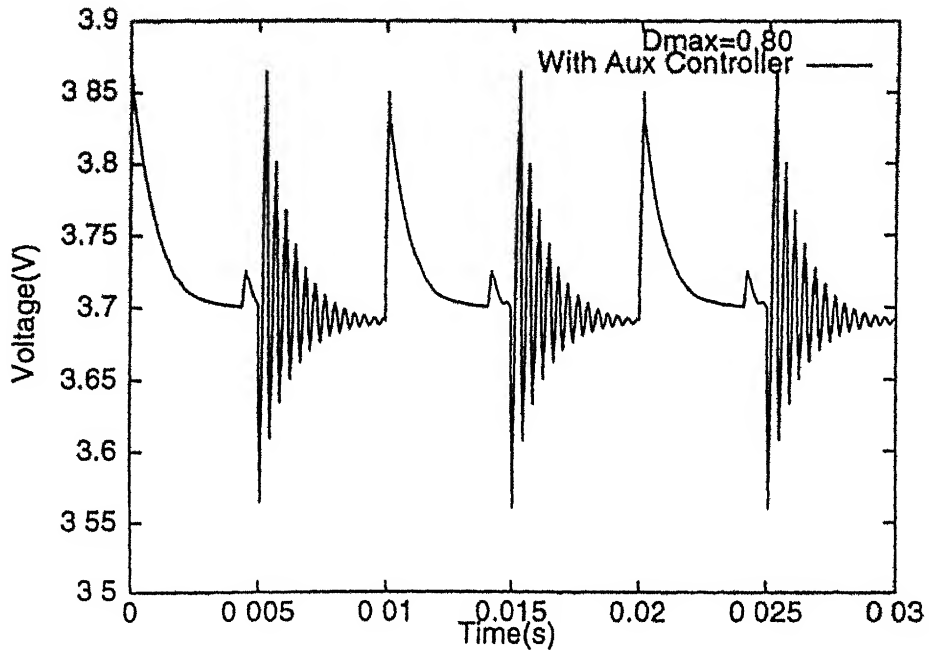


Figure 5.11 Response of the Auxiliary Controller using Simplified Small Signal Model ($D_{max}=0.80$)

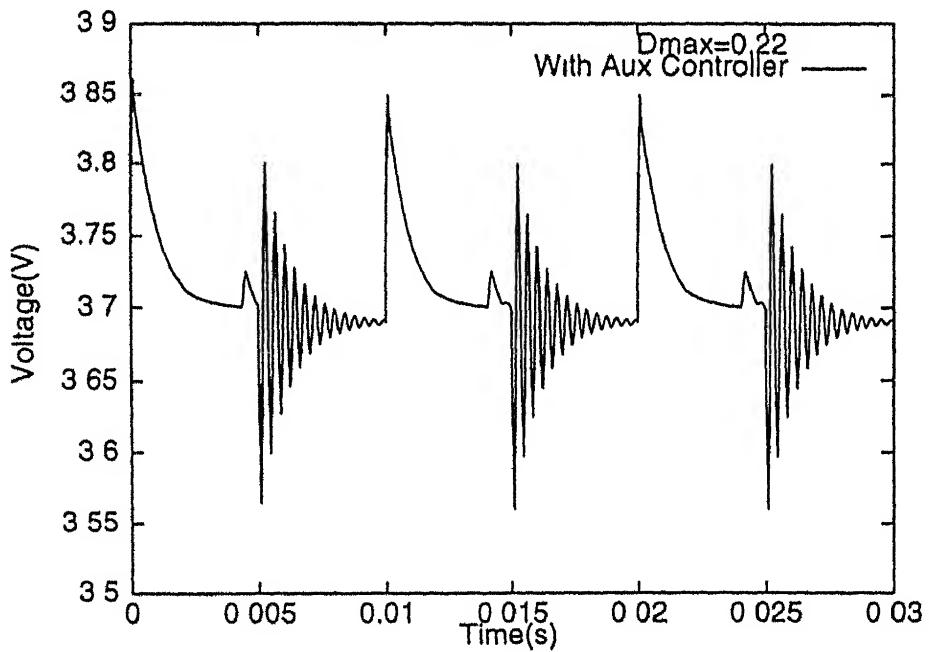


Figure 5.12 Response of the Auxiliary Controller using Simplified Small Signal Model ($D_{max}=0.22$)

Fig 5.11 shows the response for $D_{max}=0.80$ with the auxiliary controller. There is no appreciable effect on the response in this case when compared with only FLC. Fig 5.12 shows the response with the auxiliary controller with $D_{max}=0.22$. The response is better than that of with $D_{max}=0.80$ but still the change is not so significant. Therefore it can be inferred that the term containing \hat{I}_{lk} in the auxiliary controller of Section 5.4.1 can be neglected without affecting the response.

5.4.3 Auxiliary Controller Using Low Frequency D.C. Gain

The transfer function for $\hat{V}_c(s)/\hat{d}(s)$ is derived in chapter 2. Calculating the d.c. gain of the transfer function given in Section 2.1.6, the following expression is obtained

$$\hat{d}(s) = \frac{\hat{V}_c(s)}{22.88}$$

η_2 is chosen as 1.0 for this controller. Fig 5.13 shows the response with the auxiliary controller based on above algorithm with $D_{max}=0.80$. The overshoot and undershoot is less than that of without auxiliary controllers. Fig 5.14 shows the response with

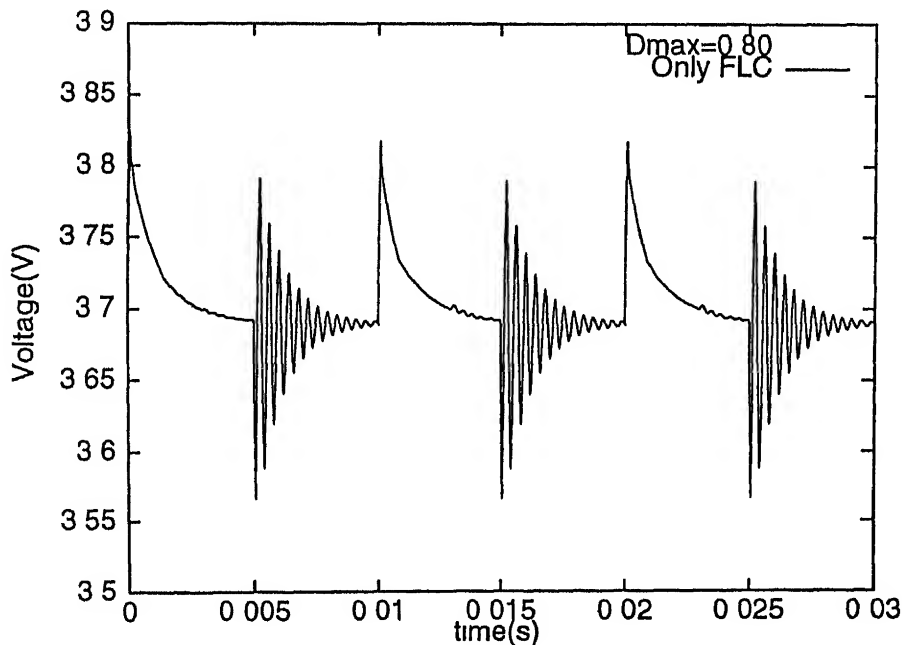


Figure 5.13 Response of the Auxiliary Controller using d.c. Gain ($D_{max}=0.80$)

the auxillary controller with $D_{max}=0.22$. The response is better in this case during load injection.

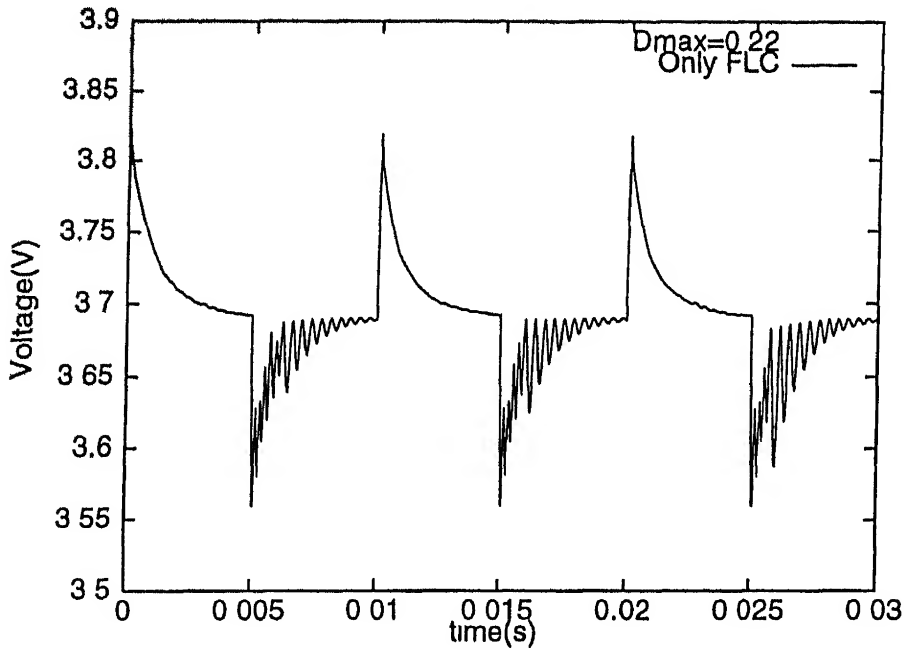


Figure 5.14 Response of the Auxillary Controller using d c Gain ($D_{max}=0.22$)

5.5 Effect of Variable Gain Factor η_1 on Response to Load Changes

In the previous section the value of η_1 has been kept constant at 0.01. In this section the effect of changing η_1 has been studied. The auxillary controller has been disconnected by assuming η_2 to be zero. The response of fuzzy logic controller can be improved by using adjustable gain factor η_1 . The following two methods are used for adjusting the gain.

- By dual value of gain factor η_1
- By Variable gain factor η_1

5.5.1 Dual Value Gain Factor

The channel gain for FLC is varied during the load variation. An increased value of gain η_1 is used only till the first zero crossing of the error in output voltage. After this the gain is again set to the initial value so that the system does not enter into unstable region. Fig 5.15 shows the response for a variable gain FLC. The gain $\eta_1=0.08$ for first few cycles and then it comes back to its initial value of 0.01 and D_{max} is set to 0.80. This gives a better response than that of with auxiliary controller. During load rejection the response is appreciably better than that of with constant gain FLC.

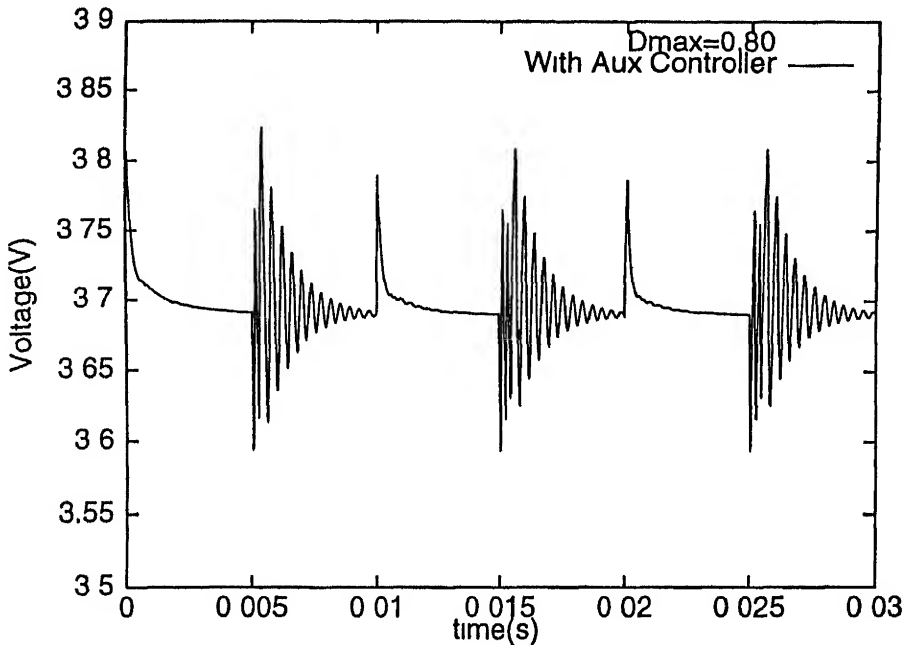


Figure 5.15 Response of Dual Gain FLC ($D_{max}=0.80$)

Fig 5.16 shows the response for variable gain FLC with $D_{max}=0.22$. Reducing the maximum limit D_{max} improves the response appreciably.

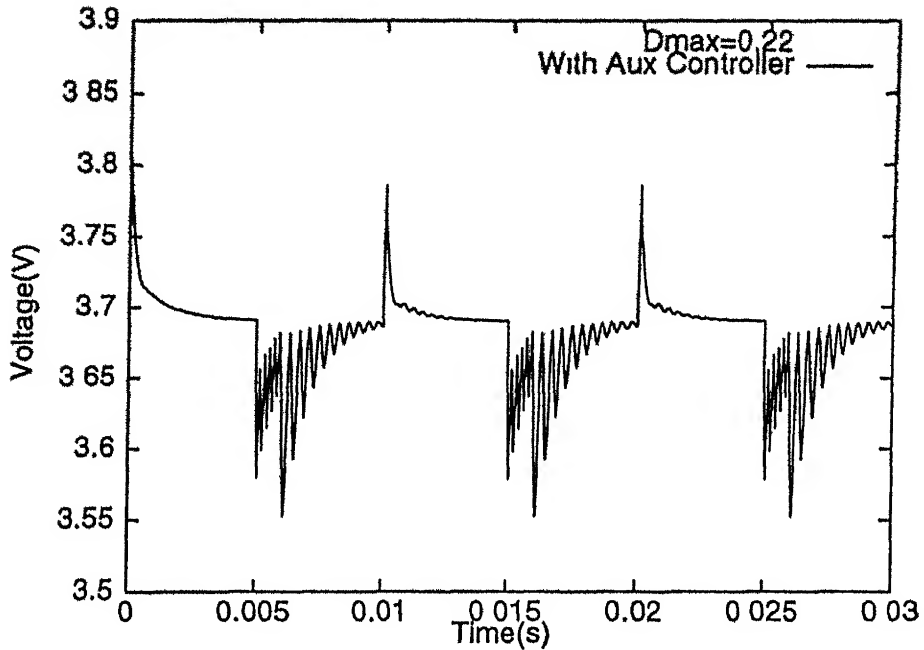


Figure 5.16 Response of Dual Gain FLC ($D_{max}=0.22$)

5.5.2 Variable Gain Factor

In the previous method the change in the value of the gain was abrupt. The gain can be decreased gradually, so that there is a smooth variation. Whenever there is a load change the gain is set to $\eta_i=0.1$ and after every converter cycle the gain is reduced by 0.0005

$$\eta_i = \eta_{i-1} - 0.0005$$

Fig 5.17 shows the response for dual valued gain with $D_{max}=0.80$. The response is much better than that of the constant gain FLC during load rejection and injection both. Reducing the limit to D_{max} i.e. $D_{max}=0.22$ improves the response while load injection as shown in Fig 5.18

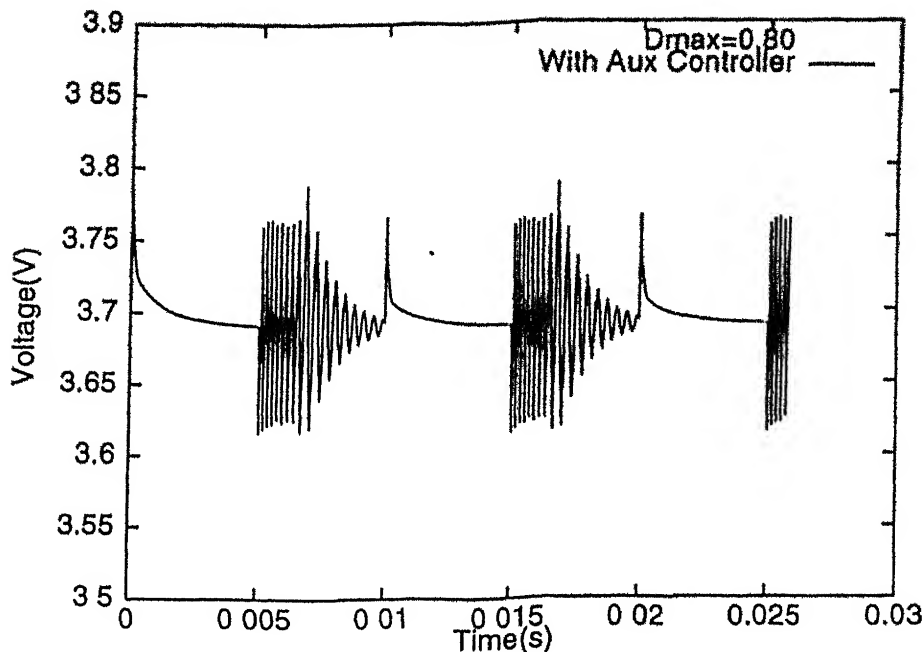


Figure 5.17 Response of Variable Gain FLC ($D_{max}=0.80$)

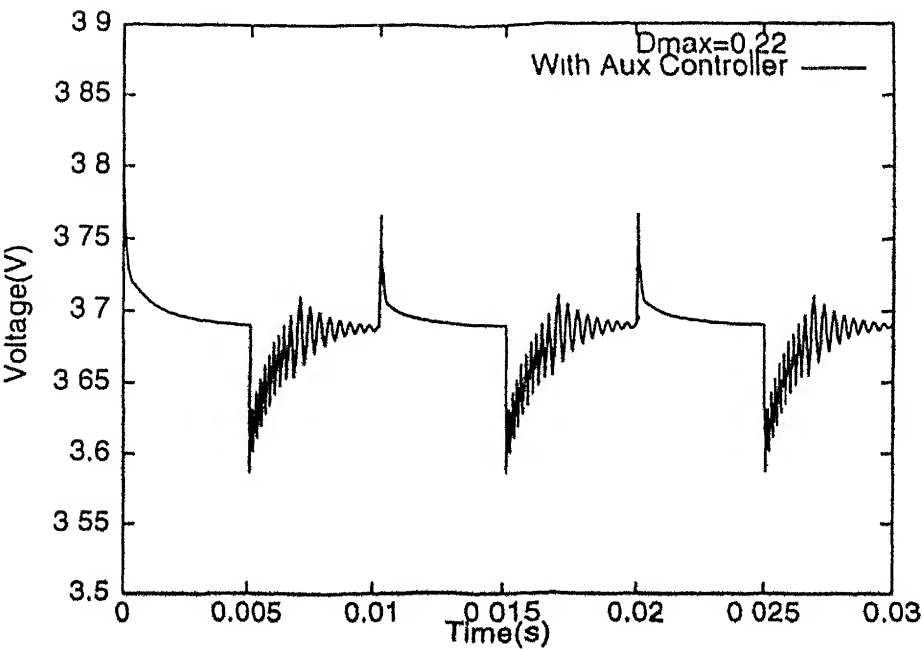


Figure 5.18 Response of Variable Gain FLC ($D_{max}=0.22$)

5.6 Conclusions

In this chapter the performance of the fuzzy logic controller has been studied. The performance is checked against variation in load, line and reference value of the voltage. The FLC is able to regulate the output voltage against these disturbances. Then the auxillary controller is introduced along with FLC in the system to damp out the overshoot and undershoot developed after load perturbations. Three auxillary controllers have been discussed which are given below:

- Auxillary controller based on small signal model of the converter
- Auxillary controller based on simplified small signal model
- Auxillary controller based on low frequency d.c. gain

The response with auxillary controller is compared to that of with only FLC. It has been seen that the response with auxillary controller is better. Auxillary controller using the small signal model gives the best response.

The gain of FLC can also be varied and it results in a better response. Two methods are proposed for varying the gain.

- Dual value gain
- Variable gain

The variable gain method gives better results than the dual valued gain method, as there is no abrupt change in the gain. Limiting the maximum value of duty cycle i.e. D_{max} around its operating point value improves the response considerably.

Chapter 6

Conclusions

A detailed analysis of Buck-Boost converter and fuzzy logic controller has been studied. The Buck-Boost converter is analysed according to the following models

1. State space differential equation models
2. Average state space model and its equivalent circuit
3. Small signal model and transfer function

The Bode plots for the transfer function are verified by the simulation.

The following types of fuzzy logic controllers have been discussed in this thesis.

1. A simple Proportional Controller
2. A simple Integral Controller.
3. Integral Control with adjustable weights
4. A P.I. Controller with crisp output
5. A P.I. Controller with fuzzy output.

The equivalence of Fuzzy Logic Controller (FLC) with a P.I. controller is established. It can be concluded that FLC is highly nonlinear in nature. The values of K_i and K_p are calculated. The responses of 3 zone and 5 zone FLC are compared.

The 5 zone FLC is faster than the 3 zone FLC. As the number of zones increase, the response becomes better, but complexity increases. The system output voltage behaviour at a frequency of 20 kHz is also shown. As the value of inductor and capacitor is increased the response time also increases.

Self-Organisation is discussed in order to tune the original response to a desired response. Two methods are discussed for self organisation. Method-2 gives better results. It has been shown that it is possible to calculate the constants of rule table starting from all zero initial values. However, there are many sets of constants which give nearly the same response. Therefore, it is possible that the self organising algorithm does not reproduce the constants known to give a specified response.

The figure of merit for any controller is its ability to damp out the oscillations i.e., undershoot and overshoot and time taken to settle the output to the set value. The fuzzy regulator used, is able to regulate the output voltage. In order to reduce the overshoot and undershoot, auxiliary controller is introduced with the FLC which acts only during transients. It has been seen that the auxiliary controller using the small signal model gives the best response to damp out the overshoot and undershoot. The FLC using different gains, dual and variable, also gives better results than the constant gain FLC.

The operator has a prior knowledge of the operating value of duty cycle i.e., D_o . Setting the limits to the maximum value of duty cycle i.e., D_{max} around its operating point value improves the response considerably with both the auxiliary controller as well as with the variable gain controller.

6.1 Recommendations for Future Work

The following aspects of this problem can be studied further.

1. Relationship between the Rule table and the Control surface can be studied further. Particularly, if the constants of the rule table can be calculated to approximate a specified surface.

- 2 General formulae for calculation of equivalent gains for multi-zone FLC can be investigated.
- 3 Self-Organisation for the responses from a non-zero initial stage to a given operating point can be studied
- 4 Auxillary Controller for line regulation can be investigated
- 5 Operation with variable gain FLC and Auxillary Controller can be studied

References

- [1] Ebrahim H. Mamdani, "*Application of fuzzy logic to approximate reasoning using linguistic synthesis*", IEEE Transactions on computers, vol 20, No 12, December 1977, pp. 1182-1191.
- [2] G. Nagib, W. Gharieb and Z. Minder, "*Application of fuzzy control to a non-linear thermal process*", Proceedings of the 31st conference on Decision and Control, December 1992, pp. 1154-1159.
- [3] Kwuk L Tang and Robert J. Muholland, "*Comparing fuzzy logic with classical controller designs*", IEEE Transactions on SMC, vol. SMC-17, No-6, November/December 1987, pp. 1085-1087.
- [4] Haoying, William Siler and James J Buckley, "*Fuzzy control theory: A nonlinear case*", Automatica, vol. 26, No-3, pp. 513-520, 1990.
- [5] Hema Khurana "*Fuzzy logic control-A tutorial*", IETE Technical review, vol 18, No-5, pp. 280-288.
- [6] Wing-Chi So, Chi-K Tse and Yim-Shu Lee, "*Development of a fuzzy logic controller for dc/dc converters Design, computer simulation, and experimental evaluation*", IEEE Transactions on Power Electronics, vol. 11, No-1, pp. 24-31, January 1990
- [7] D M Mitchell, "*DC-DC Switching regulator analysis*", Mc - Grawhill, 1988.
- [8] T J Procyk and E H Mamdani, "*A linguist self-organizing process controller*", Automatica, vol 15, pp 15-30, 1979

- [9] Shihuang Shao, "*Fuzzy self-organizing controller and its application for dynamic process*", Fuzzy Sets and Systems 26, pp 151-164, 1988

123242

123242

10

[illegible]

EE-1997-M-MAL-9M